2016

A Missing Link in the Ionoregulatory Strategy of Larval Sea Lamprey (Petromyzon marinus) and African Lungfish (Protopterus annectens): A Closer Look into the Role of the Non-gastric H+/K+-ATPase

Justine E. Doherty
Wilfrid Laurier University, dohe2690@mylaurier.ca

A Missing Link in the Ionoregulatory Strategy of Larval Sea Lamprey (*Petromyzon marinus*) and African Lungfish (*Protopterus annectens*): A Closer Look into the Role of the Non-gastric H^+/K^+-ATPase

By

Justine Elizabeth Doherty

Honours Bachelor of Science, Marine and Freshwater Biology, University of Guelph

2014

Thesis

Submitted to the Department of Biology

Faculty of Science

In partial fulfillment of the requirements for the

Master of Science in Integrative Biology

Wilfrid Laurier University, Waterloo, Ontario Canada

2016

ABSTRACT

Fishes living in freshwater need to actively compensate for the diffusive loss of ions and osmotic gain of water. The gill is the primary organ of ion regulation and contains an array of ion transport proteins to help maintain homeostasis. Two of the more well studied ion pumps are the Na^+/K^+-ATPase (NKA) and vacuolar type proton ATPase (V-ATPase). This thesis focuses on another ion pump known as the non-gastric H^+/K^+-ATPase (ngHKA). The ngHKA (gene: *atp12a*) has not been found in any of the teleost fishes, indicating loss from that lineage. In contrast, there is confirmed expression in lamprey (*Petromyzon marinus*) and lungfish (*Protopterus annectens*) and thus these species were used to investigate the role of the ngHKA in fishes. It was hypothesized that the ngHKA plays a role in potassium and/or acid-base regulation in these fishes. The first objective was to develop an antibody as a tool to study the ngHKA. Next, was to characterize tissue expression patterns to infer functional significance. Finally, I wanted to confirm the pump's functional significance by determining if potassium (fed-fasting) and acid-base challenges (3µEq/g wet mass H^+ or HCO_3^- load) modulate the expression of the ngHKA.

The pump was studied at multiple levels including; transcript expression using qPCR, protein expression using Western blotting, localization using immunohistochemistry, as well as potassium and proton ion flux measurements. Rubidium (Rb^+) was used as a surrogate flux marker for potassium. The NKA and V-ATPase were also studied in an attempt to understand overall osmoregulation strategies. A rabbit polyclonal antibody (LF12Arb2) was successfully validated for the use in Western blotting and immunohistochemistry in both lamprey and lungfish. High expression of ngHKA was found in both gill and kidney, the major ion regulatory organs in fishes. Rubidium uptake

was also successfully measured in both species. In lamprey, fed fish had significantly greater acid uptake and high Rb^+ uptake rates against the predictions. Acid loaded lamprey had higher acid excretion rates compared to controls as predicted. There were no differences in ngHKA protein expression for any of the treatments and localization did not appear to change. Transcript (mRNA) levels did not change for any treatments in either lamprey or lungfish. In lungfish, the ngHKA and NKA protein expression decreased in omeprazole treated fish although with no corresponding changes in H^+ or Rb^+ flux rates. Apical staining did appear more pronounced in the acid loaded fish compared to controls, which should be investigated further. The results show no clear support for the hypothesis that the ngHKA plays a role in potassium and/or acid-base regulation. This was the first study to investigate the ngHKA in fishes. Future studies are suggested to use radioisotopes (^{86}Rb) to advance the methods as well as perform immunohistochemistry quantification analysis.

ACKNOWLEDGMENTS

First and foremost, I would like to thank my supervisor, Dr. Jonathan M. Wilson for always having his door open and for being patient while teaching me all of the very technical and detailed methods. As well for his continuous advice, input, and expertise throughout my thesis.

I would also like to thank my committee members, Drs. Michael P. Wilkie and Dr. Tristan A.F. Long for their valuable feedback and to Dr. Wilkie for allowing me to get my hands wet in the lamprey lab. I would like to acknowledge Gena Braun for all of her technical support with the atomic absorption spectrophotometer and to the volunteer students (Claire, Amanda, and Ayden) who assisted in taking care of our fish. This work could not have been accomplished without the financial support of NSERC to J.M.W and OGS to myself.

Finally, I would like to thank my parents for their continuous love and support, and to Josh, who has been my rock throughout this entire process and has provided me with endless encouragement. Lastly, thank you to Sophie for being my therapy dog.

Table of Contents

List of Tables

List of Figures

Chapter 1:

Chapter 2:

Chapter 3:

Chapter 4:

Chapter 5:

Abbreviations

ANOVA	analysis of various
ASIC	acid-sensing ion channels
ATP	adenosine triphosphate
AUP	animal use protocol
BCA	bicinchoninic acid assay
BLAST	Basic Local Alignment Search Tool
BSA	bovine serum albumin
cDNA	complementary deoxyribonucleic acid
Cl^-	chloride ion
CO_2	carbon dioxide
CsCl	cesium chloride
CT	cycle threshold
DAPI	4,6-Diamidino-2-phenylindole, dihydrochloride
DIC	differential interference contrast
DiH_2O	deionized water
DNA	deoxyribonucleic acid
ECL	enhanced chemiluminescence
EDTA	Ethylenediaminetetraacetic acid
ELISA	enzyme-linked immunosorbent assay
FASC	formic acid and sodium citrate solution
gHKA	gastric H^+/K^+-ATPase
H_2O_2	hydrogen peroxide
H_2SO_4	sulfuric acid
H^+	proton or hydrogen ion
HCO_3^-	bicarbonate ion
HKA	H^+/K^+-ATPase

IMRC	intercalated mitochondrion rich cell
K^+	potassium ion
K_m	Michaelis-Menten constant
MRC	mitochondrion rich cell
MS222	tricaine methanesulfonate
Na^+	sodium ion
NaCl	sodium chloride
$NaHCO_3$	sodium bicarbonate
ngHKA	non-gastric H^+/K^+-ATPase
NKA	Na^+/K^+-ATPase
PBS	phosphate buffered saline
PCO_2	partial pressure of carbon dioxide
PCR	polymerase chain reactions
PNA^-	peanut lectin – insensitive
PNA^+	peanut lectin – sensitive
PVDF	polyvinylidene difluoride membrane
qPCR	quantitative polymerase chain reaction
Rb^+	rubidium ion
RbCl	rubidium chloride
RIPA	radioimmunoprecipitation assay buffer
RNA	ribonucleic acid
RO	reverse osmosis
ROMK	renal outer medullary potassium channel
SDS-PAGE	sodium dodecyl sulfate polyacrylamide gel electrophoresis
S.E.M	standard error of the mean
SEI	sucrose EDTA imidazole buffer
SEID	sucrose EDTA imidazole buffer with sodium deoxycholate
TBE	tris base, boric acid and EDTA buffer solution

TPBS	phosphate buffered saline with tween
TSA	tyramide signal amplification
TTBS	tris buffered saline with tween
V-ATPase	vacuolar type proton ATPase
V_{max}	maximum rate of enzyme reaction

Chapter 1:
General Introduction

INTRODUCTION

1.1 Overview of Fish Osmoregulation

Aquatic animals are faced with dealing with steep osmotic gradients across their body surfaces. Fishes living in seawater need to actively compensate for the gain of ions and loss of water in order to maintain homeostasis, whereas fishes living in freshwater have the opposite challenge; they need to actively compensate for the diffusive loss of ions and osmotic gain of water (Marshall and Grosell, 2006). The gill is the primary organ for ion regulation in fishes and contains ionocytes with an array of ion transport proteins which meet their ion regulatory needs (Evans et al., 2005; Hwang et al., 2011). Ionocytes are specialized cells responsible for ion transport (Wilson, 2011). Other osmoregulatory organs include the kidney, intestine, and skin (Marshall and Grosell, 2006). Ion loss in freshwater is balanced by active uptake mechanisms in the gill epithelium and ion gain from the diet (Marshall and Grosell, 2006). Ion loss in the urine of freshwater fish is minimized by tubular reabsorption of ions and glomerular filtration resulting in a dilute urine (Marshall and Grosell, 2006).

The primary ion transport proteins in the fish gill are Na^+ /K^+- ATPase (NKA) and the vacuolar type proton ATPase (V-ATPase) which use ATP to drive ion transport against unfavourable gradients using sodium (Na^+) and proton (H^+) motive forces, respectively (Evans et al., 2005). The NKA is a basolateral electrogenic pump that pumps two potassium ions (K^+) into the cell in exchange for three Na^+ ions being pumped out (Blanco and Mercer, 1998) and is one of the largest consumers of ATP (Skou, 1957). The V-ATPase is a vacuole type electrogenic proton pump that can be found in either apical or basolateral membranes in fishes (Lin and Randall, 1995; Evans et al. 2005). There are other ATPase type pumps,

and one of interest is the hydrogen/potassium (H^+ /K^+)-ATPase (HKA) which is central to stomach acidification (Shin et al., 2009) and renal acid-base and K^+ regulation in mammals (Gumz et al., 2010).

1.2 The Fish Gill

The gill not only evolved as a main respiratory organ in vertebrates, it is also the site of ion and acid-base regulation, and nitrogenous waste excretion (Evans et al., 2005). In lamprey the gills consist of seven branchiopores (in larvae) and gill pouches (in adults) protected by skin, while teleost fish have four pairs of holobranch filaments covered by an operculum (Evans et al., 2005). African lungfish have reduced gills and a well-developed lung (Glass, 2010). Their gills have fewer filaments and secondary lamellae (Laurent et al., 1978). In teleosts and lungfish, water enters through the mouth and passes over the filaments (unidirectional flow). In larval lamprey, unidirectionally ventilated gills are still used but in juvenile and adult lamprey the mechanism is different due to the fact that when they are feeding and attached to prey or other substrate, unidirectional ventilation is not an option (Youson and Potter, 1979; Lewis, 1980). Instead, post metamorphic lamprey switch to tidally ventilating their gills by using musculature in their gill pouches to move water in and out of their gills (Evans et al., 2005).

The gill epithelium is made up of two major cell types, pavement cells which cover more than 90% of the total area, and mitochondrion-rich cells (MRCs) (sometimes referred to as chloride cells or ionocytes), which cover approximately 10% of gill epithelium (Evans et al., 2005). Pavement cells are generally considered to play a passive role in physiological processes and do not contain a large amount of mitochondria or expansion of their basolateral membrane (Laurent and Dunel, 1980). However, in freshwater fish, it has been

shown that pavement cells are rich in V-ATPases (Galvez et al., 2002). In contrast, like the name suggests, MRCs contain large amounts of mitochondria as well as having an expansion of their basolateral membrane through folding (basal labyrinth or tubular system) (Wilson, 2011). These cells play a role in the majority of active physiological processes and are often found on the afferent edge of filaments and interlamellar regions (Evans et al., 2005). Different subtypes of MRCs exist for various environmental functions including changes in salinity (Evans et al., 2005). For example, in adult anadromous lamprey, two types of MRCs have been characterized, a distinct freshwater type, and a distinct saltwater type while the larval lamprey have a distinct ammocoete MRC not found in the adults (Bartels et al., 1996; Bartels et al., 1998; Bartels and Potter, 2004). Little information is known about the cell types and distribution in gill epithelium on lungfish. However, MRCs, the same cells found in the gill were characterized in the skin of *Protopterus annectens* (Sturla et al., 2001).

1.3 Mechanisms of Freshwater Ion Regulation

Fish in freshwater deal with osmotic challenges by reabsorbing ions and excreting dilute urine using the kidney and by actively taking up ions at the gills. To date there are still conflicting results and ideas regarding ion regulation in fishes that is most likely dependent upon species differences and environmental factors (Evans, 2011). Recently it was thought that Na^+ uptake was either through a Na^+/H^+ exchanger or through a Na^+ and Cl^- cotransport (Evans, 2011). However, a more recent study found that acid-sensing ion channels (ASIC) play a role in Na^+ uptake and are localized in NKA rich cells in rainbow trout gill (Dymowska et al., 2014). There is also evidence that the apical V-ATPase and Na^+/H^+ exchanger are involved in acid secretion (Evans, 2011). Cl^- is thought to be taken

up by a Cl^-/HCO_3^- exchanger driven by a basolateral V-ATPase (Evans, 2011). There are two subtypes of MRCs, peanut lectin – insensitive (PNA^-) and peanut lectin – sensitive (PNA^+). PNA^- type have more V-ATPase activity and co-location of Na^+ channels and V-ATPase pumps. The PNA^+ cells have high levels of NKA and about half the amount of V-ATPases as PNA^- cells (Glavez et al., 2002; Reid et al., 2003; Marshall and Grosell, 2006). Carbonic anhydrase catalyzes carbon dioxide (CO_2) hydration to provide intracellular H^+ and HCO_3^- ions for the pumps (Gilmour et al., 2007). See current model Figure 1.1.

1.4 Potassium and Acid-base Regulation

Homeostasis of extracellular K^+ is often overshadowed by the dominant ions, Na^+ and Cl^-. The majority of K^+ (98%) is intracellular due to active uptake by the NKA and a small change in K^+ distribution can cause dramatic extracellular changes in K^+ levels (Weiner and Wingo, 1997). In fishes, K^+ flux rates are only 3-5% of Na^+ and Cl^- (Eddy, 1985), nonetheless homeostasis of K^+ is essential in the control of the excitability of nerve and muscle cells. A small change in plasma K^+ concentration can have dramatic, adverse effects such as muscles not functioning properly due to nerve signals not firing (Crambert, 2014). With low K^+ levels, neurons can lose their ability to depolarize which is necessary for end plate potentials (Weiner and Wingo, 1997).

In mammals, low potassium diets are often linked to hypertension and hypokalemia (low blood $[K^+]$) impairs insulin release (Weiner, and Wingo, 1997). The mechanism is not fully understood, but is thought to be caused by a retention of renal Na^+ (Krishna and Chusid, 1987; Weiner and Wingo, 1997). Hypokalemia also inhibits aldosterone secretion which is important for the regulation of blood pressure and regulation of NKA production

(Weiner and Wingo, 1997). In mammals it is known that the HKA in the collecting duct of the kidney reabsorbs K^+ and secrets H^+ (Weiner and Wingo, 1998).

K^+ balance is largely met by diet in fishes (Bucking and Wood, 2006) but can also be actively taken up against electrochemical gradients from the water (Eddy, 1985). The non-dietary route would be important during periods of fasting such as during overwintering, spawning, and migration. However, there is currently no mechanism explaining K^+ uptake in fish although K^+ efflux in fish has been linked to K^+ channels K_{cnj1} (Abbas et al., 2011) and renal outer medullary potassium (ROMK) channels (Furukawa et al., 2012). Furukawa and colleagues (2012) studied ROMK channels in gill MRCs in the Mozambique tilapia. ROMK was localized at the apical side of gill MRCs and mRNA expression levels increased during high external K^+ (Furukawa et al., 2012).

In mammals, acidosis is often linked to hyperkalemia by causing a decrease in K^+ secretion and an increase in K^+ reabsorption in the collecting duct of the kidney (Stanton and Giebisch, 1982; Weiner and Wingo, 1997). As such, K^+, and acid-base balance are often linked (Hamm et al., 2013). Acid-base regulation is extremely important for a body system and any deviations away from the normal range can be devastating to cells because their enzymes cannot function properly. Metabolic alkalosis causes a stimulation of both gastric and non-gastric isoforms of the HKA in the kidney proximal tubule (Wingo and Smolka, 1995). Low K^+ levels can also effect acid-base homeostasis by inhibiting aldosterone secretion and aldosterone is important for the secretion of H^+ via the V-ATPase in the kidney (Weiner and Wingo, 1997).

In air breathing animals, acid-base balance is in part maintained through ventilation. For example an increase in breathing during metabolic acidosis raises pH by reducing

arterial PCO_2 (Gilmour et al., 2007). Air breathing animals also use their kidneys as a mechanism for acid-base disturbances (Heisler, 1986; Swenson, 2000; McNamara and Worthley, 2001). However, in fish, acid-base balance is controlled at the metabolic level (for reviews, see Goss et al., 1998; Claiborne et al., 2002; Hirose et al., 2003; Perry et al., 2003; Evans et al., 2005; Perry and Gilmour, 2006) because water breathers have a limited capacity to adjust pH by ventilation due to low plasma PCO_2 compared to tetrapods (Perry and Gilmour, 2006; Hwang et al., 2011). Conversely, lungfish have high PCO_2 (20-30 mmHg) for fish because their gills are ventilated by low volumes of water, have a low surface area, and high blood to water diffusion distance (Lenfant and Johansen, 1968; Perry et al., 2005).

The gills play a major role (90%) in acid-base transfers in fish, while the remainder is accounted for via the skin and kidney (Evans et al., 2005). The fish gill has a remarkable ability to respond to acid-base disturbances within hours (Evans et al., 2005). In the case of acidosis, this is done by increasing plasma HCO_3^-, used as a buffering system as well as increased output of acidic equivalents (H^+) to the environment (Gilmour et al., 2007). Teleost fish can correct for acid-base disturbances by manipulating Na^+ and Cl^- fluxes in order to trigger H^+ and HCO_3^- effluxes (Goss et al., 1992). Fish may be faced with acid-base perturbations through external changes in nature such as pH, salinity, temperature or internally though lactic acid build up during prey capture, predator avoidance or migration as well as hypercapnia (Heisler, 1989; Evans et al., 2005). Studying ion transport and acid-base molecules together is important in order to potentially reveal the integrated response (Marshall and Grosell, 2006).

1.5 H^+ /K^+-ATPase

The HKA, like the NKA is a heterodimer consisting of an α and β subunit (Bublitz et al., 2011). The α-subunit contains the functional properties of the pump whereby ATP hydrolysis is used to drive the exchange of intracellular H^+ for extracellular K^+ and is ~100kDa in size. The β subunit is thought to play a role in structural stability (Shin et al., 2009). There are two types of HKAs, the gastric HKA (gHKA) and the non-gastric HKA (ngHKA).

The gHKA is responsible for stomach acidification in all vertebrates (Koelz, 1992; Shin et al., 2009). It is composed of HKα1 (gene: *atp4a*) and HKβ (gene: *atp4b*) subunits and is electroneutral with stoichiometry changing with the pH gradient; $2H^+$: $2K^+$: 1ATP at neutral pH to $1H^+$: $1K^+$: 1ATP at pH < 3 (Shin et al., 2009). The gHKA undergoes phosphorylation and a conformational change to pump protons out and is dephosphorylated to return the enzyme to its original conformation (Shin et al., 2009). In its resting state, the pump is localized to the cytoplasmic tubulovesicular system and once acid secretion is stimulated, the tubulovesicular elements fuse with the apical membrane canaliculi for acid secretion (Forte et al., 1983; Galmiche et al., 2004). The gHKA has been localized in the stomach gastric glands and gills of the Atlantic stingray (Smolka et al., 1994; Choe et al., 2004) In the gill, apical HKα1 was found to colocalize in cells with basolateral NKA but not in cells that stained for V-ATPase (Choe et al., 2004). Hypercapnia (high water CO_2 levels) did not change gill gHKA transcript expression, but transcription level expression was increased during saltwater to freshwater acclimation suggesting that gHKA plays an important role in acclimation to a hypotonic environment (Choe et al., 2004).

The ngHKA is known to play a role in renal K^+ maintenance in mammals (Crambert, 2014; Hamm et al., 2013) and is composed of a HKα2 alpha subunit (gene: *atp12a*) and a β subunit, although not specific to the ngHKA (Fig. 1.2). The electrogenicity of the ngHKA is currently unknown but is thought to depend on the presence of a lysine in the fifth transmembrane domain (Crambert, 2014). The ngHKA has been found in the collecting duct of the kidney as well as the thick ascending limb and connecting tubule in rats and mice in addition to skin, colon, choroid plexus, and epididymis (Crambert, 2014). Previous studies have shown an increase in renal mRNA expression of ngHKA in rats fed a diet low in potassium (Crambert, 2014). The ngHKA (HKα2) also appears to play a role in acid-base regulation as mRNA expression levels were increased after multiple days of acid loading in mice (Crambert, 2014). Currently nothing is known about ngHKA in fishes apart from their confirmed expression in lungfish and lamprey (JM Wilson, personal communication) (Fig. 1.3).

1.6 Verifying the Presence of the *atp12a* Gene

The full length genome sequences of sea lamprey, *Petromyzon marinus* and African lungfish, *Protopterus annectens atp12a* (HKα2) have previously been determined in the lab (JM Wilson, personal communication). PCR (polymerase chain reaction) using degenerate primers was initially performed to determine if lungfish and lamprey express the *atp12a* gene. Using a RACE (rapid amplification of cDNA ends) strategy, the full length sequence was obtained. Next, a phylogenetic analysis using BLAST (Basic Local Alignment Search Tool) search and gene tree construction (Maximum likelihood MEGA 7) was performed in order to determine the relationship of the lamprey and lungfish genes to the *ATP12A* clade. They were found to be highly related. Monoclonal and polyclonal

antibodies were generated against synthetic peptide from HKα2 sequences (Abmart Inc., China; and David's Biotechnogie, Gmbh. Germany, respectively). These antibodies were tested and validated using immunohistochemistry and Western blotting as described in Wilson et al. (2007) and Wright et al. (2014). Results from PCR indicate that gill and kidney are the tissues of highest expression in both species. Gill is the main osmoregulatory organ in fish and thus was investigated further. PCR gives an idea of what is going on at the transcript level but does not necessarily reflect what is going on at the protein level and how the gene of interest is actually functioning as a protein. This is why immunohistochemistry and Western blotting were used to further support the PCR results.

1.7 Hypothesis and Objectives

My thesis will address the central hypothesis that the ngHKA plays a role in K^+ and acid-base regulation in non-teleost fishes. It will also provide some insight into the evolutionary of HKA across fish taxa. Studies involving the ngHKA have received very little attention due to its species and tissue specific variability, a lack of tools to measure expression, and the difficulty of measuring expression as there is no specific inhibitor (Crambert, 2014). The ngHKA is present in non-teleost fishes therefore larval sea lamprey (*Petromyzon marinus*) (Chapter 3) and African lungfish (*Protopterus annectens*) (Chapter 4) were used as model species. The objectives for my thesis were to:

1. Develop and validate the tools necessary for studying ngHKA in lamprey and lungfish (Chapter 2). Since the antibodies have never been used and lamprey and lungfish are both non-established model species, I first had to validate the custom designed ngHKA antibodies.
2. Characterize tissue expression and localization of the ngHKA (Chapters 3 & 4).

3. Examine the physiological role of ngHKA by determining if acid-base perturbations or K^+ challenges modulate expression of ngHKA in gill tissue (Chapters 3 and 4). Altering acid-base and K^+ levels and looking at the effects on expression may provide an indication of the functional role of the ngHKA.
4. Determine if estivation in lungfish has an effect on protein expression levels of ngHKA in the gill (Chapter 4).

A variety of techniques were used in this study, from cellular and molecular strategies, to whole animal ion fluxes, in order to gain knowledge about the role of the ngHKA. Tissue characterization was performed using Western blotting and immunohistochemistry techniques. K^+ was manipulated by comparing fasted (K^+ deficient) and fed animals. Acid and base loads were injected in to the animal to test for an acid-base regulatory role. Western blotting and immunohistochemistry was then completed for all experimental treatment animals. Rb^+ uptake and acid flux was performed to complement the protein expression and localization data. Transcript level (mRNA) expression was also done for all treatments. It was predicted that the fasted animals would upregulate expression of ngHKA and/or change localization patterns, with an increased K^+ uptake rate, while excess K^+ (fed) animals would be expected to have the opposite effect (or decreased effect). Experimental acid and base disturbances should elicit a response if the ngHKA is involved with acid-base regulations. It was predicted that animals injected with acid would upregulate expression of ngHKA and/or change protein localization, with an increased net acid efflux (and thus parallel increase in Rb^+ uptake) while base loading in fish would have the opposite effect.

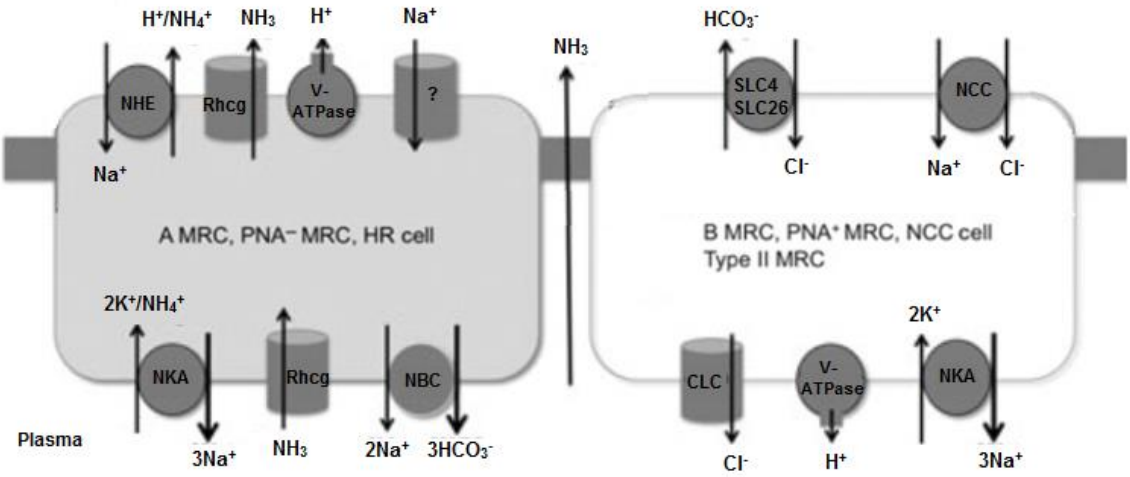

Figure 1.1: Working model for osmoregulation in freshwater fish gill from Evans 2011. Two mitochondrial rich cells (MRC) are shown, PNA^- and PNA^+. NHE: Na^+/H^+ exchanger, Rhcg: rhesus glycoprotein, V-ATPase: vacuolar type proton ATPase, SLC4/SLC26: Cl^-/HCO_3^- exchanger, NCC: Na^+ and Cl^- cotransporter, NKA: Na^+/K^+-ATPase, NBC: Na^+ and HCO_3^- cotransporter, and CLC: Cl^- channel. Circles represent active transport. The actual distribution of these pumps in various cell types are still under debate and vary depending on species and environmental factors.

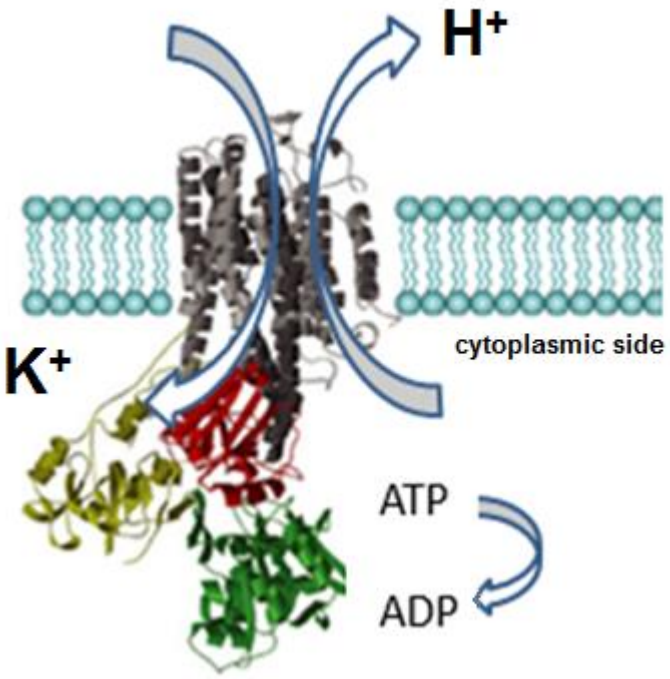

Figure 1.2: Structural representation of the non-gastric H^+/K^+ ATPase which is found in the apical membrane. Proton (H^+) ions are exchanged for potassium (K^+) ions against their concentration gradients using the energy from ATP hydrolysis (modified using structural model of related P-type ATPase NKA from Kühlbrandt 2004).

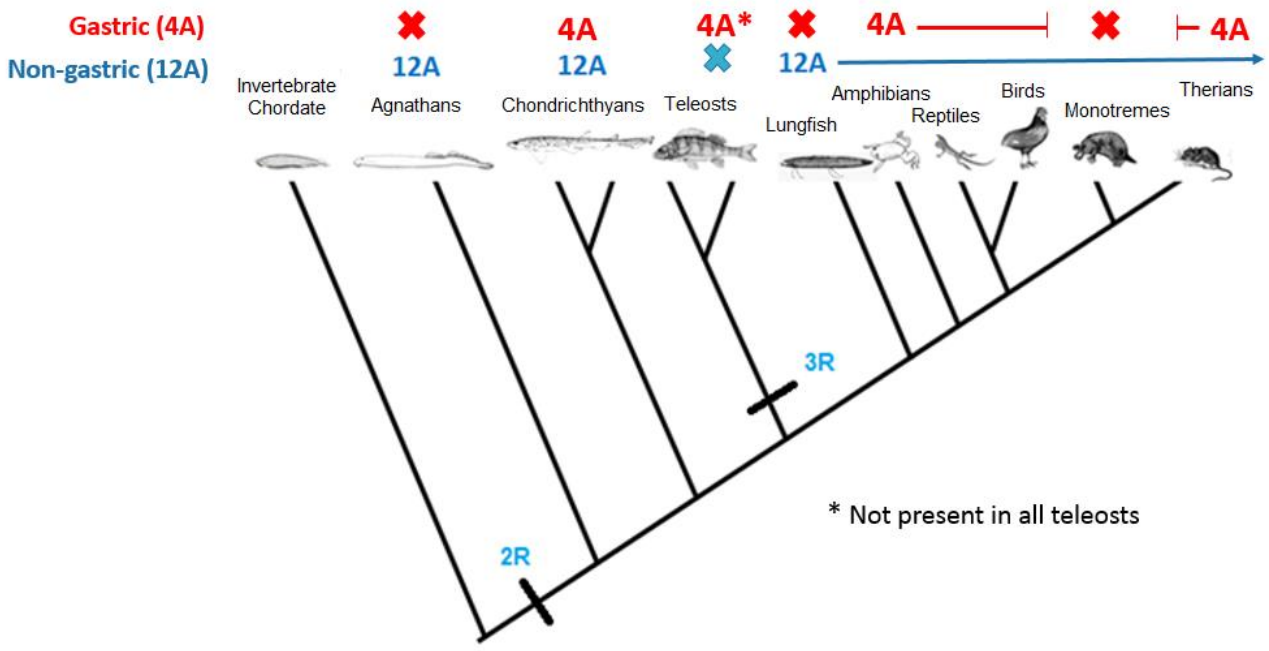

Figure 1.3: The vertebrate lineage showing the genes associated with H^+/K^+-ATPase (HKA). The *atp12a* (12A) gene corresponds to the non-gastric HKA α subunit and the *atp4a* (4A) gene corresponds to the gastric HKA α subunit. The 2R and 3R represent rounds of whole genome duplication found in the vertebrate and teleost ancestors, respectively. "X" represents genomic loss or absence of the *atp4a* or *atp12a* gene.

Chapter 2:
Antibody Validation and Methodological Development for Studying the Non-gastric H^+/K^+-ATPase

ABSTRACT

Antibodies are a fundamental tool for studying proteins because they can be highly specific probes for studying both localization (immunohistochemistry) and expression levels (Western blotting). However, antibodies first need to be validated. To date, the non-gastric H^+/K^+-ATPase (ngHKA) has not been studied in fish. The goal of this thesis was to understand the role of the ngHKA in non-teleost fishes, and thus firstly, tools (i.e. antibodies) had to be validated in order to study the ngHKA. In this chapter, I explain the various steps necessary for antibody validation, as well as the different modifications in each technique and what was successful for the validation of the ngHKA antibody (LF12Arb2).

2.1 INTRODUCTION

Antibodies are a commonly used research tool and can complement other techniques for studying proteins such as Western blotting, enzyme-linked immunosorbent assay (ELISA), immunoprecipitation, and immunohistochemistry (Harlow and Lane, 1999; Bordeaux et al., 2010). An antigen is the foreign substance that causes an immune response and the epitope is a specific region on the antigen that the antibody binds. For the first immunological studies of ion transport protein in fish, the first source of antibodies were against biochemically purified proteins (e.g. Rahim et al., 1988, Witters et al., 1996). However this can be time consuming and purity can be an issue. Now with the use of DNA sequencing, predicted protein sequences can be used to generate synthetic peptides or recombinant proteins. In my research, I used antibodies that were generated against synthetic peptides. The benefit of this technique is that you can use a computer assisted

strategy to predict the best antigenic peptide (e.g. Abdesigner https://hpcwebapps.cit.nih.gov/AbDesigner/), which can then be screened for specificity and you can chose one that is as unique as possible to the protein of interest for antibody generation (Grant, 2002). Once the antibodies are collected and purified, the next step is to validate them to ensure they are specific, selective, and reproducible. There has been no universal guidelines for antibody validation. However, Bordeaux and colleagues (2010) have described what they believe to be the best procedure for proper antibody validation.

Often times, antibody validation can be complicated due to the large number of methodological factors and all the different combinations arising from those factors that may be antibody and tissue specific impacting the outcome of the results (Bordeaux et al., 2010). These include such things such as sectioning types, fixation mediums, tissue processing, buffer compositions, polyclonal versus monoclonal antibodies, antigen retrieval steps, dilutions, incubation times, blocking reagents, and detection methods (Table 2.1) (Harlow and Lane, 1999; Wilson, 2007; Bordeaux et al., 2010).

There are two major antibody types, monoclonal and polyclonal. Monoclonal antibodies are from one cell line specific for one epitope while polyclonal antibodies can recognize multiple epitopes of an antigen (Harlow and Lane, 1999). Monoclonal antibodies are very specific and potentially create less background but sometimes do not give good signal strength because the epitope and antibody affinity is not high enough. Polyclonal antibodies, which are essentially a mix of monoclonal antibodies, provide stronger signals but sometimes have high background or non-specific binding (Harlow and Lane, 1999).
Due to processes such as post-translation modifications and differences in three dimensional conformation, knowing the amino acid sequence does not guarantee that the

antibody will work (Bordeaux et al., 2010). The antibody binding may also favour one technique over another, for example an antibody may work well for Western blotting (denatured state) and not so well for immunohistochemistry (native state) (Wilson, 2007; Bordeaux et al., 2010). Additionally, the opposite may be true, the antibody may work well on a protein in its native state conformation and not work well in its denatured form. Also, an epitope may be masked in its native state and become available only once denatured. (Bordeaux et al., 2010; Willingham, 1999). Controls are always important to run in order to assess the specificity of the observed staining (Wilson, 2007).

There are several different techniques that can be added to standard Western blotting and immunohistochemistry protocols to further improve the results. For Western blotting, immunoprecipitation is a powerful technique to concentrate proteins that are present in low abundance and can also be used as a control to check for cross-reactivity with other closely related proteins (Harlow and Lane, 1999). A technique that can be added to the regular immunohistochemistry processing that increases sensitivity of weak staining is known as tyramide signal amplification (TSA) (Wang et al., 1999) which is an ultrasensitive detection method. It allows for antibody dilutions to be increased while maintaining low background signals (Adams, 1992), helps brighten weak staining caused by harsh fixation procedures or simply low levels of target expression (Hunyady et al., 1996; Van Heusden et al., 1997). Additionally, antigen retrieval through the use of detergents such as sodium dodecyl sulfate (SDS) (Brown et al., 1996) and heat with additives such as citraconic anhydride (Namimatsu et al., 2005) have significantly increased staining performance of many antibodies (Wilson, 2007; Shi et al., 1993). Another alternative to paraformaldehyde processing is cryostat sectioning using frozen

tissue, which is less harsh on the tissue compared to paraffin embedding (heat and chemical processing) and therefore helps preserve epitope binding sites. Because there is currently no standardization for antibody validation, it is ultimately up to the researcher to go through proper validation steps (Bordeaux et al., 2010).

One of the main reasons why the non-gastric H^+/K^+-ATPase (ngHKA) has received very little attention in non-mammalian species is because there have been no antibodies designed to study this protein (Crambert, 2014). In this chapter, I go through all the steps and protocols that were attempted in order to validate an antibody for the ngHKA and explain what worked and what did not. This included the techniques of Western blotting, immunoprecipitation, and immunohistochemistry using antigen retrieval and tyramide signal amplification.

2.2 MATERIALS AND METHODS

2.2.1 Antibodies

Six mouse monoclonal antibodies (P12 and P14; *P.marinus*, P16, P19/P20, P21, and P22; *P. annectens*) (Abmart Inc, China) (Table 2.2) were tested on gill and kidney of *P.marinus* and *P. annectens* at various dilutions ranging from 1:200 – 1:20 000 for both Western blotting and immunohistochemistry. Four rabbit polyclonal antibodies (Pm12Arb1 and Pm12Arb2; *P.marinus*, LF12Arb1 and LF12Arb2; *P. annectens*) (Davids Biotechnologie GmbH, Germany) (Table 2.2) were also tested on various *P.marinus* and *P. annectens* tissue at a dilution of 1:1000 for both Western blotting and 1:500 for immunohistochemistry. The commercial, well validated antibodies used were the α5 (1:1000) mouse monoclonal, for the Na^+/K^+-ATPase (NKA) α subunit, developed by

Douglas Fambrough (Johns Hopkins University) (Takeyasu, 1988). This antibody was obtained as culture supernatant from Developmental Studies Hybridoma Bank, University of Iowa under contract N01- HD-7-3263 from National Institute for Child Health and Human Development (NICHD). In addition, the αR1 antibody (1:1000), a rabbit polyclonal anti-peptide antibody against NKA α subunit was used (Ura et al. 1996; Wilson et al., 2007) and the B2 antibody (1:500), a rabbit polyclonal anti-peptide antibody against the V-ATPase B subunit (Wilson et al., 2007). A mouse tubulin monoclonal known as 12g10 (1:200) was used as a reference protein for Western blotting (Developmental Studies Hybridoma Bank, University of Iowa, Iowa City, IA, USA, under contract N01-HD-7-3263 from the National Institute of Child Health and Human Development). For Western blotting, the secondary antibodies were the appropriate (anti-mouse or anti-rabbit) horseradish peroxidase conjugated secondary antibody (Novus Biologicals, Littleton, CO). For immunohistochemistry the secondary antibodies used were goat anti-rabbit Alexa Fluor 488 and goat anti-mouse Alexa Fluor 568 conjugates (Life Technologies). For Western blotting antigen pre-absorption negative controls were run. For immunohistochemistry negative controls, equivalently diluted isotyped culture supernatant known as J3 was used for mouse monoclonals, as well as LF12Arb pre-immune serum (Davids Biotechnologie GmbH, Germany) control were also run.

2.2.2 Tissue Preparation

Western blotting

Tissues were flash frozen in liquid nitrogen and stored in SEI (sucrose EDTA immidazole) buffer at -80°C. Sodium deoxycholate was added to a final concentration of

0.1% just prior to homogenization from a 3x SEID stock solution. Tissues were also flash frozen and stored in 1.5 mL centrifuge tubes and radioimmunoprecipitation assay (RIPA) buffer was added just prior to homogenization. Samples were homogenized with a Precellys 24 bead homogenizer (Bertin) (6800 2x15s with a 30s pause) and centrifugation (14 000 xg for 15 mins at 4°C). Three hundred µL of supernatant was then mixed with an equal volume of 2x Laemmli's buffer, heated at 70°C for 10 mins, and stored in the fridge. Remaining supernatant was used for a BCA Protein Assay (G-Biosciences, St. Louis USA). The protein concentrations of the samples in Laemmli's buffer were then adjusted to 1µg/µl.

Immunohistochemistry

Gill tissue were placed in embedding cassettes in 3% paraformaldehyde, phosphate buffered saline (pH 7.4) fixative for 24 hours. Gills were then transferred to FASC decalcification solution (30% formic acid 13% sodium citrate) for 48 hours, and then transferred to 70% ethanol (histological grade) for at least 24 hours. Tissues were then embedded in paraffin using a Shandon Citadel 1000 processor (Thermo Scientific, Pittsburgh PA) (see Appendix A).

2.2.3 Western Blotting Protocol

Tissue protein expression levels were determined using SDS-PAGE (polyacrylamide gel electrophoresis) and Western blotting according to Wilson et al. (2007). Twenty µg of various tissue samples was loaded onto the 1.5mm discontinuous gels (4%T stacking gel and 10%T resolving gel). Gels were run using a Bio-Rad MiniPROTEAN® Tetra cell system (Bio-Rad, Hercules, CA) for 15 minutes at 75V and

then for 1 hour at 150V. Membranes were transferred to Immobilon PVDF membranes (pore size 0.45 µm, Millipore, Billerica USA) or Immu-Blot® PVDF membranes (pore size 0.2 µm, Bio-Rad) for 1 hour at 100V in a Hoefer TE22 transfer cell (Holliston, USA). The membranes were rinsed in TTBS (0.05% Tween-20 in Tris-buffered saline) and stained in Ponceau S (0.5% in 1% acetic acid) to confirm the transfer efficiency. Membranes were then rinsed again and blocked using 5% skim milk powder, 1% and 5% fish skin mucus, casein, or 1% and 5% BSA for 1 hour at room temperature. Membranes were then incubated with the primary antibodies in 1% BSA/TTBS with 0.05% sodium azide as a preservative. Various dilutions and incubations times were tried (1:200-1:5000, 1 h-overnight). Membranes were rinsed 3x in TTBS and placed in TTBS with appropriate secondary antibody for 1 h at room temperature. Membranes were rinsed and imaged using the c300 Azure Biosystems documentation system using enhanced chemiluminescence (ECL) (Clarity™ Western blotting substrate, Bio-Rad). Bands were quantified using Multi Gauge Software (V3.1 Fujifilm). The QL/pixel2 was subtracted from the grayscale pixel value of 65,535 and normalized to the tubulin control. Antigen pre-absorption negative controls were run (Appendix C for complete details).

2.2.4 Immunoprecipitation Protocol

Immunoprecipitation is a technique used to precipitate a protein antigen and to concentrate/purify low abundant proteins. Immunoprecipitation was done according to the Bio-Rad SureBeads™ Magnetic Beads for Protein A standard protocol. SureBeads were resuspended in their solution by vortexing, then magnetized, and the supernatant was discarded. Beads were washed and resuspended 3x with phosphate buffered saline (PBS)

and 3 µl of the antibody was added. Washing eliminates irrelevant molecules as the antibody-antigen complex are bound to the beads (Harlow and Lane, 1999). Again beads were washed 3 times. RIPA buffer was added to the frozen samples, homogenized, and centrifuged (same conditions as stated above) and the supernatant was added to the prepared SureBeads and antibody containing tube for 1 hour at room temperature. The beads were then washed and resuspended in 40 µl of 1x Laemmli's buffer and incubated for 10 min at 70°C. The beads were magnetized one last time and the sample in Laemmli's buffer was moved to a new tube and used for SDS-PAGE Western blotting.

2.2.5 Immunohistochemistry Protocol

Paraffin blocks were sectioned 5 µm thin using a Leica RM2125 RTS microtome and air dried and stored. Before use, slides were dewaxed at 60°C for 30 mins, placed in 3x xylene (5 min each), and rehydrated through an ethanol series to water (Appendix B). Antigen retrieval was performed using 0.05% citraconic anhydride pH 7.4 for 30 min in a boiling water bath (Namimatsu et al., 2005) and a 1% sodium dodecyl sulfate (SDS) in PBS soak (Brown et al., 1996). Immunohistochemistry was also performed without the antigen retrieval steps. Slides were rinsed in 3x DiH_2O following each antigen retrieval step and TPBS then blocked in either 5% normal goat serum with 1% BSA in TPBS, BlockAid™ (Molecular Probes by Life Technologies), or BLØK (Millipore, Temecula USA). Primary antibodies were incubated on the slides for various times (1 h at 37°C – overnight at 4°C) with a range of dilutions (1:500-1:5000). Secondary antibodies were applied for 1 h at 37°C. Sections were imaged using a LEICA DM5500 B microscope and Hamamatsu C11440 Orca-Flash 4.0 digital camera. A tyramide signal amplification (TSA)

(Life technologies, Carlsbad USA) technique was also tried according to manufacturer's instruction as an addition to the standard immunohistochemistry protocol using fluorophore (Alexa 555 or 488) conjugated secondary antibodies. A 2% hydrogen peroxide in PBS step is done after the SDS treatment for the TSA protocol. The block and primary antibody addition were the same. After the secondary antibody incubation (goat anti-rabbit or goat anti-mouse horseradish peroxidase conjugates), the TSA (Alexa Fluor® 488, Life Technologies, Carlsbad USA) is added to the sections for 10 minutes (1:100 TSA in amplification buffer/0.0015% H_2O_2) (Appendix B for complete details).

2.3 RESULTS

2.3.1 Western Blotting

The Abmart mouse monoclonal antibodies either did not detect bands of the correct predicted molecular mass or background immunoreactivity was very high obscuring any bands (Fig. 2.1). Varying antibody dilutions and blocking buffers did not make a difference, nor did differences in the incubations times or membranes used. The immunoprecipitation technique was successful for the mouse monoclonal antibody P19 (Fig. 2.2). There was a band for the immunoprecipitated membrane probed with P19, but none using the standard Western blotting technique. When the P19 immunoprecipitated membrane was probed with αR1 for the NKA, there was no band for the immunoprecipitation tissue, indicating no cross-reactivity with the NKA.

However, for the rabbit-polyclonal antibodies, two of the antibodies (LF12Arb1 and LF12Arb2) did immunoreact with bands in the 100 kDa size range. The strongest signal was detected in samples homogenized in RIPA buffer, transferred to the Immobilon

membrane and incubated overnight with LF12Arb2 antibody at 1:1000 dilution (Fig. 2.3) compared to all other combinations of variables (Table 2.1). The antibody pre-incubated with the peptide showed no signal or bands. The bands appeared stronger in lamprey compared to lungfish. Both species showed high expression in gill and kidney tissue. The Pm12Arb1 and rb2 failed to work for Western blotting.

2.3.2 Immunohistochemistry

The mouse monoclonal antibodies did not work using any variations of the immunohistochemistry technique including the TSA detection technique. With the standard immunohistochemistry protocol, there was high background and non-specific staining (Fig. 2.4). The various combinations of dilutions, blocking reagents, incubations times, antigen retrieval, or TSA did not appear to make a difference. The LF12arb2 antibody showed some promising staining from the standard protocol but there was also unexpected staining around the nuclei (Fig. 2.5). Staining was improved with a combination of the blocking reagent BLØK and TSA (Fig. 2.6). Primary antibodies were incubated overnight at 4°C and secondary antibodies for 1 h at 37°C. The negative control was the pre-immune serum that showed no staining comparable to the ngHKA antibody (Appendix E). Sections were double labelled with NKA which showed basolateral staining. The ngHKA showed staining in the entire epithelium in the majority of cells and no sharper apical staining in the controls for both lamprey and lungfish. The Pm12Arb1 and rb2 failed to work for immunohistochemistry.

2.4 DISCUSSION

The use of antibodies is an excellent tool to study proteins but since there are no set guidelines in place for suppliers to validate antibodies, it is ultimately up to the researcher to validate and run proper controls (Bordeaux et al., 2010), and to interpret results cautiously so that false conclusions are not drawn. Additionally, an antibody that works for one technique does not necessarily work for another and should be validated independently (Willingham, 1999).

The mouse monoclonal antibodies did not work for western blotting but since the immunoprecipitation technique did detect an immunoreactive band, it can be concluded that the ngHKA is either a low abundant protein or there are differences in antigenic sites (Wilson, 2007). The LF12Arb2 antibody did work for western blotting in both lamprey and lungfish, most likely due to the fact that this is a polyclonal antibody versus a monoclonal antibody thus providing more flexibility and variety in the epitope binding region. The LF12Arb2 antibody produced multiple bands on the blot. This is not surprising since Major et al. (2006) showed that 25% of 441 antibodies tested produced multiple bands. The presence of multiple bands in both lamprey and lungfish gill and kidney tissue could be from product degradation, different post-translational modification steps, or splice variants (Bordeaux et al., 2010). The antibody was confirmed to be specific for the ngHKA by not only the correct size marker, but by the complete disappearance of all bands when incubated with the excess antigenic peptide. Also, although the LF12Arb2 antibody was generated against a lungfish specific peptide, it still cross reacts with the lamprey protein. In lamprey 12 of 19 amino acids of the corresponding peptide are identical to the immunogenic peptide.

For both the monoclonal and polyclonal antibodies, the regular immunohistochemistry technique was not successful regardless of trying various dilutions, incubation times and conditions, or removal of certain processing steps. Tissue fixation processing techniques can be harsh and damage or mask the epitope, but are important to preserve the original structure of the tissue (Wilson, 2007). The tissue is processed in strong chemicals including paraformaldehyde and xylene. Cross reactivity is a common problem with immunohistochemistry because deparaffinised, heat antigen retrieval can expose new potentially misleading cross-reactivity that would not be seen by Western blotting a fresh lysate straight from the animal (Bordeaux et al., 2010). However, the removal of the antigen retrieval steps did not appear to decrease any of the non-specific staining. When the TSA technique was tried for both types of antibodies, the mouse monoclonal antibodies showed no promising results, while the rabbit polyclonal did. Therefore it can be concluded that the regular immunohistochemistry technique was a failure not because of the harsh processing on the tissue but most likely because of a low affinity of the antibody for the single epitope type. The TSA technique was successful in increasing the intensity of weak staining of the polyclonal (LF12Arb2) antibody and was validated by showing no staining in the pre-immune serum. In conclusion, even though the P19 mouse monoclonal worked using the immunoprecipitation Western blotting technique, this technique is not suitable or practical for semi-quantitative protein expression analysis. Therefore the LF12Arb2 antibody was chosen for both western blotting and immunohistochemistry.

Table 2.1: Variations of different steps used in Western Blotting and immunohistochemistry protocols

Step	Variation
Sectioning	Cryostat Paraffin Microtome
Fixation	Paraformaldehyde Frozen
Sample preparation buffer	SEI(D) RIPA
Antibody type	Monoclonal Polyclonal
Antigen retrieval	SDS Citraconic anhydride
Dilutions	1:200 – 1:20 000
Blocking reagents	Skim milk Casein Fish skin mucus Bovine serum albumin BLØK BlockAid
Incubations times	1 hour – 24 hours
Incubation temperatures	4°C – 37°C
Membrane type	PVDF (Immobilon or Bio-Rad) Nitrocellulose

Table 2.2: List of epitopes for mouse monoclonal antibodies (Abmart Inc, China) and for rabbit polyclonal antibody production (Davids Biotechnologie GmbH, Germany) for the non-gastric H^+/K^+-ATPase (*atp12a)* in *Petromyzon marinus* (Pm) and *Protopterus annectens* (Pa).

Target Protein	Type	Epitope sequence	AB name
ATP12A_Pm	Mouse monoclonal	DVDRMDKKGDNP	P12
		RKGLRAKWVGRQ	P14
ATP12A_Pa		EDAVTPPNDEKK	P16
		QSRSNEFTHDNP	P19/20
		YWENVNDHELED	P21
		RHPGSWYEQNMF	P22
ATP12A_Pm	Rabbit polyclonal	DKKGDNPGATCKKRKGLRAK	Pm12Arb1, rb2
ATP12A_Pa		KAESDIMNRKPRRKLQDRL	LF12Arb1, rb2

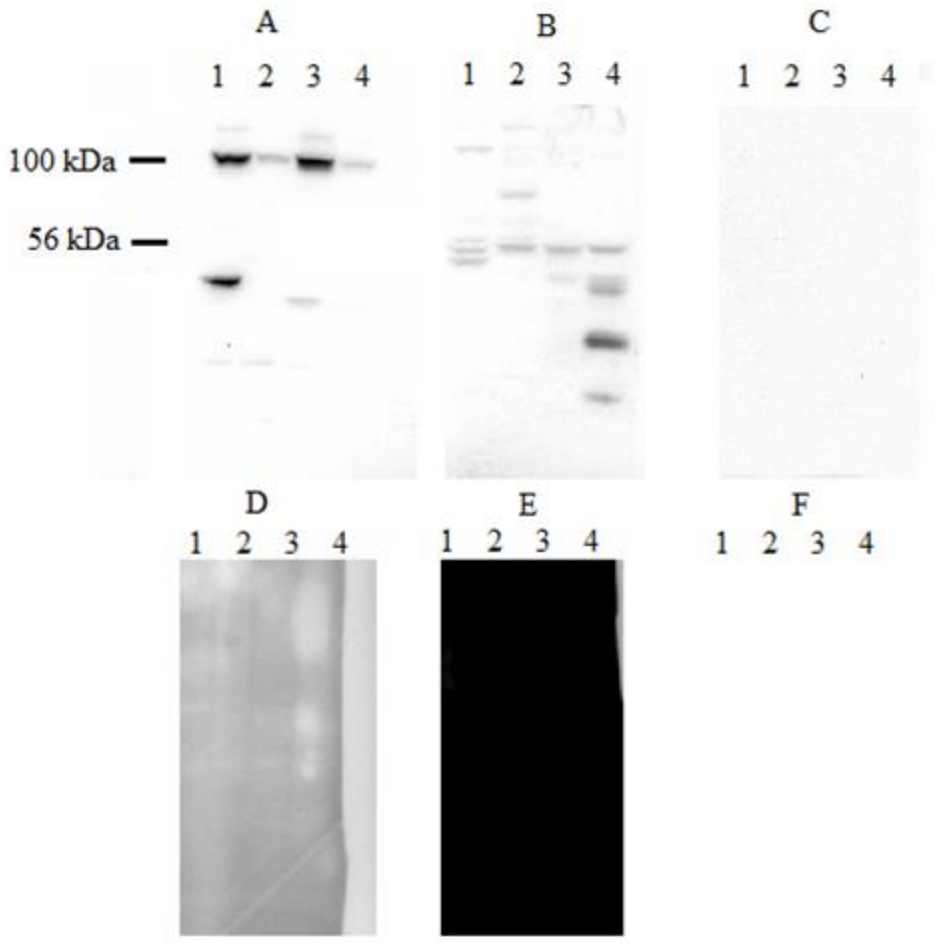

Figure 2.1: SDS-PAGE Western blot for various tissues in *Petromyzon marinus* and *Protopterus annectens.* The 1º antibodies used was αR1 1:1000 (A), B2 1:1000 (B), P19 1:1000 (C), P20 1:1000 (D), P21 1:1000 (E), and P22 1:1000 (F). The 2º was goat anti-rabbit or goat anti-mouse at 1:50 000. *P.marinus* kidney (lane 1), *P.marinus* gill (lane 2), *P. annectens* kidney (lane 3), and *P. annectens* gill (lane 4). Detection method is ECL.

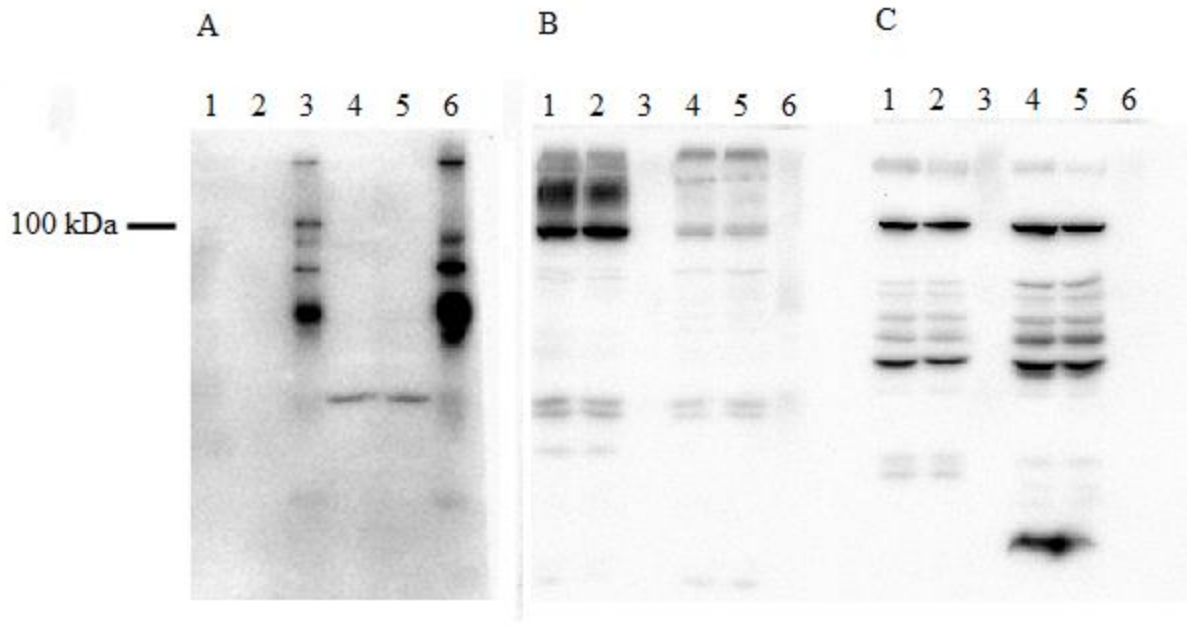

Figure 2.2: Immunoprecipitation of *Petromyzon marinus* kidney and gill samples with the mouse monoclonal P19 antibody. Blots were probed with (A) P19 (1:1000), (B) αR1 (1:1000) and (C) LF12Arb2 (1:1000). The 2º antibody was a goat anti-mouse-HRP (1:50 000) in A and goat anti-rabbit-HRP (1:50 000) in B and C. Kidney homogenate (lane 1), kidney preclearing (lane 2), kidney immunoprecipitation (lane 3), gill homogenate (lane 4), gill preclearing (lane 5), gill immunoprecipitation (lane 6). Detection method is ECL.

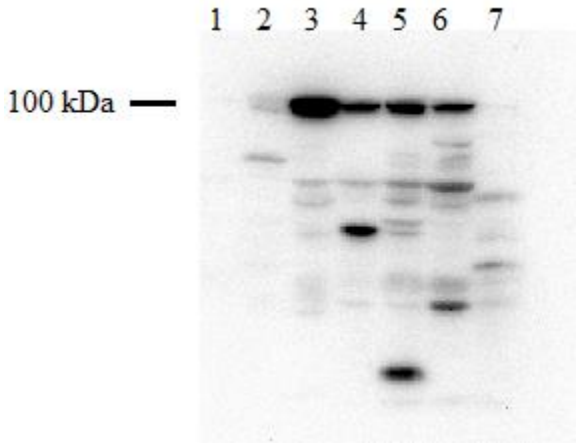

Figure 2.3: SDS-PAGE Western blot for *Petromyzon marinus* tissue. The 1º antibodies used was a rabbit monoclonal LF12Arb2 1:1000. The 2º was goat anti-rabbit (1:50 000). Brain (lane 1), muscle (lane 2), kidney (lane 3), skin (lane 4), gill (lane 5), liver (lane 6), intestine (lane 7). Detection method is ECL.

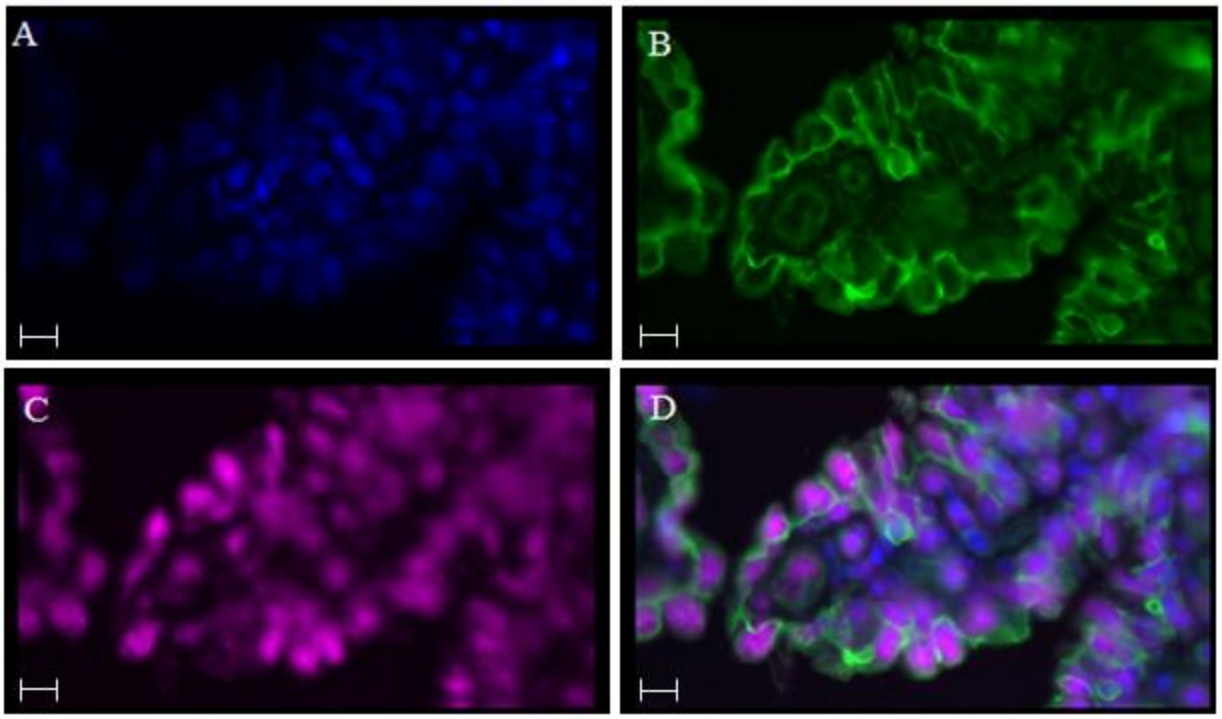

Figure 2.4: Immunohistochemistry of *Protopterus annectens* gill. Blue is DAPI staining the nuclei (A), green is the αR1 staining for the Na^+/K^+-ATPase (B) and fuschia is the P19 staining for the non-gastric H^+/K^+-ATPase (C). Panel D is the overlay of all three channels. Scale bar is 10 µm.

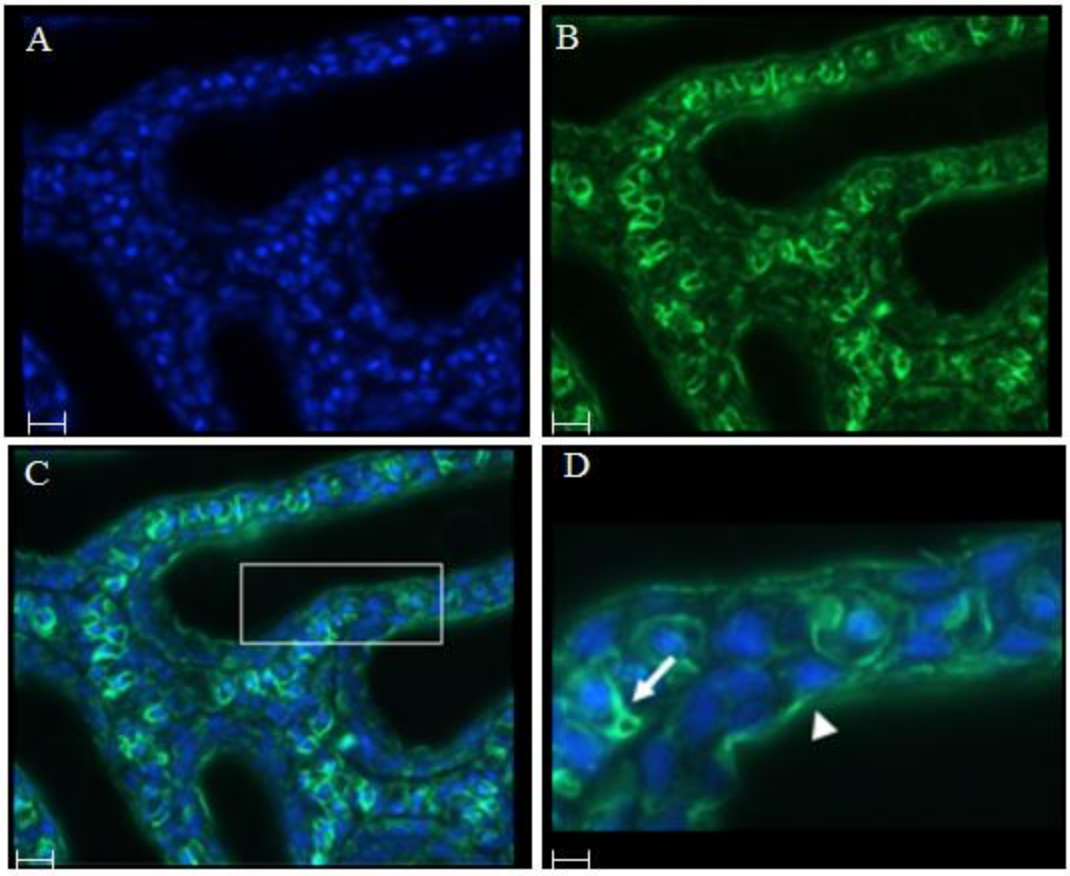

Figure 2.5: Immunohistochemistry of a larval *Petromyzon marinus* gill. Blue is DAPI staining the nuclei (A) and green is the LF12Arb2 antibody for the non-gastric H^+/K^+-ATPase (ngHKA) (B). Panel C is an overlay of the two channels and D is a magnified section of C. There is some ngHKA staining around the nuclei (arrow) and some epithelial staining (arrowhead). Scale bar is 20 μm A-C, 10 μm D.

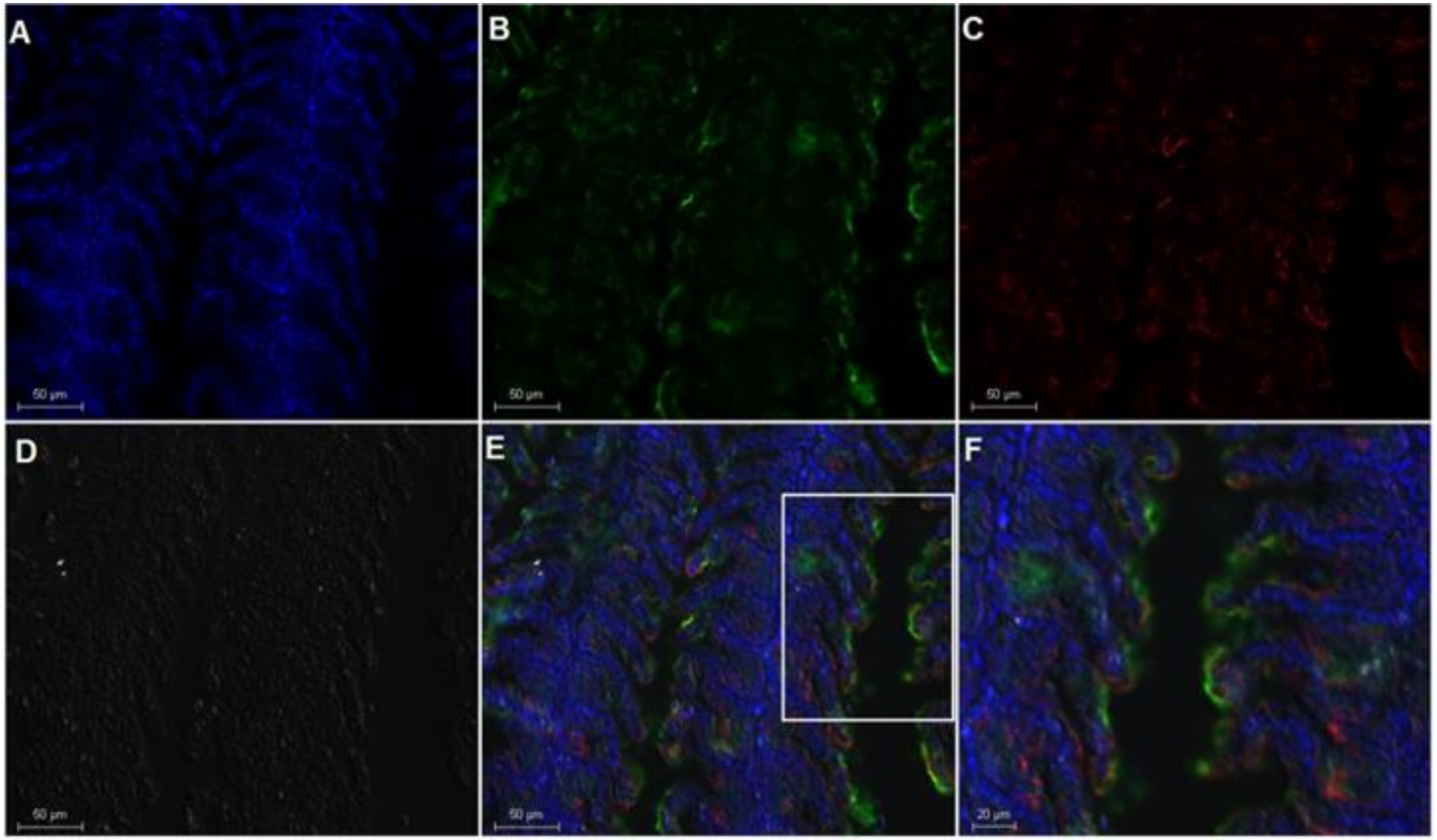

Figure 2.6: Immunohistochemistry of *Petromyzon marinus* gill. A) DAPI (blue), B) non-gastric H^+/K^+-ATPase (green), C) Na^+/K^+-ATPase (red), D) DIC, E) overlay of A-D, F) magnification of highlighted section in E. Scale bar 50 µm A-E, 20 µm F.

Chapter 3:
Potassium and Acid-base Regulation in the Larval Sea Lamprey (*Petromyzon marinus*): A Role for the Non-gastric H^+/K^+-ATPase?

ABSTRACT

Sea lamprey (*Petromyzon marinus*) begin their life cycle as filter feeding larvae in freshwater and then undergo a complicated metamorphosis into parasitic fish that feed on the blood of other fishes. Currently, there is no mechanism to explain branchial potassium (K^+) uptake in lamprey. It was hypothesized that an ion pump known as the non-gastric H^+/K^+-ATPase (ngHKA) plays a role in K^+ and acid-base regulation in lamprey. The objective of this chapter was to characterize the potential roles of the ngHKA in the larval sea lamprey by studying the pump's response to K^+ and acid-base disturbances through transcript level, protein expression, localization, and ion fluxes. Rubidium was used as a surrogate flux marker for K^+ and uptake was successfully measured, although fasted fish did not show increased uptake rates. Fed fish had a higher net acid uptake rate compared to fasted fish and acid loaded lamprey had a higher acid efflux compared to controls. However, there were no significant differences in transcript or protein expression of the ngHKA for any of the experimental treatments. Immunolocalization staining patterns were characterized and also did not change with treatments. This is the first study to investigate the ngHKA in the larval sea lamprey and although expressed in the gills, no evidence was found for an active role in K^+ uptake and compensation for acid-base disturbances.

3.1 INTRODUCTION

Of all jawless vertebrates, lamprey are one of the two groups that are still alive today. Sea lamprey (*Petromyzon marinus*) are osmoregulating anadromous fish that begin their life cycle in freshwater where they remain for 3-7 years burrowed in the sediments (Beamish and Potter, 1975), filter feeding and maintaining a low metabolic rate (Lewis,

1980). After sufficient energy stores are accumulated, sea lamprey undergo metamorphosis into parasitic juvenile sea lamprey that feed on the blood of larger host fishes by attaching to the animals with their oral disc or sucker. They then migrate back to freshwater as adults to spawn and die (Beamish, 1980). This euryhaline capability of sea lamprey make them ideal to study ion regulatory proteins in both freshwater and saltwater providing insight into their roles for osmoregulation. Reis-Santos and colleagues (2008) found that Na^+/K^+-ATPase (NKA) activity and abundance increases with salinity and V-ATPase expression decreases with salinity. Lampreys are the earliest extant vertebrates to adapt a true osmoregulatory strategy, and just like teleost fishes, the gills and kidneys are the main water and ion regulating organs (Bartels and Potter, 2004; Reis-Santos et al., 2008).

Lamprey are basally derived vertebrates diverging on their own separate trajectory approximately 550 million years ago (Bartels and Potter, 2004). Lamprey and teleost fishes are not closely related but they use similar mechanisms in the gill and kidney for regulating ion concentrations (Morris, 1972; Beamish, 1980; Hardisty et al., 1989). There is less known about lamprey osmoregulatory strategies but there is evidence for different types of mitochondria rich cells (MRCs) for the different life stages. Current lamprey osmoregulation strategies are highlighted in figure 3.1 (Bartels and Potter, 2004). This proposal is consistent with other teleost models which suggests that ionic transport strategies originated more than 500 million years ago (Evans et al., 2005) and pre-date divergence.

However, lamprey were used to study the non-gastric H^+/K^+-ATPase (ngHKA) because they have the gene *atp12a*, unlike the teleost fish. Lamprey are also stomach-less and lack the gastric HKA genes (*atp4a* and *atp4b*) which will simplify the interpretation

of the results because only the ngHKA (*atp12a*) is present (Wilson and Castro, 2010; Castro et al., 2014). Food is an important source of ions (Patel et al., 2009), but potassium (K^+) can be taken up from the water when food is not readily available. Early studies suggest branchial uptake from the water is a possibility, but the mechanism remains unknown (Eddy, 1975; Gardaire et al, 1991; Gardaire and Isaia, 1992). The goal of this chapter is to further the current knowledge of osmoregulation in lampreys and specifically the role of the ngHKA. I tested the hypotheses that the ngHKA plays a role in K^+ and acid-base regulation in lamprey. To this end, K^+ and acid-base disturbances were placed on the fish and the response of the pump were examined at the mRNA level, protein expression, localization, and ion fluxes. Additionally, the ion pumps, NKA and V-ATPase were examined in conjunction with the ngHKA because they also move K^+ and proton ion across the plasma membrane.

3.2 METHODS

3.2.1 Experimental Animals

Larval sea lamprey (*Petromyzon marinus)* were captured via backpack electrofishing in June 2015 from a stream in Richibucto, New Brunswick. Animals were transported back to Waterloo, Ontario, Canada in 70 L coolers filled with stream water, cotton (to act as a burrowing substrate) and aerator pumps. Upon arrival, the fish were placed in 25 L tanks supplies with flowing well water at 12-13°C and 5 cm of sand on the bottom. Sea lamprey were fed 1g of baker's yeast per animal once a week. The room temperature was 20°C ± 1°C with a 12h: 12h light: dark photoperiod. This project was

approved by Wilfrid Laurier University's Animal Care Committee and followed the guidelines from the Canadian Council of Animal Care (AUP R14002).

3.2.2 Rubidium Kinetics

Rubidium (Rb^+) is similar to K^+ in physico-chemical behaviour and its use as a surrogate flux marker for K^+ has been validated (Sanders and Kirschner, 1983, Tipsmark and Madsen, 2001). Rb^+ and K^+ are both alkali metals and their hydration radii are similar (Mähler and Persson, 2012). Uptake kinetics of Rb^+ were characterized using Michaelis-Menten kinetics. V_{max} and K_m were calculated by non-linear regression analysis of kinetic data to the Michaelis-Menten equation using GraphPad Prism (version 6.01 for Windows, GraphPad Software, La Jolla, CA). Concentrations tested were 0, 0.1, 1, 5, and higher concentrations of 10, 25 and 75 mM. RbCl added to 2:1 dechlorinated tap water: reverse osmosis water in a static system and rubidium uptake was measured after 6h using an atomic absorption spectrophotometer in flame mode (see below).

3.2.3 Experiment 1: K^+ Disturbance

Potassium was manipulated through diet. Fish were fasted for 14 days and control animals were fed three days a week, with the last feeding 24 hours prior to the experiment. For ion flux measurements (see below), larval *P.marinus* were placed in 75 mL of 2 parts dechlorinated tap water, 1 part reverse osmosis (RO) water and RbCl was added to a final concentration of 1 mmol/L just prior to the start of the experiment (static system). Water was aerated during the course of the experiment. A 15 mL water sample was taken at time

0, 6, and 12 h for ammonia and titratable acidity measurements. The tank volume was maintained by replacement of the sample with fresh 1 mM RbCl solution.

3.2.4 Experiment 2: Acid-base Disturbance

Fish were fasted for 24 hours prior to the start of the experiment. Fish were anesthetized in 0.75 g/L of tricaine methanesulfonate (MS222, Sigma-Aldrich) with 1.5 g/L sodium bicarbonate and weighed and given intraperitoneal injections (5 µl/g) of acid, base or saline. Treatments for the acid-base experiments included acid and base loads of 1.5 µmol/kg H_2SO_4 (e.g. Cameron and Kormanik, 1982), and 3 µmol/kg $NaHCO_3$ (e.g. Tresguerres et al., 2007), respectively along with a 0.75 µmol/kg NaCl control. Flux measurements were conducted as described in section 3.2.2.

3.2.5 Experiment 3: Omeprazole

Fish were fasted for 24 hours prior to the experiment. Treatments for the omeprazole experiments include a 0.6 µmol/kg omeprazole (Alfa Aesar. Ward Hill MA) injection made with 2% DMSO. The control was an equivalent injection volume of 0.9%NaCl with 2% DMSO giving 0.75 µmol/kg NaCl. Before being injected (5 µl/g), fish were anesthetized in 0.75g/L MS222 and 1.5g/L of sodium bicarbonate. Fish were injected twice with omeprazole (or saline control), the first time was 16h before the start of the experiment to ensure adequate inhibitory response and at time 0. Flux measurements were then conducted as described in section 3.2.2.

3.2.6 Sampling

Fish were then euthanized at 6 or 12 hours in 1.5 g/L of MS222 and 3g/L of sodium bicarbonate. The head and gills were removed and the remaining carcass was taken and placed in a pre-weighed tube and dried at 70°C for 48 hours. Five mL of concentrated HNO_3 was then added to digest the tissue in order to determine Rb^+, Na^+, and K^+ concentrations for uptake rate calculations. Whole body gill cross sections were snap frozen in liquid nitrogen or dry ice for Western blotting and RNA extractions or fixed for immunohistochemistry.

3.2.7 Analytical Techniques

Western Blotting

Protein expression was measured using SDS-PAGE (sodium dodecyl sulfate polyacrylamide gel electrophoresis) and Western blotting according to Wilson et al. (2007) (see chapter 2 and appendix C for a more detailed description of the protocol). In short, samples were homogenized in radioimmunoprecipitation assay (RIPA) buffer, and centrifuged (14 000 xg for 15 mins at 4°C). The supernatant was mixed with an equal volume of 2x Laemmli's buffer, and heated at 70°C of 10 min. The final concentrations of samples were adjusted to 1 µg/µl. Gels were run and transferred to Immobilon PVDF membranes (pore size 0.45 µm, Millipore, Billerica USA). Membranes were blocked with 5% skim milk/TTBS solution and probed with LF12Arb for ngHKA (1:1000), αR1 for NKA (1:1000), B2 for V-ATPase (1:500), and 12g10 for tubulin (1:200) overnight at room temperature. Secondary antibodies were goat anti-rabbit or anti-mouse horse radish

peroxidase (1:50 000) and membranes were imaged using the c300 Azure Biosystems documentation system using enhanced chemiluminscence (ECL) (Clarity, Bio-Rad).

Immunohistochemistry

Localization of ion pumps were determined using the techniques outlined in Wilson et al. (2007), with the addition of tyramide signal amplification (Life technologies, Carlsbad USA, according to manufacturer's instructions). More details are also found in chapter 2 and appendix B. In short, gill tissue was fixed using 3% paraformaldehyde in PBS and embedded in paraffin. Sections were dewaxed at 60°C, run through a xylene and alcohol series, and antigen retrieval was preformed including 0.05% citraconic anhydride for 30 min at pH 7.4 at 100°C (Namimatsu et al., 2005) followed by 1% SDS/PBS soak (Brown et al., 1996). Sections were blocked with BLØK (Life Technologies). Sections were probed with the primary antibodies LF12Arb2 (1:500) + α5 (1:250), pre-immune serum (1:500) + J3 (1:250), or B2 (1:500) + α5 (1:250), and incubated overnight at 4°C. The secondary antibodies were goat anti-rabbit horseradish peroxidase (1:200) and Alexa-555 (1:500) (Life Technologies) applied for 1 hour at 37°C. Labelled tyramide (Alexa488) made in amplification buffer (Bio-Rad) and 0.0015% H_2O_2 was applied for 10 minutes. Negative controls included the pre-immune serum. Sections were imaged using a LEICA DM5500 B microscope and Hamamatsu C11440 Orca-Flash 4.0 digital camera.

Transcript Level Expression (mRNA)

Total RNA was extracted from gill tissue using Bio-Rad PureZOL™ RNA Isolation Reagent and Bio-Rad Aurum™ Total RNA Mini Kits using the spin protocol with on-column DNase I treatment according to manufacturer's instruction. The quantity and purity of RNA was checked using BioTek Synergy HT Spectrophotometry (Take 3 plate). RNA

quality was checked by running samples on an agarose formaldehyde gel to make sure there was no genomic DNA contamination or degradation of samples. RNA was then reverse transcribed to cDNA using High Capacity cDNA Reverse Transcriptase Kits (Applied Biosystems). Gene-specific primers (Table 3.1) were then used to amplify cDNA fragments by PCR. A PCR reaction was initially completed for actin and samples were then run on a 2% TBE agarose gel for quality control. All primers were standardized by running a dilution series of the pooled samples in order to create standard curves to determine qPCR efficiency (E=0.9-1.1). The qPCR (CFX96 Real-Time, Bio-Rad) reactions were run in 5µl of 50x diluted samples using gene-specific primers (Table 3.1) and Bio-Rad SybrGreen Mix in a 20 µl reaction volume. The comparative cycle threshold method ($2^{-\Delta\Delta CT}$ method) was used to analyze expression levels of the genes of interest with actin used as a reference gene (Livak and Schmitthen, 2001). The qPCR results were then analyzed using Bio-Rad CFC Manager software (Appendix D).

Flux Measurements - Rb^+, K^+, and Na^+

Carcasses were digested in concentrated nitric acid and diluted accordingly. *Rb^+, K^+, and Na^+* concentrations were measured on PinAAcle 900T Atomic Absorption Spectrophotometer (Perkin Elmer Waltham MA) in flame mode. HNO_3 and CsCl were added to the samples at final concentrations of 0.1% and 0.2%, respectively. Standards ranged from 0-5 µM for Rb^+, 0-7.5 µM for K^+, and 0-22 µM for Na^+ and samples were also diluted 50x, 10000x, and 1000x , respectively, with milliQ (ultrapure) water to avoid any saturation problems. Uptake rates were calculated in µmol/kg/h and muscle concentrations in µmol/g wet weight.

Ammonia and Titratable Acidity

Ammonia in water samples was measured spectrophotometrically (Spectramax 190, Molecular Devices, Sunnyvale, CA) using a standard ammonia assay (Verdouw et al., 1978). Samples were diluted 10 times to fall within the standard curve range of 0-150 µM and read at 650 nm. Total ammonia efflux rates (J_{amm}) were calculated in µmol/kg/h. Ammonia is a good buffer and traps some of the acid which is why it is taken into account. Titratable acidity (J_{TA}) was determined using Radiometer Copenhagen TTT80 Titrator and ABU80 Autoburret with a PHM84 pH and Hamilton pH electrode. Samples (10mL) were aerated for 1 hour prior to measurements in order to remove CO_2 and with continued aeration, titrated with 0.01 N HCl until a pH of approximately 4.5 and then brought to a final pH of 4 using 0.005 N HCl. Titrant volumes were then multiplied by the respective HCl concentration to give µmol H^+ in 10 mL water samples. Those values were then multiplied by 7.5 to correct for the total volume of water the fish was in (75 mL), divided by fish mass (kg) and flux period time (h) to give flux rates as µmol/kg/h. The net acid flux (J_{H+}) was calculated in µmol/kg/h using the relationship:

$$J_{H+} = J_{TA} + J_{amm}$$

(Wood and Caldwell, 1978).

3.2.8 Statistical Analyses

Data is reported as mean values ± standard error the mean (s.e.m). Two-way and one-way ANOVAs as well as t-tests were used to test for differences between treatment groups and flux times. If a significant difference was found by ANOVA, a post hoc Holm-Sidak test was done. In the case of non-normality and/or unequal variance, an equivalent, non-parametric test was used (Mann-Whitney rank sum test, Kruskal-Wallis). $P<0.05$ was

deemed the level of significance for all tests that were done using SigmaPlot (11, Systat, San Jose USA).

3.3 RESULTS

The tissue profile Western blotting results were consistent with the qPCR data showing gill and kidney to have high expression levels of the ngHKA (lanes 3 and 5, Fig. 3.3). Rubidium uptake was successfully measured. In the lower physiological range, the data shows a hyperbolic Michaelis-Menten relationship. The Rb^+ V_{max} was 90.1 µmol/kg/h and the K_m value was 1.5 mM (Fig. 3.2). At the higher water Rb^+ concentrations, Rb^+ uptake shows a linear relationship. Average control uptake rates were 41 µmol/kg/h and 31.5 µmol/kg/h at 6 and 12 hours respectively using a water concentration of 1 mM of RbCl.

3.3.1 Experiment 1: K^+ Disturbance

There was a significant net acid uptake (J_{H+}) in fed (n=4) compared to fasted (n=4) lamprey (p=0.038) but no difference between 6 and 12 hours (p=0.6) (Fig. 3.4). The fasted (n=4) group had a significantly lower Rb^+ uptake rate compared to the fed (n=4) group (p=0.027), but no differences between time were detected (p=0.08) (Fig. 3.5). There were no differences in *atp12a* (ngHKA) or any of the other ion transport genes between fed (n=6) and fasted (n=7) animals (all values p>0.05) (Table 3.2). At the protein level of expression, there were no differences between fed (n=8) and fasted (n=8) lamprey in the ngHKA (p=0.27), or NKA (p=0.05), or V-ATPase (p=0.32) (Fig. 3.6). Fed fish (n=8) had significantly higher [Na^+] uptake compared to fasted (n=8) (p=0.04), and no differences

were seen in [K^+] in muscle (Table 3.3). Localization of ngHKA, NKA, and V-ATPase of fed versus fasted lamprey are shown in figure 3.9. NKA staining is basolateral at the tips of the secondary lamellae and in the interlamellar cell mass. The ngHKA and V-ATPase staining is found throughout the epithelium mostly along the ends of the secondary lamella. The controls for the NKA, ngHKA, and V-ATPase show similar staining patterns (fig 3.7, 3.8). The pre-immune controls show negative LF12Arb2 staining (Appendix E).

3.3.2 Experiment 2: Acid-base Disturbance

In acid loaded fish (n=4), there was significant net acid excretion (J_{H+}) compared to the control group (n=4, p=0.03) and between 6 and 12 hours (p=0.03) (Fig. 3.10). For Rb^+ uptake there was a significant interaction (p=0.015) between treatment and time. The acid loaded (n=4) Rb^+ uptake at 12 hour was significantly lower than the control (n=4) uptake rate at 12 hours (p=0.004) (Fig. 3.11). There was also a significant decrease in Rb^+ uptake between 6h and 12h in the acid loaded fish (p=0.002).

At the transcript level of expression, there were no differences in *atp12a* or any of the other transporter genes between the controls (n=8), acid (n=7), or base (n=8) loaded animals except for carbonic anydrase (*ca19*) which was significantly lower in acid loaded fish (p=0.025) (Table 3.2). At the protein level of expression there were no differences between the control, acid, or base loaded lamprey (n=8) in the ngHKA (p=0.28), or V-ATPase (p=0.27), but there was a significant decrease in acid treated NKA protein compared to the controls (p=0.02) (Fig. 3.12). There were no differences in [Na^+] or [K^+] uptake (n=8) (Table 3.3). Localization of ngHKA, NKA, and V-ATPase are shown in figure 3.13. NKA stains basolaterally at the tips of the secondary lamellae and in the

interlamellar cell mass, showing no differences between the treatments. The ngHKA staining is throughout the epithelium with some areas that show sharper, apical staining; however, showing no differences between the treatments. The V-ATPase staining in the acid loaded lamprey is more punctate compared to the control and base loaded fish.

3.3.3 Experiment 3: Omeprazole

There was no significant difference in J_{H+} (n=4, p=0.27) (Fig. 3.14) or Rb^+ uptake between the controls (n=4, 75.6 ± 28.2 μmol/kg/h) or omeprazole (n=4, 60.1 ± 23.6 μmol/kg/h) treated lamprey (p=0.34). At the transcript level of expression, there were no differences in any of the genes between the controls (n=4) and omeprazole (n=4) treated lamprey (Table 3.2). At the protein level of expression there were no differences between the control (n=4) or omeprazole loaded lamprey (n=4) in ngHKA (p=0.27) or V-ATPase (p=0.18), but there was significantly lower NKA expression (p=0.003) (Fig. 3.15). There were no differences in $[Na^+]$ or $[K^+]$ uptake (n=4) (Table 3.3). Localization of ngHKA, NKA, and V-ATPase are shown in figure 3.16. NKA stains basolaterally at the tips of the secondary lamellae and in the interlamellar cell mass and the ngHKA staining is throughout the epithelium at the ends of the secondary lamellae, showing no differences between groups. The V-ATPase staining in the omeprazole treated lamprey is more punctate compared to the control.

3.4 DISCUSSION

As predicted, the ngHKA showed high expression levels in the gill and kidney as they are believed to be the main osmoregulatory organs in lamprey, the same as teleost fish.

Because the gill is in direct contact with the environment, and a potential mechanism for K^+ uptake from the water was being investigated, the gill was further studied.

The average control Rb^+ uptake rates were 36 µmol/kg/h. The results for Rb^+ uptake in the fed and fasted *P. marinus* were not as predicted. It was predicted that fasted animals would have an increased uptake because they were not obtaining K^+ from their diet. The opposite however was found. This result possibly could be explained by the fact that only uptake flux rates were measured and perhaps an increased influx is also accompanied with an increased efflux with an overall net efflux. Eddy (1985), found that K^+ flux rates in rainbow trout are approximately 3-5% of Na^+ and Cl^-. When comparing these flux rates to flux rates measured in the adult sea lamprey (Wilkie et al., 1998), the values fall within the range of post exercised fish, suggesting that the lamprey were either not at resting state during the experiment or that K^+ uptake in lamprey are higher than those found in teleost fishes. Under resting conditions the Rb^+ uptake rate would be 10% and 20% of Cl^- and Na^+ uptake rate, respectively measured by Wilkie et al. (1998). The Rb^+ uptake rates are also 10% and 20% of Cl^- and Na^+ resting rates found in ammocoete sea lamprey (Wilkie et al., 2001). It should be noted that teleost fishes lack the *atp12a* gene and thus this potential uptake mechanism. There were no differences in K^+ muscle concentrations between any of the treatments. Due to the sedentary lifestyle of larval sea lamprey, the two week fasting period was most likely not long enough to trigger a K^+ disruption. Fed fish showed significantly higher Na^+ levels likely attributed from their diet.

Amino acids absorbed after ingestion are catabolized in the liver and there is an increase in plasma ammonia in fish (Bucking and Wood, 2008). Similarly to the result found in the present study, Wood et al. (2010) showed a post-prandial metabolic acidosis in the

freshwater acclimated agastric killifish. The results for the net acid flux in acid and base challenged lamprey makes sense in that acid injected animals excreted more acid compared to the controls, however again, the Rb^+ data does not parallel this. The Rb^+ uptake rates in fish injected with an acid load for 12 hours were significantly lower than the controls, which is opposite of what was predicted. It is possible that the acid injected fish did not fare well with the treatment. Muscle discolouration was noted at the site of injection and during trial experiments, some animals did not recover from the acid injections. Future studies are suggested to measure intracellular pH of the muscle and extracellular pH of the plasma, as this would be useful information. NKA protein expression decreased in acid loaded animals and those treated with omeprazole. Lamprey have a remarkable capacity to quickly restore blood pH after acid build up from exercise. Migrating adult lamprey are able to restore control pH levels after 1 h (Wilkie et al., 1998), while other teleost fish usually take 4-12 h (Holeton et al. 1983; Milligan and Wood, 1986; Kieffer et al., 1994). It was determined that lamprey are able to do this through proton excretion into the environment (Wilkie et al., 1998). Perhaps this short 1 h correction was masked from the longer interval time points chosen in this study and may possibly explain why increases were not seen.

There were no differences in mRNA expression in any of the pumps examined between any of the treatments, with the exception of a significant decrease in carbonic anhydrase activity in acid treated fish. Carbonic anhydrase catalyzed CO_2 to produce intracellular protons. Gilmour et al. (2007) investigated the effects of metabolic acid-base disturbance in *P. annectens* and found no differences in mRNA expression in the carbonic anhydrase, V-ATPase, or Na^+/HCO_3- cotransporter. However, in other species of fish such as rainbow

trout, transcriptional regulation of proteins during acid-base disturbances have been found (Galvez et al., 2002; Hirata et al., 2003; Perry et al., 2003a; Perry et al., 2003b; Georgalis et al., 2006). It could be that the stressors were not strong enough to elicit any changes or that the increase in activity is not needed to deal with the disturbance (Gilmour et al., 2007). Additionally, the sampling times used may have missed transient changes in transcript levels (Gilmour et al., 2007) or post-translational modifications may be involved (Tresguerres et al., 2005; Tresguerres et al., 2006). NetPhos (http://www.cbs.dtu.dk/services/NetPhos/) predicted 22 phosphorylation sites, with 80% confidence set as the threshold in lamprey Atp12a. Unfortunately these factors were the product of limited animal availability and trying to find a good balance for the need to simultaneous measure flux rates in the same animals.

In the control sections, NKA staining is basolateral which is consistent with immunolocalization in a previous study (Reis-Santos et al., 2008). The ngHKA staining was spread throughout the epithelium and the majority of NKA staining was in separate cells, however there did appear to be a few cells where ngHKA and NKA were within the same cell. In rat colon cell, ngHKA and NKA have been observed to colocalize (Li et al., 2004) and in rat pancreatic ducts, ngHKA was at the apical side of the cell which suggests it plays a role in extruding protons generated by intracellular carbonic anhydrase (Novak et al., 2011) The pre-immune serum control, showed no immunostaining indicating that the LF12arb2 antibody staining was specific. The gastric HKA has been localized in tubulovesicular membranes in pig stomachs (Sachs et al., 1976). In mammalian stomachs, when acid secretion occurs during digestion, it causes the protein vesicle to fuse with a canaliculus on the apical membrane (Rabon and Reuben, 1990). The immunolocalization

of V-ATPase shows granular staining spread throughout the epithelium indicating possible storage in intracellular vesicles, with some sharp apical staining. Similar findings were reported by Reis-Santos et al. (2008).

In the fed versus fasted *Petromyzon marinus*, there appears to be no difference in the ngHKA staining pattern compared to the controls. However the V-ATPase staining does appear to be reduced in the fasted fish although this was not evident from Western blotting. This would make sense if no digestion is occurring, since there would be less acid from amino acid deamination, but there is still overall net acid secretion, which could be due to lactic acid build up from handing stress.

For the acid-base loading experiments, it does not look like there is a difference in ngHKA localization compared to control fish. The V-ATPase staining appears to be more punctate in the acid treatment group, but requires further quantitative analysis. There were no changes in gill protein expression levels of these transporters either, however, acid loading did significantly decrease NKA protein levels as determined by Western blotting.

No differences were seen between the NKA or ngHKA localization in omeprazole treated fish either. The gHKA has been shown to decrease in protein expression with omeprazole (Crothers et al., 1993). Western blotting did detect a decrease in gill NKA protein levels. Omeprazole is acid activated (Sachs et al., 1994) and Iwata et al. (1988) showed that omeprazole inhibited the NKA activity in both the brain and kidney of rat. From these results, it does not appear that omeprazole is inhibiting the ngHKA. Im and colleagues (1985) showed that 50% of the ATPase activity was inhibited after 3 hours from dosage in rat gastric mucosa, so the sampling time should not have affected inhibitory response. The V-ATPase appears to be staining more sharply in the omeprazole treated

lamprey suggesting a possible compensatory increase. Choe and colleagues (2004) studied the gHKA in Atlantic stingray gill and found it to colocalize with NKA cells but not with V-ATPase rich cells. Similar to the present results in lamprey, Choe et al. (2004) did not observe unambiguous apical staining of the gHKA even in stingrays exposed to hypercapnia (respiratory acidosis). They did however, find increased transcript level expression of the gHKA in freshwater acclimated stingray, suggesting a role in K^+ uptake in hypotonic environments (Choe et al., 2004).

In conclusion, the results show no clear support for the hypothesis that the ngHKA play a role in acid-base or K^+ regulation in larval sea lamprey. Perhaps the ngHKA is important for intracellular K^+ regulation or for secondary active transport mechanisms. However, the development and validation of the ngHKA antibody will allow for future studies to investigate more precisely the localization of the ngHKA, test other potential inhibitors, and use radiolabelled isotopes to trace K^+ movement.

Table 3.1: Primer pairs for qPCR in *Petromyzon marinus.*

Gene	Forward primer 5'-3'	Reverse primer 5'-3'	Reference
atp12a	CTCACCAAGAACATCGCTGA	CGCTCTCGGGTTTCTCATAG	
atp1a1	CGTGGAATCGTCATCAACAC	GCGACAGGATGAAGAAGGAG	Ferreira-Martins *et al.* 2016
atp6v1e	GTGAAGGAAGCCATGGAGAA	TGGGGTTGACTTTGAAGAGC	Ferreira-Martin *et al*. 2016
ca18	GCTGAAGCAGTTCCACTTCC	CCCTTGCTCCTGATGATGTT	Ferreira-Martin *et al.*
scnn1	GCATCATGGTACACGACCAG	AGGCGGAGGAGTAGAGGTTC	Ferreira-Martin *et al*. 2016
slc12a3	GTCATCACGGTCACCTTCCT	ACACCGGAGTGAAATTCTCG	Ferreira-Martin *et al.* 2016

Table 3.2: Mean ± sem normalized transcript expression levels of *atp12a*= ngHKA, atp1a1= NKA, atp6v1e1= V-ATPase, *ca19*= carbonic anhydrase, *scnn1*= epithelial sodium channel, *slc12a3*= sodium chloride cotransporter in the gills of *Petromyzon marinus*. Exp1: fed (n=6) and fasted (n=7); Exp2: acid (n=7) and base (n=8) loading, control (n=8); Exp3: omeprazole (OPZ) treatment (n=8). Each gene was analyzed separately using a t-test or Mann-Whitney rank sum test (*) (experiments 1 and 3) or a One-way ANOVA or Kruskal-Wallis ANOVA on ranks (†) (experiment 2). Groups with like letters are not significantly different from each other.

		atp12a	***atp1a1***	***atp6v1e1***	***ca19***	***scnn1***	***slc12a3***
Exp1	Fed	1.0 ± 0.18	1.0 ± 0.43	1.0 ± 0.33	1.0 ± 0.44	1.0 ± 0.70	1.0 ± 0.31
	Fasted	1.35 ± 0.28	1.10 ± 0.44	1.88 ± 0.58	1.31 ± 0.35	1.25 ± 0.77	1.21 ± 0.47
Exp2	Ctrl	1.0 ± 0.20	1.0 ± 0.36†	1.0 ± 0.15†	1.0 ± 0.20[a]	1.0 ± 0.38†	1.0 ± 0.62†
	Base	0.97 ± 0.14	1.60 ± 0.63	1.49 ± 0.40	1.20 ± 0.10 [a]	2.78 ± 1.80	1.26 ± 0.43
	Acid	1.17 ± 0.18	0.96 ± 0.38	2.04 ± 0.77	0.52 ±0.15[b]	1.94 ± 0.92	1.21 ± 0.33
Exp3	Ctrl	1.0 ± 0.38*	1.0 ± 0.32	1.0 ± 0.48*	1.0 ± 0.53	1.0 ± 0.35	1.0 ± 0.34
	OPZ	2.53 ± 0.22	1.08 ± 0.83	2.13 ± 1.54	2.21 ± 1.91	1.83 ± 1.45	0.67 ± 0.53

Different letters represent a significant difference (One way ANOVA, p=0.032).

Table 3.3: Sodium (Na^+) and potassium ion (K^+) concentrations ± s.e.m in fed and fasted (n=8), acid and base loaded (n=8), and omeprazole injected (n=4) *Petromyzon marinus* muscle (µmol/g wet weight)

		Na^+	K^+
Exp1	Fed	59.3 ± 10.5	84.5 ± 12.6
	Fasted	31.5 ± 6.8 *	101.0 ± 2.3
Exp2	Ctrl	31.4 ± 6.0	101.2 ± 23.9
	Base	43.5 ± 12.7	112.5 ± 16.3
	Acid	29.8 ± 4.2	168.0 ± 67.6
Exp3	Ctrl	41.8 ± 4.5	147.8 ± 39.7
	OPZ	33.2 ± 2.2	130.9 ± 18.1

* Represents statistically significant difference from fed *P. marinus* (Mann Whitney rank sum test, p=0.04)

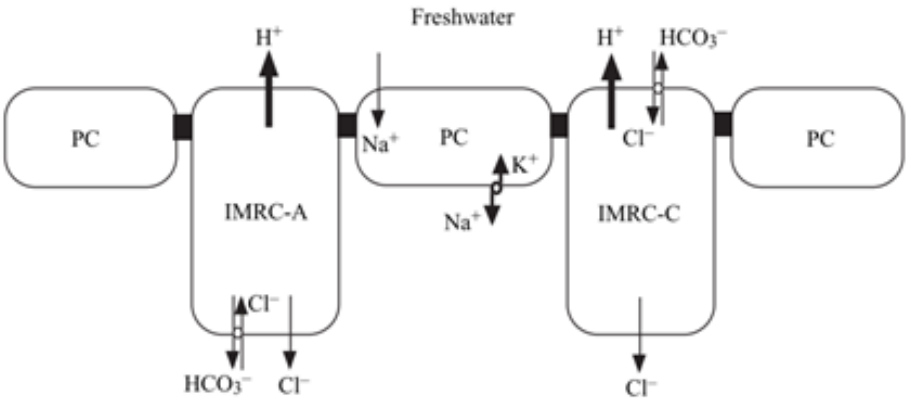

Figure 3.1: Current working model for osmoregulation in freshwater lamprey adapted from Bartels and Potter (2004). Two types of intercalated mitochondrion rich cells (IMRC) are shown (A and C) and a pavement cell (PC). Thick arrows represent active transport, while thinner arrows represent passive movement.

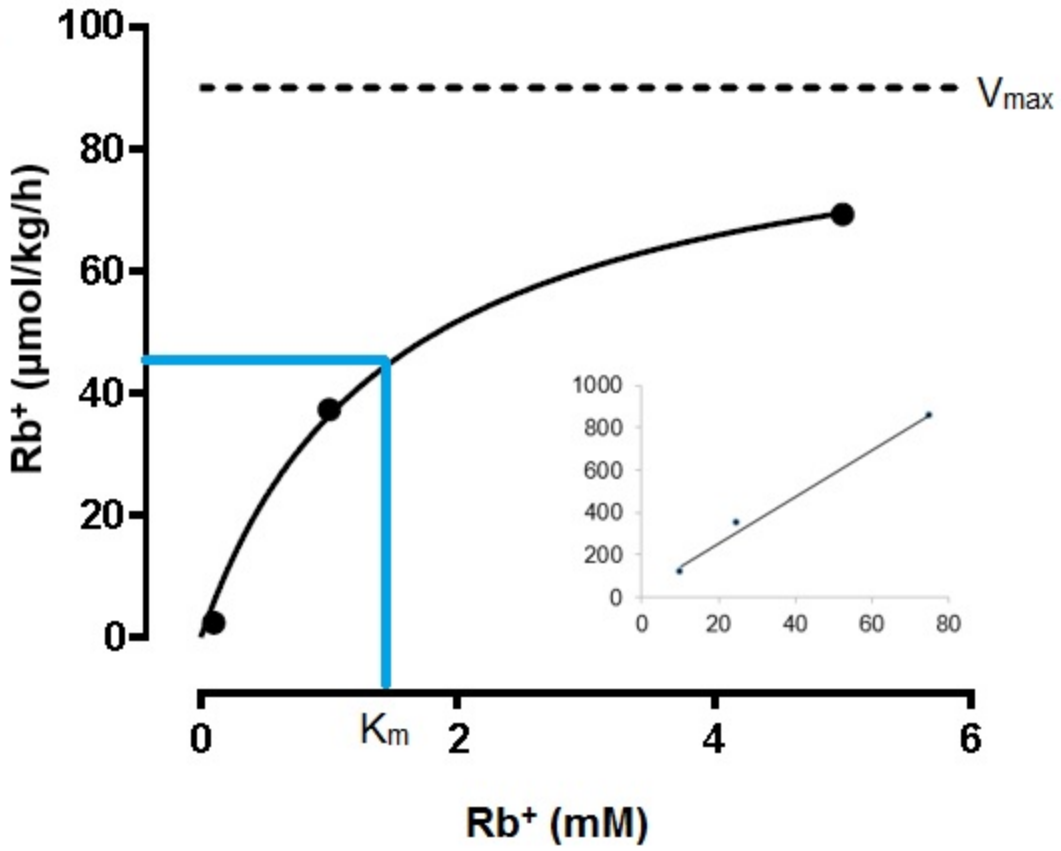

Figure 3.2: *In vivo* Rubidium (Rb^+) uptake in *Petromyzon marinus* (n=4) over lower and higher (inset) physiological range of concentrations of rubidium chloride. Uptake kinetics of Rb^+ were characterized using Michaelis-Menten kinetics. V_{max}=90.09 and K_m=1.48 were calculated by non-linear regression analysis of kinetic data to the Michaelis-Menten equation using GraphPad Prism (version 6.01 for Windows, GraphPad Software, La Jolla, CA).

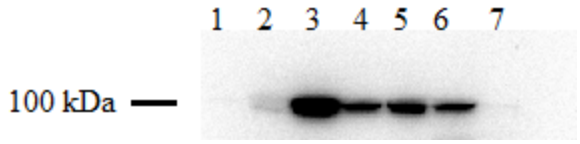

Figure 3.3: SDS-PAGE Western blot for *Petromyzon marinus* tissues probed with a rabbit polyclonal LF12Arb2 antibody 1:1000. The 2º antibody was a goat anti-rabbit HRP detected with ECL. Lane: 1 brain, 2 muscle, 3 kidney, 4 skin, 5 gill, 6 liver, 7 intestine.

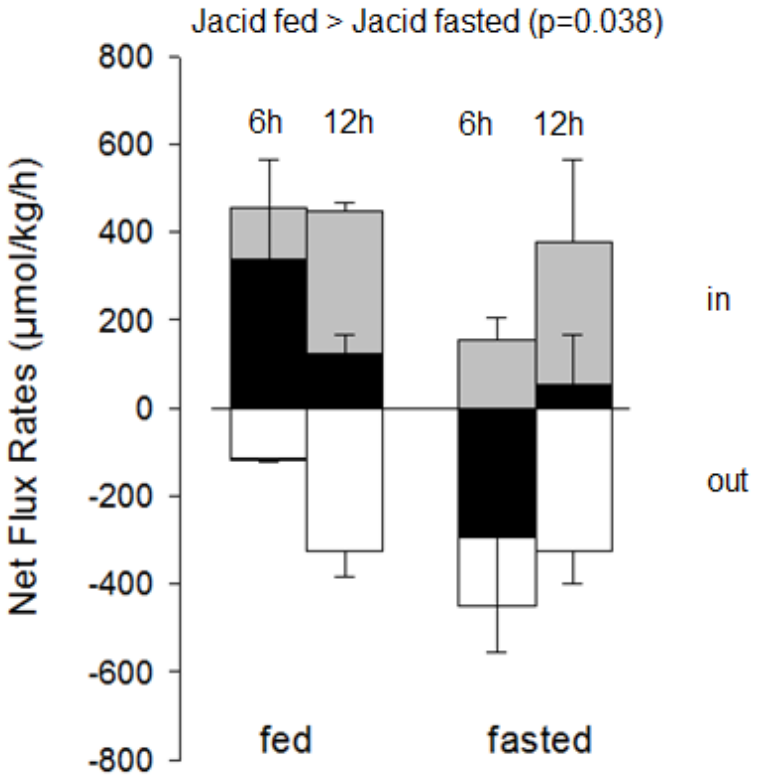

Figure 3.4: Net flux rates of ammonia (white; J_{amm}), titratable acidity (grey; J_{TA}) and acid (black; J_{H+}) in fed and fasted (n=4) *Petromyzon marinus* at 6 and 12 hours. J_{H+} in fed fish was significantly higher than J_{H+} in fasted fish (p=0.038, Two-way ANOVA, Holm-Sidak post hoc). Positive values indicate uptake while negative values indicate excretion.

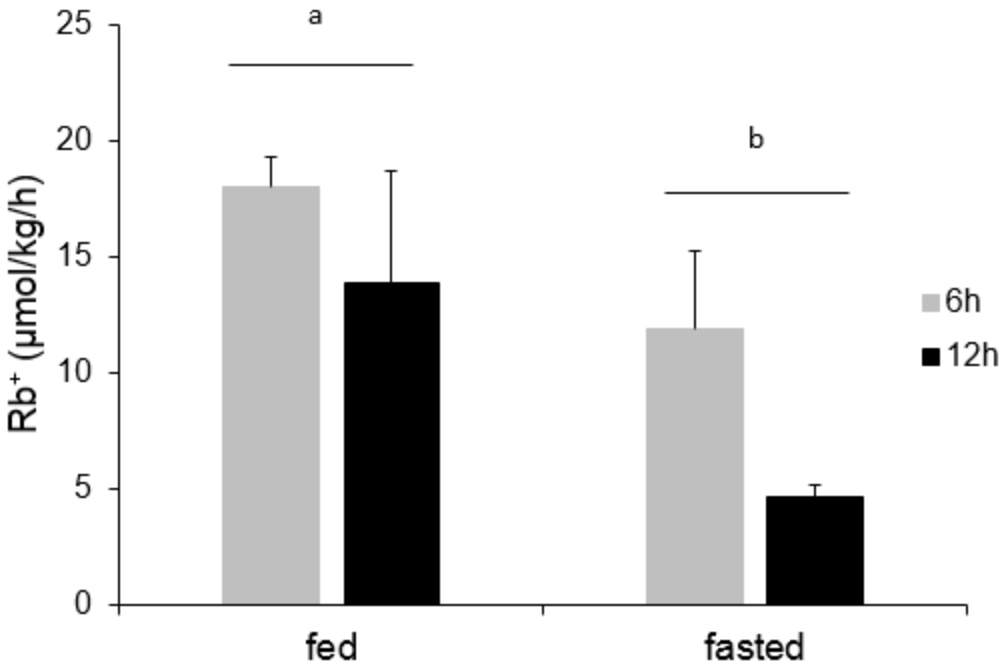

Figure 3.5: Rubidium (Rb^+) uptake rates in fed and fasted *Petromyzon marinus* at 6 hours (grey) and 12 hours (black) (n=4). Different letters represent significant differences (p=0.027, Two-way ANOVA, Holm-Sidak post hoc).

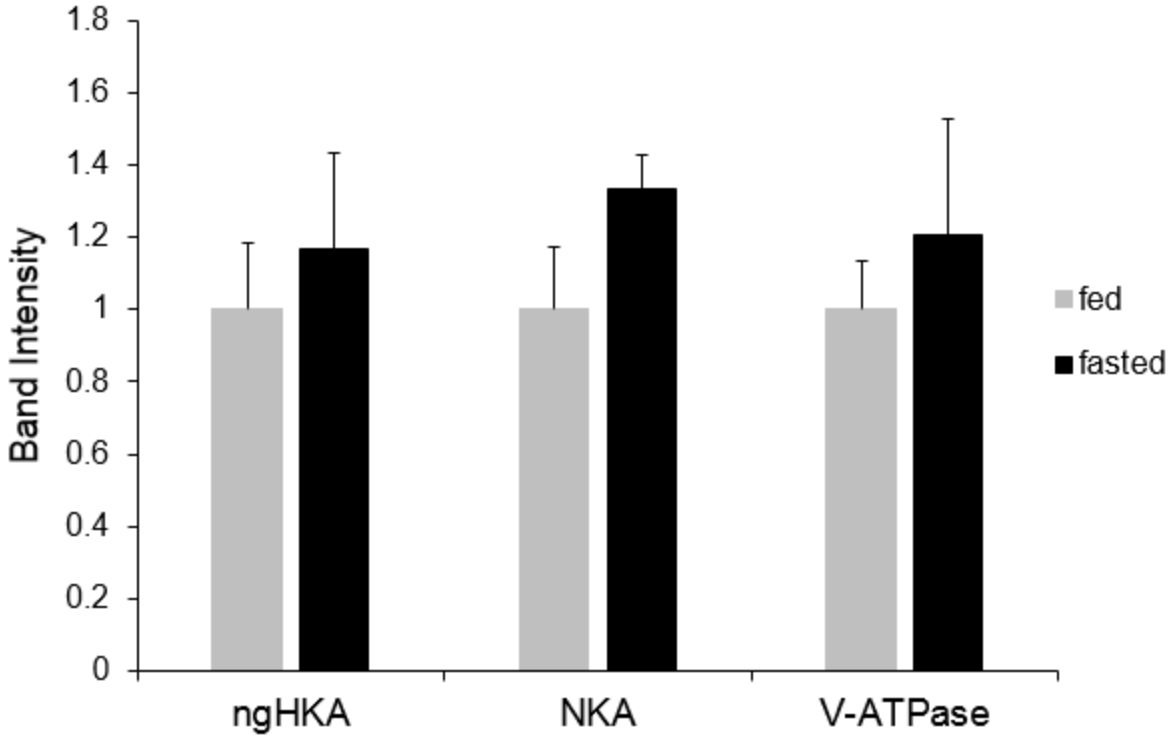

Figure 3.6: Relative band intensity of the non-gastric H^+/K^+-ATPase (ngHKA) α subunit, the Na^+/K^+-ATPase (NKA) α subunit, and the vacuolar proton pump V-ATPase B subunit in fed (grey) and fasted (black) (n=8 for all) *Petromyzon marinus* gill. No statistically significant differences were found (t-test, p=0.27, 0.05, 0.32 for ngHKA, NKA, V-ATPase, respectively).

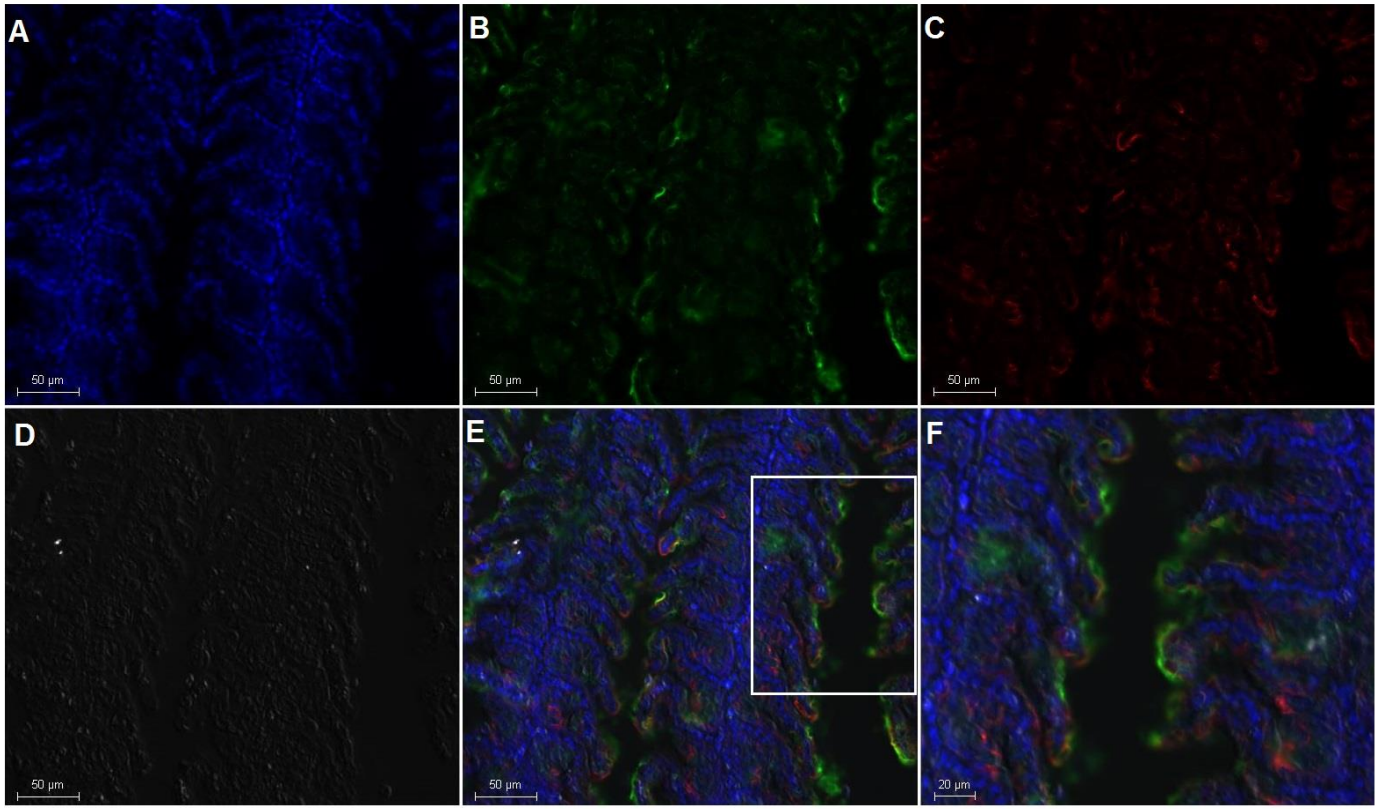

Figure 3.7: Immunohistochemistry of control lamprey *Petromyzon marinus* gill A) DAPI (blue), B) non-gastric H^+/K^+-ATPase (green), C) Na^+/K^+-ATPase (red), D) DIC E) overlay of A-D and F) enlarged area of E. Scale bar is 50 µm A-E, 20 µm in F.

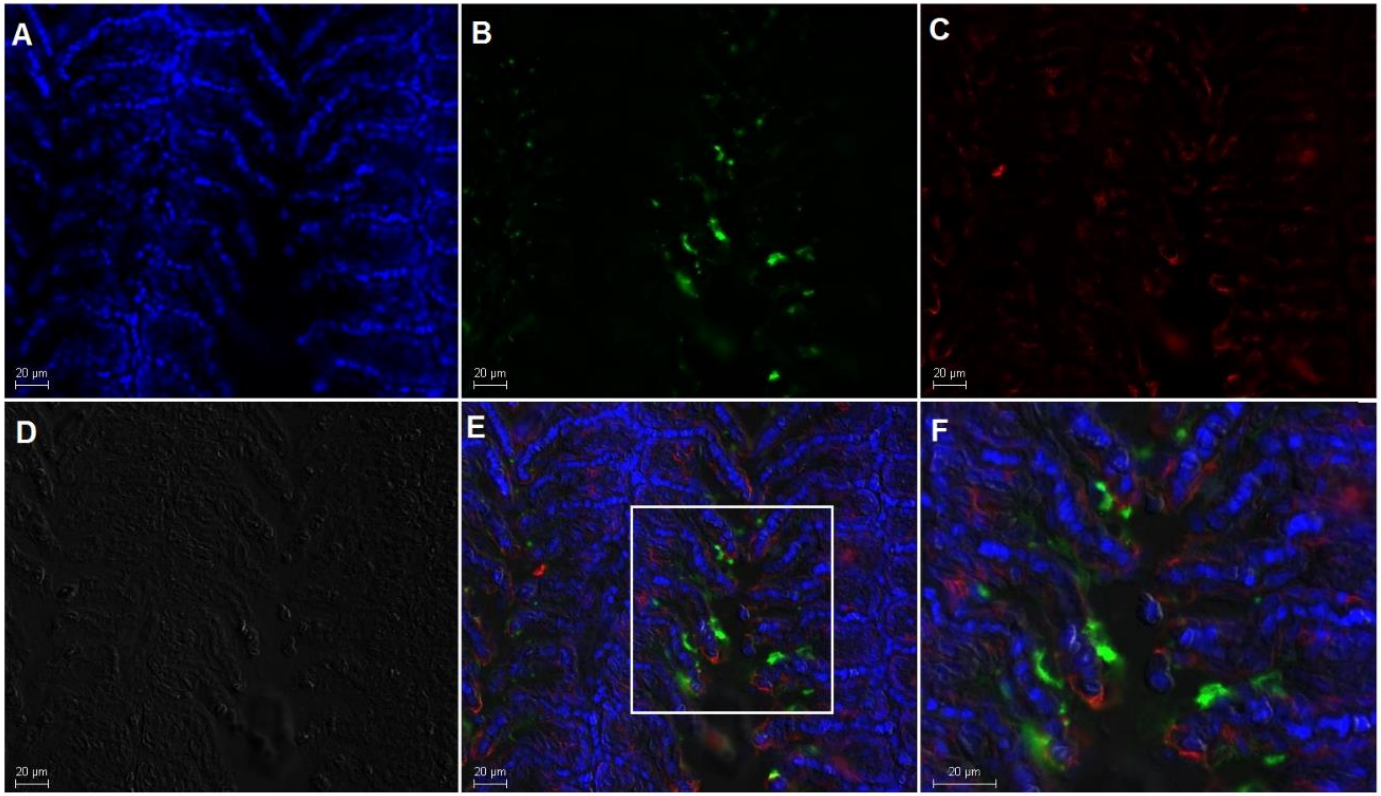

Figure 3.8: Immunohistochemistry of control lamprey *Petromyzon marinus* gill A) DAPI, B) V-ATPase (green), C) Na^+/K^+-ATPase (red), D) DIC, E) overlay of A-D, and F) magnification of highlighted section in E. Scale bar is 20 µm.

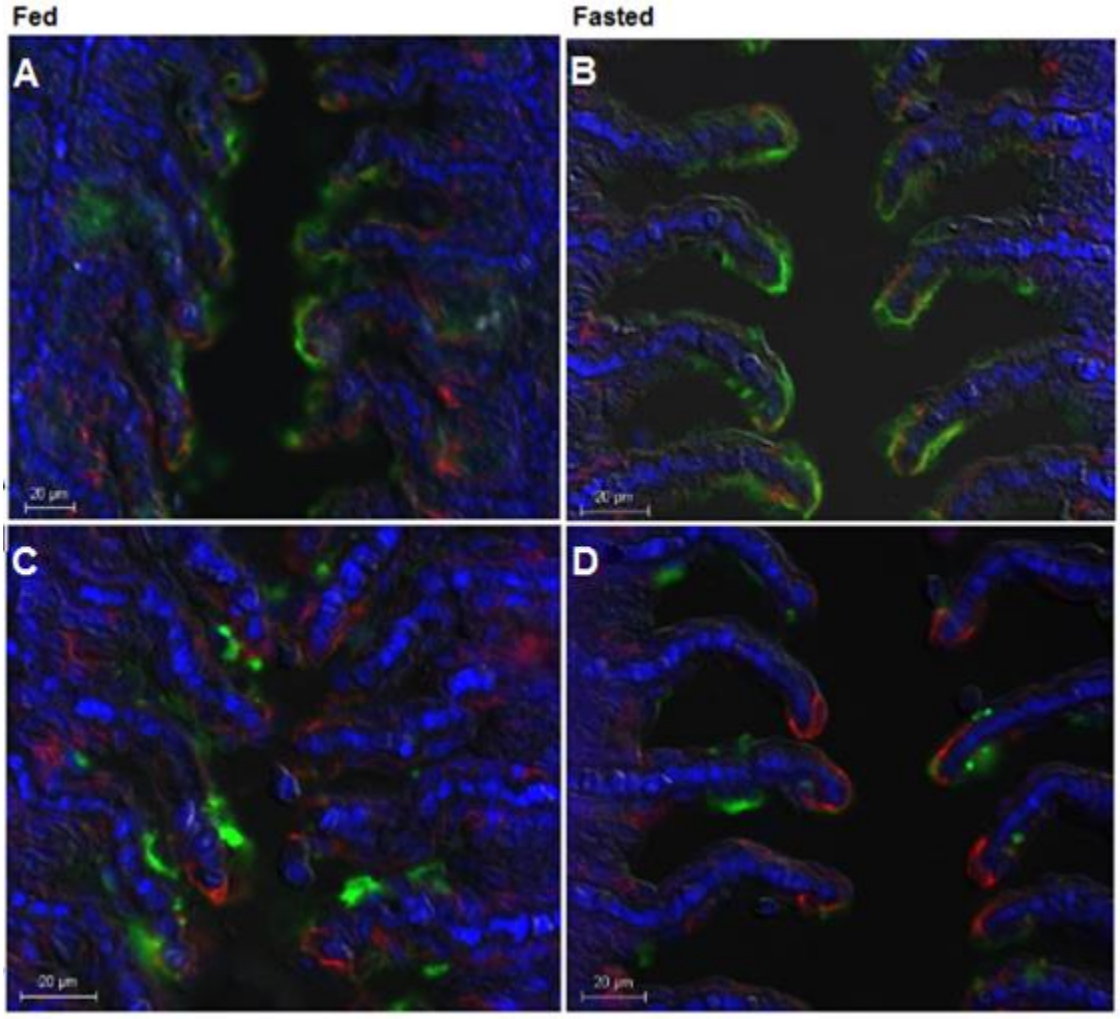

Figure 3.9: Immunohistochemistry of fed (A and C), and fasted (B and D) lamprey *Petromyzon marinus* gill. In the top panels DAPI (blue), non-gastric H^+/K^+-ATPase (green), and Na^+/K^+-ATPase (red). In the bottom panels DAPI (blue), V-ATPase (green), and Na^+/K^+-ATPase (red). Scale bar is 20 µm.

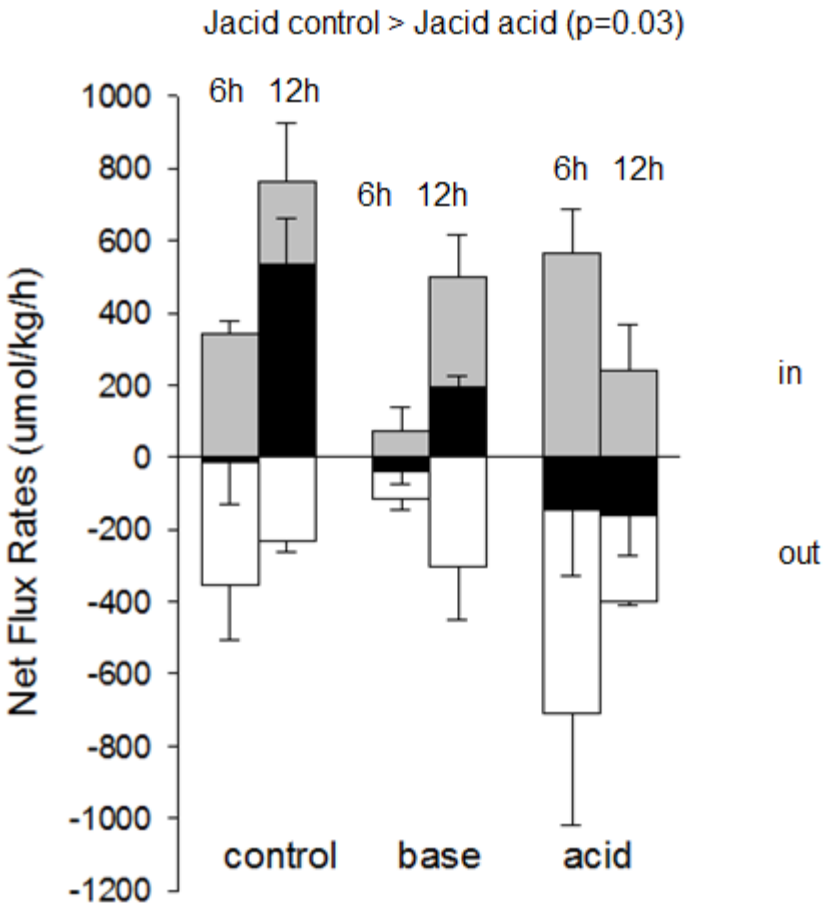

Figure 3.10: Mean ± sem ammonia flux (J_{amm}, white), titratable acidity (J_{TA}, grey) and overall net acid flux (J_{H+}, black) in control, base and acid loaded *Petromyzon marinus* at 6 and 12 hours (n=4 for all). The acid efflux of acid injected lamprey was significantly greater than the control group (p=0.03, Two-way ANOVA, Holm-Sidak post-hoc).

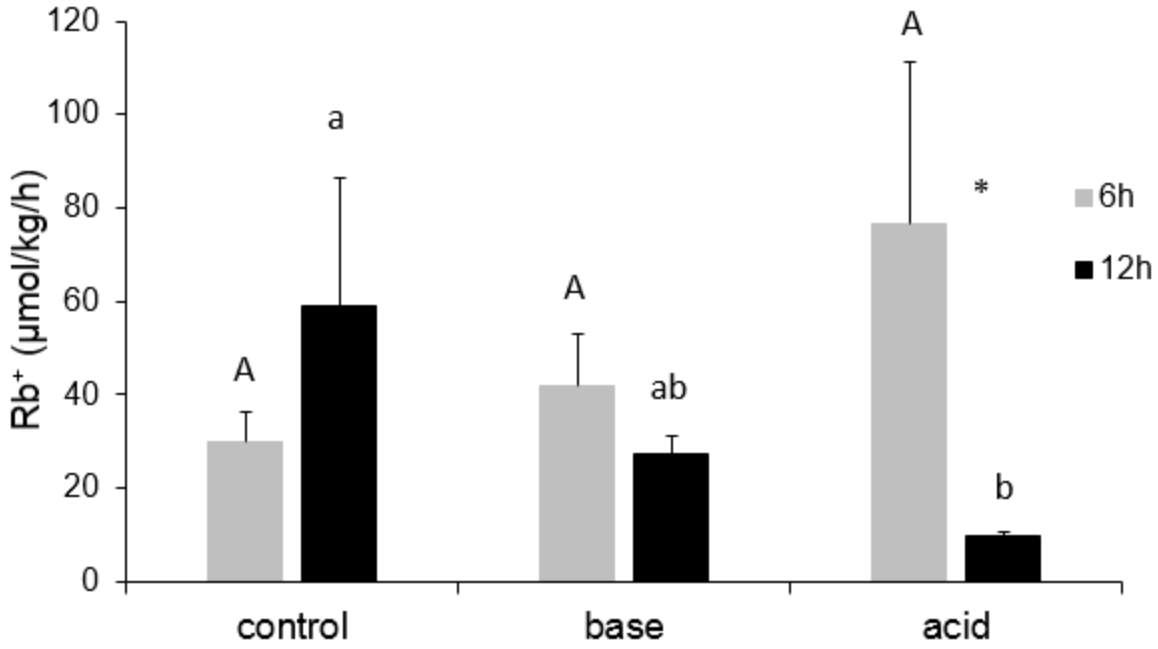

Figure 3.11: Mean ± sem rubidium (Rb^+) flux rate in control, base and acid loaded *Petromyzon marinus* at 6 hours (grey) and 12 hours (black) (n=4 for all). Different letters represent significant differences within sampling time groups (capital for 6 hours, lowercase for 12 hours, p=0.004). Asterisk represents a significant difference between 6 hours and 12 hours within a treatment group (p=0.002) (Two-way ANOVA, Holm-Sidak post hoc).

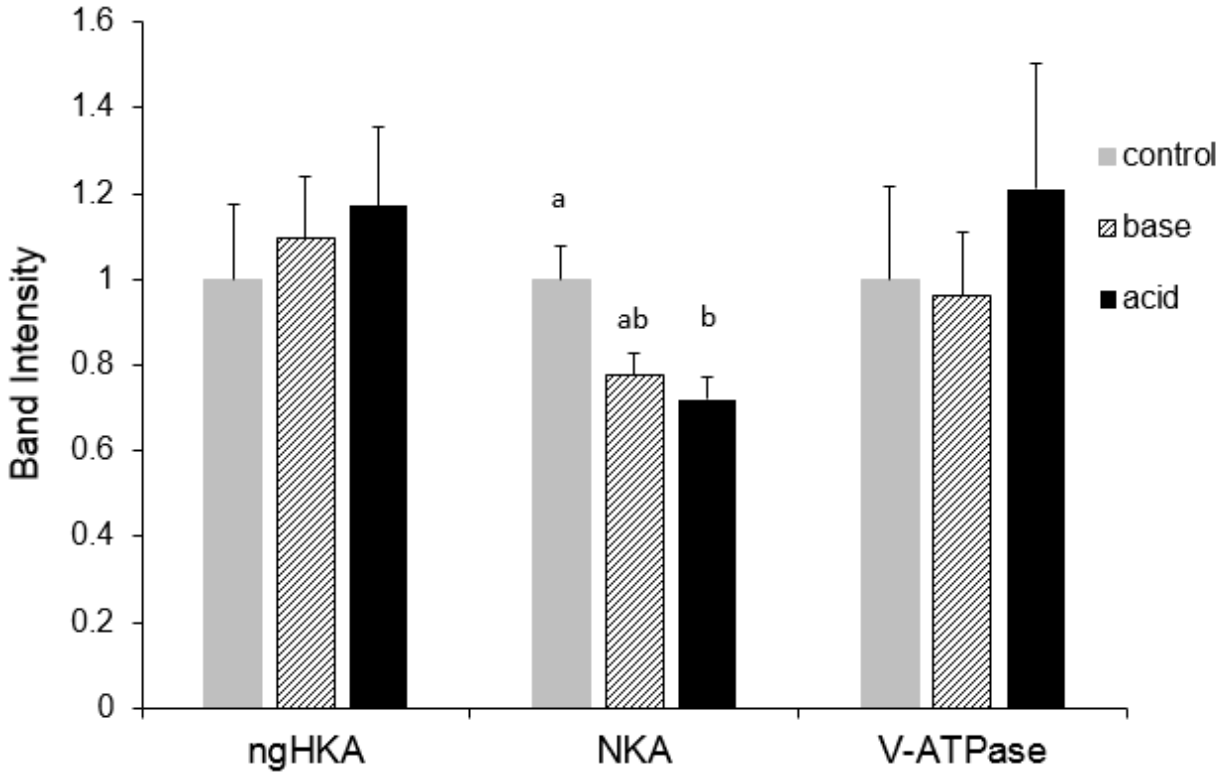

Figure 3.12: Semi-quantitative analysis of the non-gastric H^+/K^+-ATPase (ngHKA) α subunit, the Na^+/K^+-ATPase (NKA) α subunit, and the vacuolar proton pump V-ATPase B subunit in the gills of control (grey) base loaded (stripes) and acid loaded (black) *Petromyzon marinus* (n=8 for all). Different letters represent significant differences (p=0.02) (One-way ANOVA for ngHKA, Kruskal-Wallis One Way ANOVA for V-ATPase and NKA with Tukey test).

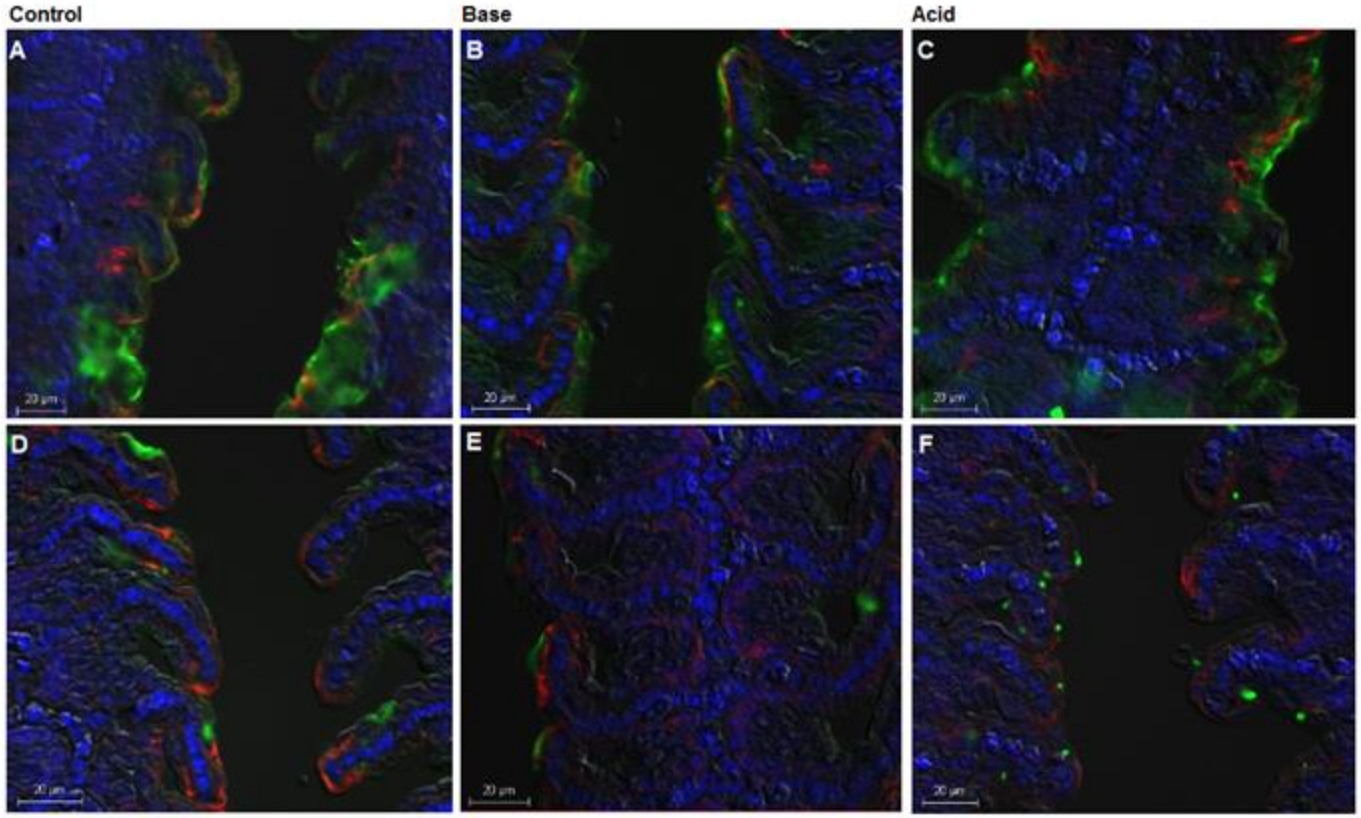

Figure 3.13: Immunohistochemistry of control (A and D), base loaded (B and E), and acid loaded (C and F) lamprey *Petromyzon marinus* gill. In A, B, C sections are labelled with DAPI (blue), non-gastric H^+/K^+-ATPase (green), and Na^+/K^+-ATPase (red). In D, E, F, sections are labelled with DAPI (blue), V-ATPase (green), and Na^+/K^+-ATPase (red). Scale bar is 20 µm.

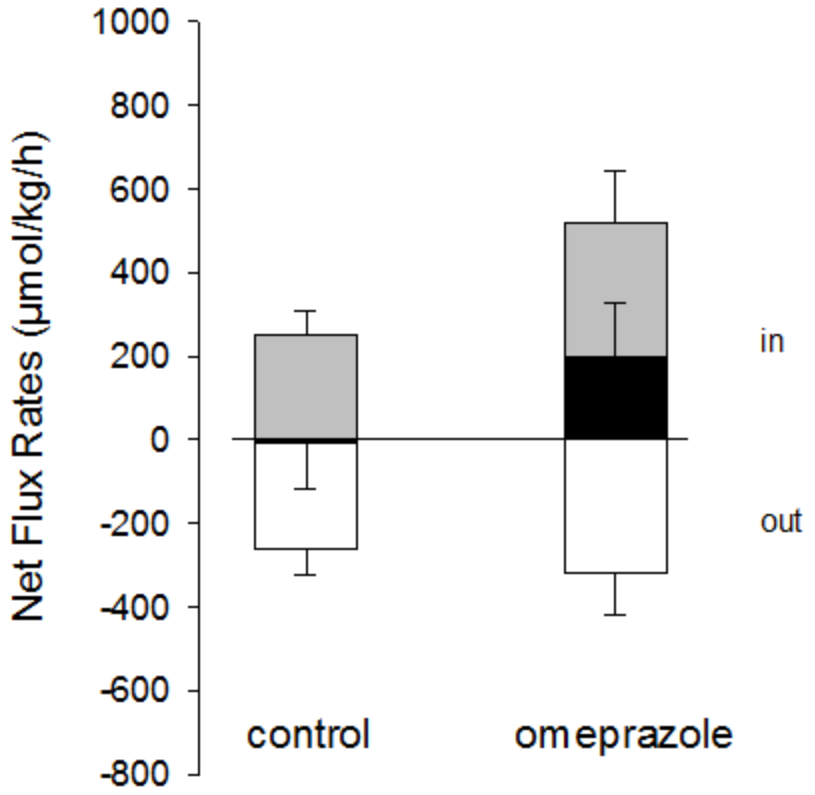

Figure 3.14: Mean ± s.e.m ammonia flux (J_{amm}, white), titratable acidity (J_{TA}, grey) and overall net acid flux ($J_{H+,}$ black) in controls and omeprazole injected *Petromyzon marinus* at 6 hours (n=4). No statistically significant differences were found (Mann-Whitney rank sum test, p=0.27).

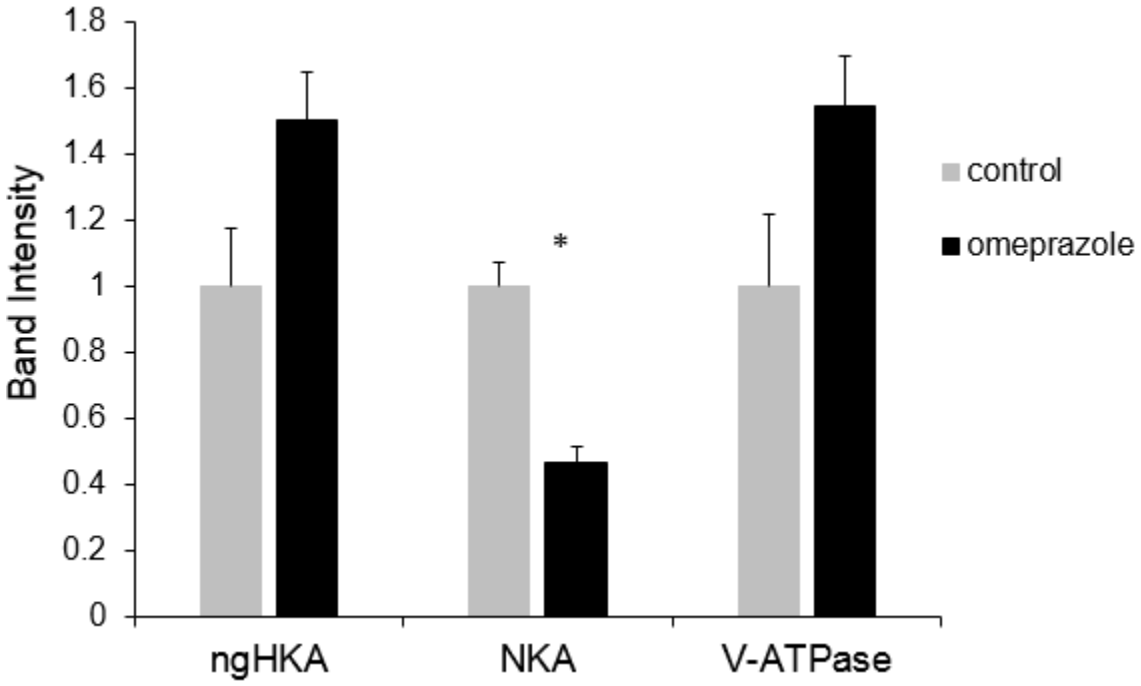

Figure 3.15: Mean ± sem relative band intensity of three ion pumps, the non-gastric H^+/K^+-ATPase (ngHKA) α subunit, the Na^+/K^+-ATPase (NKA) α subunit and the vacuole proton pump V-ATPase β subunit in control (grey) and omeprazole injected (black) *Petromyzon marinus* gill (n=4 for all). The asterisk indicates a significant difference between control an omeprazole groups (t-test, p=0.003).

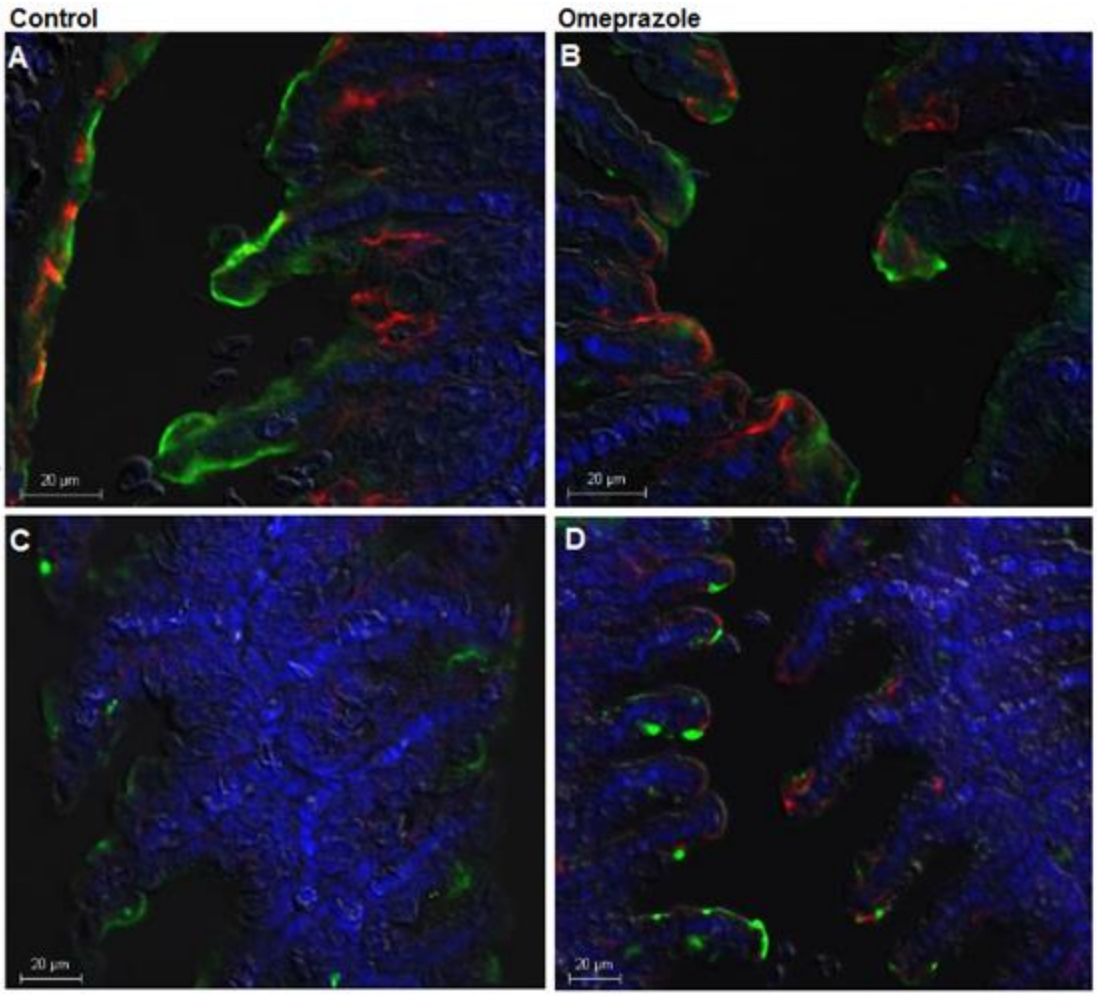

Figure 3.16: Immunohistochemistry of control (A and C), and omeprazole injected (B and D) lamprey *Petromyzon marinus* gill. In the top panels, DAPI (blue), non-gastric H^+/K^+-ATPase (green), and Na^+/K^+-ATPase (red). In the bottom panels, DAPI (blue), V-ATPase (green), and Na^+/K^+-ATPase (red). Scale bar is 20 µm.

Chapter 4:
Potassium and Acid-base Regulation in the Lungfish (*Protopterus annectens*): A Role for the Non-gastric H^+/K^+-ATPase?

ABSTRACT

African lungfish (*Protopterus annectens*) are a unique fish, with the capability to breathe air and enter a state of estivation during unfavourable environmental conditions. Currently, there is no mechanism to explain branchial potassium (K^+) uptake in lungfish. It was hypothesized that an ion pump known as the non-gastric H^+/K^+-ATPase (ngHKA) plays a role in K^+ and acid-base regulation in lungfish. The objective of this chapter was to characterize the potential roles of the ngHKA in the African lungfish by studying the pump's response to K^+ and acid-base disturbances. Responses of the pump were examined by qPCR, Western blotting, immunohistochemistry, and rubidium (Rb^+) and proton fluxes. There was Rb^+ (K^+) uptake but no significant differences in Rb^+ or proton fluxes in any treatments. Transcript or protein expression also did not change during any of the K^+ or acid-base disturbances. The Na^+/K^+-ATPase (NKA) and ngHKA protein levels were decreased in the omeprazole treated groups. Immunolocalization staining patterns showed epithelial and apical staining (which appeared stronger in the acid treated fish) of ngHKA. This is the first study to investigate the ngHKA in lungfish and although expressed in the gills, no evidence was found for an active role in K^+ and compensation for acid-base disturbances.

4.1 INTRODUCTION

Sarcopterygians or lobe finned fishes, including the lungfishes are the closest ancestors of tetrapods (Brinkmann et al., 2004). The African lungfish (*Protopterus* annectens) are obligate air breathers, meaning they must breathe air or they will die (Ballantyne and Frick, 2006). Lungfish have true lungs and reduced gills with fewer

filaments and irregular secondary lamellae (Laurent et al. 1978; Burggren and Johansen 1986). Ninety percent of respiration occurs through air breathing via the lungs but lungfish still rely on their gills for ion regulation and nitrogenous waste excretion (Evans, 1979; Glass, 2010). *P. annectens* can enter a state of torpor or estivation for years at a time during times of drought (Smith, 1931; Ballantyne and Frick, 2006). In lungfish and amphibians, during estivation there is a downregulation of many normal body functions including gas exchange, heart rate, and cardiac work (Glass et al., 1997). In the species *P. aethiopicus*, estivation caused a 50% reduction in oxygen consumption (Smith, 1931; Lahiri et al., 1970, Fishman et al., 1986), and in *P. annectens* there was a decrease in mRNA expression of the epithelium sodium channel (ENaC) (Uchiyama et al., 2015). Therefore, it was predicted that a downregulation of the ngHKA would also occur during estivation.

Teleost fish have branchial O_2 receptors that monitor the oxygen in the water and blood (Glass, 2010) but lack CO_2/pH chemoreceptors (central chemoreceptors) (Gilmour and Perry, 2007). Like land vertebrates, lungfish can also monitor and adjust acid-base status through respiratory ventilation (Gilmour et al., 2007; Glass, 2010). Gilmour and colleagues (2007) provided evidence for CO_2/pH chemoreceptors in *P. annectens* that initiate ventilation adjustments in response to acid-base disturbances. An increased ventilation response has been seen with increased PCO_2 as well as decreased pH in lungfish, amphibians and mammals (Glass, 2010). Air breathing can become crucially important during times of hypoxia and hypercapnia and it is believed that vertebrates developed lungs before they developed proper limbs and locomotory systems to invade terrestrial habitats. Studying lungfish can provide some interesting evolutionary insight

regarding the transition from aquatic living to terrestralization (Ballantyne and Frick, 2006).

Lungfish have mitochondrion-rich cells (MRCs) in the gills and skin epithelia (Sturla et al., 2001; Marshall and Grosell 2006). There is not much known about osmoregulatory strategies in lungfish. Wilkie and colleagues (2007) concluded that lungfish gills have low permeability to water and ions and rather the ventral surface of the skin is important for ion regulation in air exposed fish. The function of the external gills are currently unknown.

Lungfish were used to study the non-gastric H^+/K^+-ATPase (ngHKA) because they have the gene *atp12a*, unlike the teleost fish. Lungfish are also stomach-less and lack the gastric H^+/K^+-ATPase (gHKA) genes (*atp4a* and *atp4b*) which will simplify the interpretation of the results because only ngHKA is present (Wilson and Castro, 2010; Castro et al., 2014). Currently, information regarding osmoregulatory strategies is lacking, and there is no research on the ngHKA in lungfish. Food is an important source of ions (Patel et al., 2009), but potassium (K^+) can be taken up from the water when food is not readily available. Early studies in rainbow trout suggest branchial uptake from the water is a possibility, but the mechanism remains unknown (Eddy, 1975; Gairdaire et al., 1991, Gardaire et al., 1992).

The goal of this chapter is to understand lungfish osmoregulation and specifically the role of the ngHKA. I tested the hypotheses that the ngHKA plays a role in K^+ and acid-base regulation in lungfish. To do this, K^+ and acid-base disturbances were placed on fish and the response of the pump was examined at the mRNA level, as well as protein expression, localization, and ion fluxes. Additionally, the ion pumps, Na^+/K^+-ATPase

(NKA) and V-ATPase were also examined in conjunction with the ngHKA because they also move K^+ and proton ions in and out of the cell.

4.2 METHODS

4.2.1 Experimental Animals

African lungfish (*Protopterus annectens)* were flown from Nigeria to Waterloo, Ontario, Canada (Fish Orchard Company, Lagos Nigeria) (n=50). Upon arrival, lungfish were placed in individual 5 L containers with 2-3 L of 2:1 dechlorinated city water to reverse osmosis (RO) water at a room temperature of 27°C ± 2°C. Lungfish were fed approximately 2 g of basa fillets (*Pangasius bocourti*) containing about 8.6 mg of K^+ (Monday, Wednesday, Friday) and the tank water was changed 3 times a week or when soiled by defecation. The room light was set to a 12h: 12h light: dark photoperiod. This project was approved by Wilfrid Laurier University's Animal Care Committee and followed the guidelines from the Canadian Council of Animal Care (AUP R14002).

4.2.2 Experiment 1: K^+ Disturbance

Fasted lungfish for 14 days were considered low K^+ treatments. Fed fish were given a regular diet (3 days a week), which ceased 24 hours prior to the experiment. For flux measurements, lungfish were placed in individual boxes with 1L of 2 parts dechlorinated tap water, 1 part RO water and RbCl was added to a final concentration of 1mmol/L just prior to the start of the experiment (static system). A 15 mL water sample was taken at time 0, 6, and 12 h for ammonia and titratable acidity measurements.

4.2.3 Experiment 2: Acid-base Disturbance

Fish were fasted for 24 hours prior to the experiment. Treatments for the acid-base experiments included 1.5 µmol/kg H_2SO_4 injections (e.g. Cameron and Kormanik, 1982), and 3 µmol/kg M $NaHCO_3$ (e.g. Tresguerres et al., 2007), along with a 0.75 µmol/kg NaCl control. Before being injected (0.5 ml/kg), fish were anesthetized with 0.75 g/L of tricaine methanesulfonate (MS222, Sigma-Aldrich) and 1.5 g/L of sodium bicarbonate, and weighed for calculation of the injection volume. Water samples were taken according to 4.2.2.

4.2.4 Experiment 3: Omeprazole

Fish were fasted for 24 hours prior to the experiment. Treatments for the omeprazole experiments include a 0.6 µmol/kg omeprazole injection made with 2% DMSO. The control was 0.75 µmol/kg NaCl injection made with 2% DMSO. Before being injected (0.5 ml/kg), fish were anesthetized with 0.75 g/L of MS222 and 1.5 g/L of sodium bicarbonate. Fish were injected twice with omeprazole (or saline control), the first time was 16h before the start of the experiment and at time 0. Water samples were taken according to 4.2.2.

4.2.5 Experiment 4: Estivation

In an experiment conducted at National University of Singapore (Y.K. Ip), lungfish internal and external gill samples were taken during estivation from 3 to 46 days in both air and mud. Additionally, some fish were returned to water for 1 day or 2 days following

the 46 days of estivation. Gills samples were prepared for Western blotting and analyzed for ngHKA.

4.2.6 Sampling

Fish were euthanized at 6 or 12 hours using 1.5 g/L of MS222 and 3 g/L of sodium bicarbonate. Blood samples were taken by caudal puncture and spun down (1 min, 14 000 rcf) and the plasma was separated from the red blood cells in order to measure plasma K^+ concentrations. Gill tissues were dissected and placed in either a homogenization tube for Western blotting, fixative for immunohistochemistry, or in foil for RNA extractions and snap frozen in liquid nitrogen or dry ice. Approximately 1 gram of muscle was excised from the posterior-dorsal region and placed in a pre-weighed tube where it was dried in an oven for 48 hours at 70°C. Five mL of concentrated HNO_3 was then added to the tube to digest the muscle so rubidium (Rb^+), Na^+, and K^+ uptake could be measured.

4.2.7 Analytical Techniques

Western Blotting

Protein expression was measured using SDS-PAGE (sodium dodecyl sulfate polyacrylamide gel electrophoresis) and Western blotting according to Wilson et al. (2007) (see chapter 2 and appendix C for further details). In short, samples were homogenized in RIPA buffer and centrifuged. The supernatant was mixed with equal volume of 2x Laemmli's buffer and heated at 70°C for 10 min. The final concentrations were adjusted to 1 µg/µl. Gels were run and transferred to Immobilon PVDF membranes (pore size 0.45 µm, Millipore, Billerica USA). Membranes were blocked with a 5% skim milk/TTBS

solution and probed with LF12Arb for ngHKA (1:1000), αR1 (1:1000) for NKA, B2 for V-ATPase (1:500), and 12g10 for tubulin (1:200) overnight at room temperature. Secondary antibodies were goat anti-rabbit or anti-mouse horse radish peroxidase (1:50 000) and membranes were imaged using the c300 Azure Biosystems documentation system using enhanced chemiluminscence (ECL) (Clarity, Bio-Rad).

Immunohistochemistry

Localization of ion pumps was determined using the techniques outlined in Wilson et al. (2007), with the addition of tyramide signal amplification (Life Technologies, Carlsbad USA), according to manufacturer's instructions. More details are also found in chapter 2 and appendix B. In short, gill tissue was fixed using 3% paraformaldehyde in PBS and embedded in paraffin. Sections were dewaxed at 60°C, run through a xylene and alcohol series, rehydrated, and antigen retrieval performed including 0.05% citraconic anhydride (Namimatsu et al., 2005) and 1% SDS/PBS (Brown et al., 1996). Sections were blocked with BLØK (Life Technologies). Sections were probed with the primary antibodies LF12Arb2 (1:500) + α5 (1:250), pre-immune serum (1:500) + J3 (1:250), or B2 (1:500) + α5 (1:250), incubated overnight at 4°C. The secondary antibodies were goat anti-rabbit HRP (1:200) and Alexa-555 (1:500) (Life Technologies) applied for 1 hour at 37°C. Labelled tyramide (Alexa 488) in amplification buffer/0.0015% H_2O_2 was applied for 10 minutes. Negative controls include the pre-immune serum. Sections were imaged using a LEICA DM5500 B microscope and Hamamatsu C11440 Orca-Flash 4.0 digital camera.

Transcript Level Expression (mRNA)

Total RNA was extracted from gill tissue using Bio-Rad PureZOL™ RNA Isolation Reagent and Bio-Rad Aurum™ Total RNA Mini Kits using the spin protocol with on-

column DNase I treatment according to manufacturer's instruction. The quantity and purity of RNA was checked using BioTek Synergy HT Spectrophotometry (Take 3 plate). RNA quality was checked by running samples on an agarose formaldehyde gel to make sure there was no genomic DNA contamination or degradation of samples. RNA was then reverse transcribed to cDNA using High Capacity cDNA Reverse Transcriptase Kits (Applied Biosystems). Gene-specific primers were then used to amplify cDNA fragments by PCR. A PCR reaction was initially completed for actin and samples were then run on a 2% TBE agarose gel for quality control. All primers were standardized by running a dilution series of the pooled samples in order to create standard curves to determine qPCR efficiency (E=0.9-1.1). The qPCR (CFX96 Real-Time, Biorad) reactions were run in 5 µl of 50x diluted samples using gene-specific primers (Table 4.1) and Bio-Rad SybrGreen Mix in a 20 µl reaction volume. The comparative CT method ($2^{-\Delta\Delta CT}$ method) based on cycle threshold (CT) values were used to analyze expression levels of the genes of interest with actin used as a reference gene (Livak 2001). The qPCR results were then analyzed using Bio-Rad CFC Manager software (Appendix D).

Flux Measurement - Rb^+, K^+, and Na^+

Fish were placed in individual flux boxes. A final concentration of 1 mmol/L of RbCl was added to the water, mixed and water samples were taken at 0, 6 and 12 hours to monitor Rb^+ appearance in the animal in order to determine Rb^+ uptake rates. Rb^+, K^+ and Na^+ concentrations were measured on PinAAcle 900T Atomic Absorption Spectrophotometer (Perkin Elmer Waltham MA) in flame mode. HNO_3 and CsCl were added to the samples at final concentrations of 0.1% and 0.2%, respectively. Standards ranged from 0-5 µM for Rb^+, 0-7.5 µM for K^+, and 0-22 µM for Na^+. Muscle samples were

diluted 50x, 10000x, and 1000x for Rb^+, K^+ and Na^+ respectively, with milliQ water to avoid any saturation problems. Plasma K^+ and Na^+ samples were diluted 1000x and 10000x respectively. Uptake rates were calculated in µmol/kg/h, muscle concentrations in µmol/g wet weight, and plasma concentrations in mmol/L.

Ammonia and Titratable Acidity

Ammonia in water samples was measured spectrophotometrically (Spectramax 190, Molecular Devices, Sunnyvale, CA) using a standard ammonia assay (Verdouw et al., 1978). Samples were diluted 10x to fall within the standard curve range of 0-150 uM and read at 650 nm. Ammonia (J_{amm}) efflux rates were calculated in µmol/kg/h. Ammonia is a good buffer and traps some of the acid which is why it is taken into account. Titratable acidity (J_{TA}) was determined using Radiometer Copenhagen TTT80 Titrator and ABU80 Autoburret with a PHM84 pH and Hamilton pH electrode. Samples (10mL) were aerated for 1 hour to remove CO_2 and titrated with 0.01 N HCl with continued aeration until a pH of approximately 4.5 and then brought to a final pH of 4 using 0.005 N HCl. Titrant volumes were then multiplied by the respective HCl concentration to give µmol H^+ in 10 mL water samples. Those values were then multiplied by 100 to correct for the total volume of water the fish was in (1 L), divided by fish mass (kg) and flux period time (h) to give flux rates as µmol/kg/h. The net acid flux (J_{H+}) was calculated in µmol/kg/h using the relationship:

$$J_{H+} = J_{TA} + J_{amm}$$

(Wood and Caldwell, 1978).

4.2.8 Statistical Analyses

Data are reported as mean values ± standard error the mean (s.e.m). Two-way and one-way ANOVAs as well as t-tests were used to test for differences between treatment groups and flux times. If a significant difference was found by ANOVA, a post hoc Holm-Sidak test was done. In the case of non-normality and/or unequal variance, an equivalent, non-parametric test was used (Mann-Whitney rank sum test, Kruskal-Wallis). $P<0.05$ was deemed the level of significance for all tests and were done using SigmaPlot (11, Systat, San Jose USA).

4.3 RESULTS

The tissue profile Western blotting results were consistent with the qPCR data showing gill and kidney to have high expression levels of the ngHKA (lanes 7 and 9, Fig. 4.1). Rb^+ uptake was successfully measured. Average control uptake rates were 26 µmol/kg/h and 18 µmol/kg/h at 6 and 12 hours respectively.

4.3.1 Experiment 1: K^+ Disturbance

There was no significant difference in the net acid excretion (J_{H+}) between the fed (n=4) and fasted (n=4) lungfish (p=0.55) or between 6 and 12 hours (p=0.23) (Fig. 4.2). Rb^+ uptake rates were significantly lower at 12 hours compared to 6 hours in both the fed (n=4) and fasted (n=4) fish ($p<0.0001$) (Fig. 4.3). At the transcript level of expression, there were no differences in *atp12a* or any of the other ion transport genes between fed (n=6) and fasted (n=8) animals (Table 4.2). At the protein level of expression there were no differences between fed (n=8) and fasted (n=8) lungfish in the ngHKA (p=0.44), NKA

(p=0.51) or V-ATPase (p=0.48) (Fig. 4.4). No differences were seen in fed (n=8) and fasted (n=8) muscle [Na^+] or plasma [K^+] (Table 4.3). Control localization is shown in figures 4.5-4.6. The ngHKA staining is spread throughout the entire epithelium with NKA basolateral staining. V-ATPase staining is also throughout the epithelium, with some cells staining sharper apically. Unfortunately the immunohistochemistry samples for fed and fasted lungfish were ruined due to an embedding machine malfunction.

4.3.2 Experiment 2: Acid-base Disturbance

There was no significant difference in the net acid excretion (J_{H+}) between the acid loaded, based loaded, or control lungfish (n=4, p=0.07) or between 6 and 12 hours (p=0.66) (Fig. 4.7). No significant difference was found in Rb^+ uptake between any of the treatment groups (n=4, p=0.87) or between time (p=0.16) (Fig. 4.8). At the transcript level of expression, there were no differences in any of the genes between the controls, acid, or base loaded animals (n=8) (Table 4.2). At the protein level of expression there were no differences between the control, acid, or base loaded lungfish (n=8) in the ngHKA (p=0.11), NKA (p=0.92), or V-ATPase (p=0.47) (Fig. 4.9). There were no differences in muscle or plasma [Na^+] or [K^+] (n=8) (Table 4.3). Localization of ngHKA, NKA, and V-ATPase are shown in figure 4.10. The NKA stains basolaterally, some cells have near continuous, weaker staining, while other isolated cells are staining stronger and are more isolated all along the secondary lamellae. The ngHKA staining is throughout the epithelium in the control and base loaded lungfish, with some areas staining apical in the acid treated fish. The V-ATPase staining in the base treated lungfish is punctuate and more apical staining appears in the acid loaded fish.

4.3.3 Experiment 3: Omeprazole

There was no significant difference in J_{H+} between the control (n=4) or omeprazole (n=4) treated lungfish (p=0.55) (Fig. 4.11). No significant differences in Rb^+ uptake rates were found between control (25.4 µmol/kg/h ± 2.6) and omeprazole, (25.4 µmol/kg/h ± 0.7) lungfish (n=4, p=0.34). At the transcript level of expression, there were no differences in any of the genes between the two treatment groups (n=4) (Table 4.2). At the protein level of expression there were no differences between the control or omeprazole loaded lungfish (n=8) for the V-ATPase (p=0.65), but there was significantly lower expression of ngHKA (p=0.045) and in the NKA (p=0.025) in omeprazole treated fish (Fig. 4.12). There were no differences in muscle or plasma [Na^+] or [K^+] (n=4) (Table 4.3). Localization of ngHKA, NKA, and V-ATPase are shown in figure 4.13. The NKA staining is basolateral in isolated cells along the sides of the secondary lamellae. The ngHKA and V-ATPase is staining through the entire epithelium in all groups.

4.3.4 Experiment 4: Estivation

There were no differences in either internal (n=3-5, p=0.6) (Fig. 4.14) or external gill (n=3-4, p=0.06) protein expression of the ngHKA between the estivating fish and controls.

4.4 DISCUSSION

As expected, the ngHKA expression was high in the gill and kidney tissue. Because the gill is the main ion regulation organ in fish (Evans et al., 2005), this was the tissue that

warranted further investigation. The gills are in direct contact with the water which allows for the transfer of ions between the animal and their environment. Lungfish however do differ from other fish by having reduced gills and the ability/reliance to breath air. The reduced gills affect water O_2 uptake, but the gill is still thought to be important for ionic exchange (Gilmour et al., 2007). The ability of lungfish to survive in air, may shift to a higher reliability on the kidney for ion regulation, similar to tetrapods, and should be further investigated in future studies. There were no differences in ngHKA expression during estivation. Wilkie et al. (2007) and Patel et al. (2009) found no differences in plasma Na^+ and Cl^- levels during estivation in *P. dolloi*. Lungfish awaken and recover quite quickly, perhaps explaining the maintenance of important ion proteins during estivation (Wilkie et al., 2007). It is important to note that the gills are not functional in air and the ventral skin should be a tissue of investigation in estivation studies.

It has been predicted that lungfish ion flux rates are much lower compared to teleost fish (approximately 90% lower) (Wilkie et al., 2007). Na^+ and Cl^- flux rates in *P. dolloi* were found to be 44 and 100 µmol/kg/h in fed fish respectively (Patel et al., 2009). Eddy (1985) predicted that K^+ rates were 3-5% of Na^+ rates. In this study, fed lungfish had average Rb^+ flux rates of 22 µmol/kg/h in fed *P. annectens*. These rates are lower than Na^+ flux rates (22-50%), however not as low as Eddy (1985) predicted (1.3-5.0 µmol/kg/h), possibly due to the already low flux rates compared to teleost fish. Additionally, teleost fish do not have the ngHKA and lack this potential K^+ uptake mechanism. However, Oduleye (1977) predicted Na^+ efflux to be 200-500 µmol/kg/h in *P. annectens* which the rates found in this study also using *P. annectens* are 3-5% of those, suggesting there may be species differences in *P. dolloi* and *P. annectens* such as the case in CO_2 unloading

strategies (Perry et al., 2005; Wilkie et al., 2007). It has been suggested that these low flux rates and ion levels are beneficial by minimizing ionic gradients and thus being more metabolically favourable (Iftikar et al., 2008). It is also possible that the cold Rb^+ and atomic absorption spectrometer does not provide enough resolution to detect the very small changes that may be occurring. The use of radiolabelled rubidium ^{86}Rb may provide more resolution. The flux rates are also lower in the 12 hour samples possibly due to the fish being calmer. Future studies are advised to allow for a longer acclimation time before beginning the experiment.

There were no differences in mRNA expression in any of the pumps examined between any of the treatments. Gilmour et al. (2007) investigated the effects of metabolic acid-base disturbance in *P. annectens* and found no differences in mRNA expression in carbonic anhydrase, V-ATPase, or Na^+/HCO_3^- cotransporter either. However, in other species of fish such as rainbow trout, transcription regulation of proteins during acid-base stressors has been previously found (Galvez et al., 2002; Hirata et al., 2003; Perry et al., 2003a; Perry et al., 2003b; Georgalis et al., 2006). It could be that the challenges were not strong enough to elicit any changes or that the increase in activity is not needed to deal with the disturbance (Gilmour et al., 2007). Additionally, post-translational modifications may be involved (Tresguerres et al., 2005; Tresguerres et al., 2006), or perhaps the sampling times did not parallel the changes (Gilmour et al., 2007). Unfortunately it was not possible to address these factors because of limited numbers of animals and the need to try and find a good balance with the flux rate sampling time points. NetPhos (http://www.cbs.dtu.dk/services/NetPhos/) predicted 19 possible phospohorylation sites, with 80% confidence set as the threshold. Another point to consider is the possibility for

aerial breathing. Aerial breathing was available to the lungfish and was not measured in this study. Gilmour et al. (2007) concluded that respiratory compensation accounted for 77% of the acid load and 46% of the base injected lungfish. This could also explain why there were no differences in the net acid excretion to the water.

It was predicted that fasted and acid loaded lungfish would have an upregulation in ngHKA protein expression in order to take up K^+ or pump out protons, respectively. However only a downregulation in ngHKA and NKA expression was seen in the omeprazole treated fish, but this was not paralleled with a difference in Rb^+ uptake. No measured differences in protein expression could be explained by the fact that if de-novo synthesis is not occurring and the pump is stored in vesicles and gets translocated to the apical membrane when needed, similar to the gHKA (Sachs et al., 1976). However this was not seen from in the immunohistochemistry results.

The NKA staining in control animals is basolateral which is well characterized in other studies (e.g. Wilson and Laurent 2002; Wilson, 2011) but to my knowledge, has not been shown to date in lungfish. The control ngHKA staining is spread throughout the epithelium and the majority of NKA is staining is in separate cells, however there does appear to be a few cells where ngHKA and NKA are within the same cell. In rat colon cell, ngHKA and NKA have been observed to colocalize (Li et al., 2004) and in rat pancreatic ducts, ngHKA was at the apical side of the cell (suggesting a role in extruding protons generated by carbonic anhydrase) (Novak et al., 2011). The pre-immune serum control, shows no ngHKA staining, meaning it is specific. The V-ATPase control shows strong staining spread throughout the epithelium (stored in vesicle systems) with some sharp apical staining and once again NKA staining basolateral in separate cells.

For the acid-base experiments the control and base appear to have no major differences while the acid treatment group may have more strongly apical ngHKA staining. This observation requires further investigation and quantification. In mammalian stomachs, acid secretion causes the protein vesicle to fuse with a canaliculus on the apical membrane (Rabon and Reuben, 1990). The V-ATPase staining appears to be more punctate in the base treatment group and translocated to the apical membrane in the acid animals. No differences were seen between the NKA, V-ATPase or ngHKA in omeprazole treated fish. Choe and colleagues (2004) studied the gHKA in Atlantic stingray gill and found it to colocalize with NKA cells but not with V-ATPase rich cells. Similar to present results, Choe et al. (2004) did not observe unambiguous apical staining even in stingrays exposed to hypercapnia. They did however, find increased transcript level expression of the gHKA in freshwater acclimated stingray, suggesting a role in K^+ uptake in hypotonic environments (Choe et al., 2004). This also may become important during periods of starvation in fish, such as when migrating, however this was not seen in the fed and fasted lungfish. Perhaps the two weeks without food was not long enough in lungfish considering they can go years at a time without eating during estivation.

In conclusion, the results show no clear support for the hypothesis that the ngHKA plays a role in acid-base or K^+ regulation in African lungfish. Perhaps the ngHKA is important for intracellular K^+ regulation or for secondary active transport mechanisms. Development and validation of the ngHKA antibody is novel and will allow for future studies to investigate more precisely the localization of the ngHKA and further develop K^+ uptake methods by using radiolabelled ^{86}Rb.

Table 4.1: Primer pairs for qPCR in *Protopterus annectens.*

Gene	Forward primer 5'-3'	Reverse primer 5'-3'	Reference
atp12a	CTCACCAAGAACATCGCTGA	CGCTCTCGGGTTTCTCATAG	
PanAtp1a1q	ACAAGATCTCCTGAATTTTCCA	TGTGTTGTCACCAGTGTTAATG	Hiong *et al*. 2014
PanAtp1a2q	AGACATTGCAGCACGTCTC	CATTCATTTCCTTCAAATCCGAA	Hiong *et al.* 2014
PanAtp1a3q	CTCATGAGGGAAAAGTACAGA	CGATTATCATTAGGGTCTTCGG	Hiong *et al.* 2014
PanAtp6v1b	CCATGAAGGCGGTAGTCGGTGAG	TTGGGGAAGATTCGCAGCAGC	Gilmour *et al*. 2007
PanCAq	TGGACCCCTTGCTGGACACTTCA	ACCAATAACAGCCAGCCCGTCAG	Gilmour *et al*. 2007
PanScnn1q	TCCTTCAGAGACTTATGTACATCC	TAATACTAGTCTGGCTCATTCGTC	Gilmour *et a*l. 2007
PanNBCq	TTTCTGGGGCTGTCTTCTGT	AATGCTGACCACAAGCCAAT	Gilmour *et a*l. 2007
Pan18Sq	GGCGCTCCCTCGATGCTCTTAACT	GTCCCTCTTAATCATGGCCCCAGTTC	Gilmour *et al*. 2007

Table 4.2: Mean ± s.e.m normalized transcript expression levels of *atp12a* = ngHKA, *atp1a1, atp1a2, atp1a3* = NKA, *atp6v1b* = V-ATPase, *ca* = carbonic anhydride, *scnn1* = epithelial sodium channel, *nbc* = sodium bicarbonate exchanger in the gills of *Protopterus annectens*. Exp1: fed (n=6) and fasted (n=8); Exp2: acid-base loading (n=8); Exp3: omeprazole (OPZ) treatment (n=4). No statistically significant differences were found. Each gene was analyzed separately using a t-test or Mann-Whitney rank sum test (*) (experiments 1 and 3) or a One-way ANOVA or Kruskal-Wallis ANOVA on ranks (†) (experiment 2).

		atp12a	***atp1a1***	***atp1a2***	***atp1a3***	***atp6v1b***	***ca***	***scnn1***	***nbc***
Exp1	Fed	1.0 ± 0.30*	1.0 ± 0.18	1.0 ± 0.30	1.0 ± 0.46*	1.0 ± 0.31	1.0 ± 0.95*	1.0 ± 0.50*	1.0 ± 0.33
	Fasted	2.43 ± 1.24	1.30 ± 0.12	1.57 ± 0.27	0.68 ± 0.20	0.71 ± 0.16	0.08 ± 0.04	0.77 ± 0.11	1.01 ± 0.27
Exp2	Ctrl	1.0 ± 0.34†	1.0 ± 0.12†	1.0 ± 0.13	1.0 ± 0.10	1.0 ± 0.24†	1.0 ± 0.15†	1.0 ± 0.09†	1.0 ± 0.19†
	Base	1.61 ± 0.65	0.99 ± 0.11	1.30 ± 0.16	1.15 ± 0.13	1.47 ± 0.31	1.29 ± 0.29	1.02 ± 0.12	1.17 ± 0.22
	Acid	1.27 ± 0.34	1.21 ± 0.25	0.94 ± 0.10	0.83 ± 0.13	1.47 ± 0.38	0.97 ± 0.22	1.54 ± 0.30	1.10 ± 0.32
Exp3	Ctrl	1.0 ± 0.20	1.0 ± 0.18	1.0 ± 0.14	1.0 ± 0.17	1.0 ± 0.15	1.0 ± 0.13	1.0 ± 0.17	1.0 ± 0.21
	OPZ	0.70 ± 0.16	0.65 ± 0.13	0.95 ± 0.23	1.01 ± 0.36	1.01 ± 0.51	1.31 ± 0.39	0.55 ± 0.10	0.95 ± 0.37

Table 4.3: Sodium (Na^+) and potassium ion (K^+) concentrations ± s.e.m in fed and fasted (n=8), acid-base loaded (n=8), and omeprazole treat (n=4) *Protopterus annectens* muscle and plasma (µmol/g wet weight, mmol/L respectively). No statistically significant differences were found (Exp1 and 3: t-test, Exp3: One way ANOVA)

			Na^+	K^+
Muscle	Exp1	Fed	28.5 ± 15.3	26.7 ± 1.6
		Fasted	9.9 ± 3.0	27.2 ± 1.1
	Exp2	Ctrl	4.6 ± 1.5	27.6 ± 1.4
		Base	16.2 ± 4.6	26.4 ± 0.7
		Acid	13.8 ± 5.0	24.3 ± 1.5
	Exp3	Ctrl	7.5 ± 3.7	23.8 ± 0.9
		OPZ	6.5 ± 1.4	22.9 ± 1.0
Plasma	Exp1	Fed		8.7 ± 1.4
		Fasted		6.5 ± 0.4
	Exp2	Ctrl		7.1 ±1.4
		Base		6.7 ± 0.8
		Acid		7.5 ± 0.7
	Exp3	Ctrl		6.9 ± 1.0
		OPZ		7.5 ± 1.2

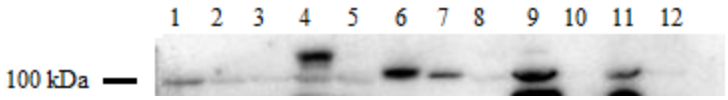

Figure 4.1: SDS-PAGE Western blot for *Protopterus annectens* tissues probed with a rabbit polyclonal LF12Arb2 antibody 1:1000. The 2º antibody was a goat anti-rabbit HRP detected with ECL. Lane: 1 anterior intestine, 2 mid intestine, 3 posterior intestine, 4 liver, 5 skin, 6 brain, 7 kidney, 8 muscle, 9 gill, 10 lung, 11 heart, 12 testes.

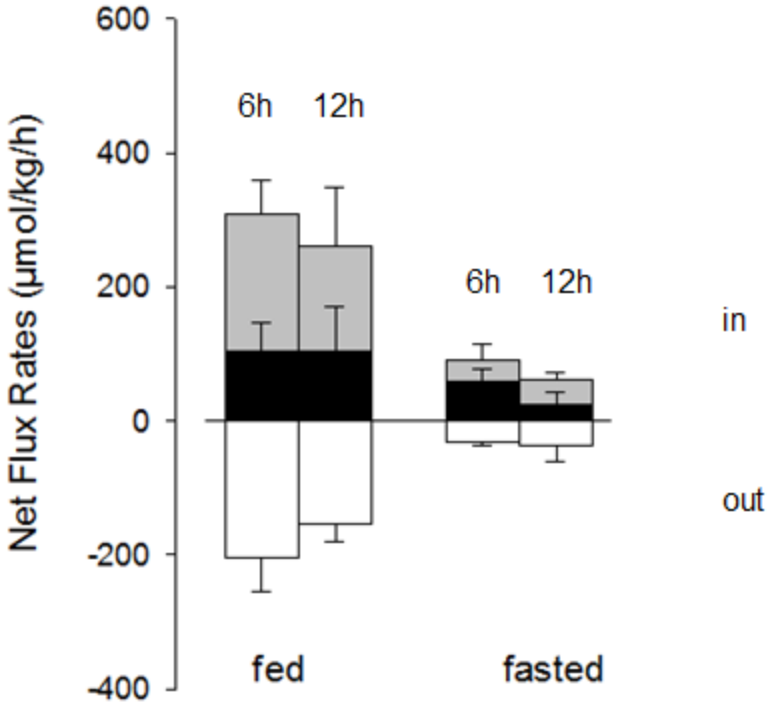

Figure 4.2: Net flux rates of ammonia (white; J_{amm}), titratable acidity (grey; J_{TA}) and acid (black; J_{H+}) in fed and fasted *Protopterus annectens* at 6 and 12 hours (n=4). No significant differences were found (Two-way ANOVA, p=0.55). Positive values indicate uptake while negative values indicate excretion.

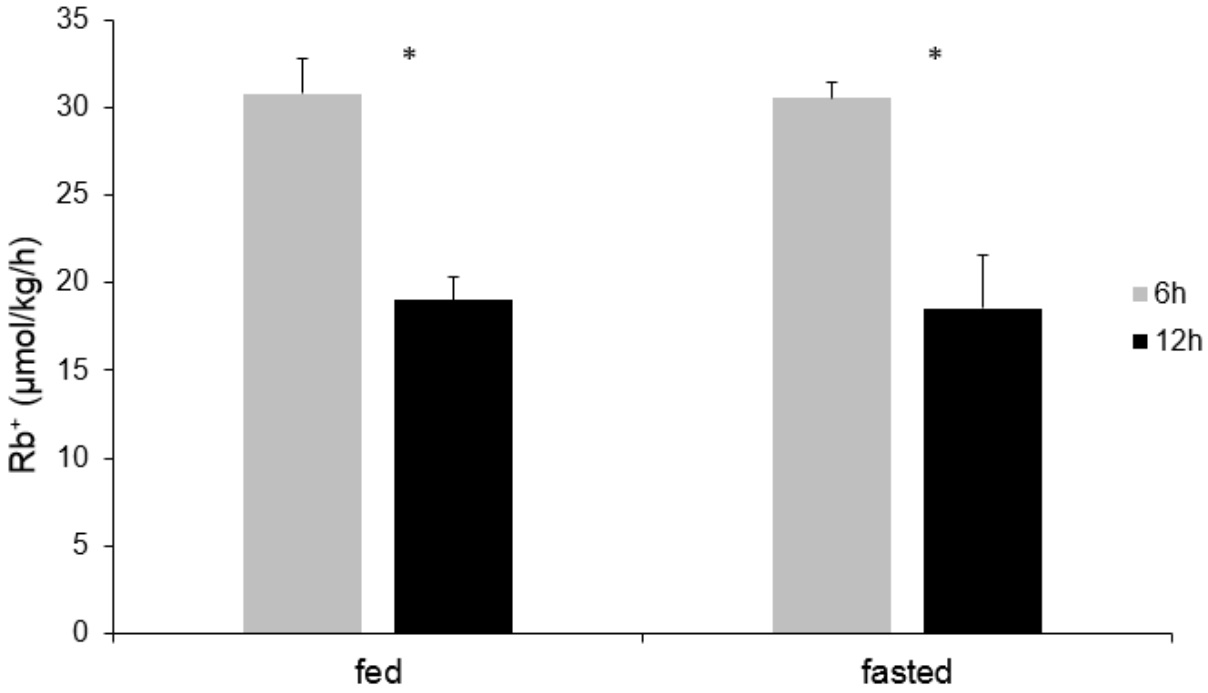

Figure 4.3: Rubidium (Rb^+) uptake rates in fed and fasted *Protopterus annectens* at 6 hours (grey) and 12 hours (black) (n=4). Asterisks represent significant differences between 6h and 12h ($p<0.0001$, Two-way ANOVA, Holm-Sidak post hoc).

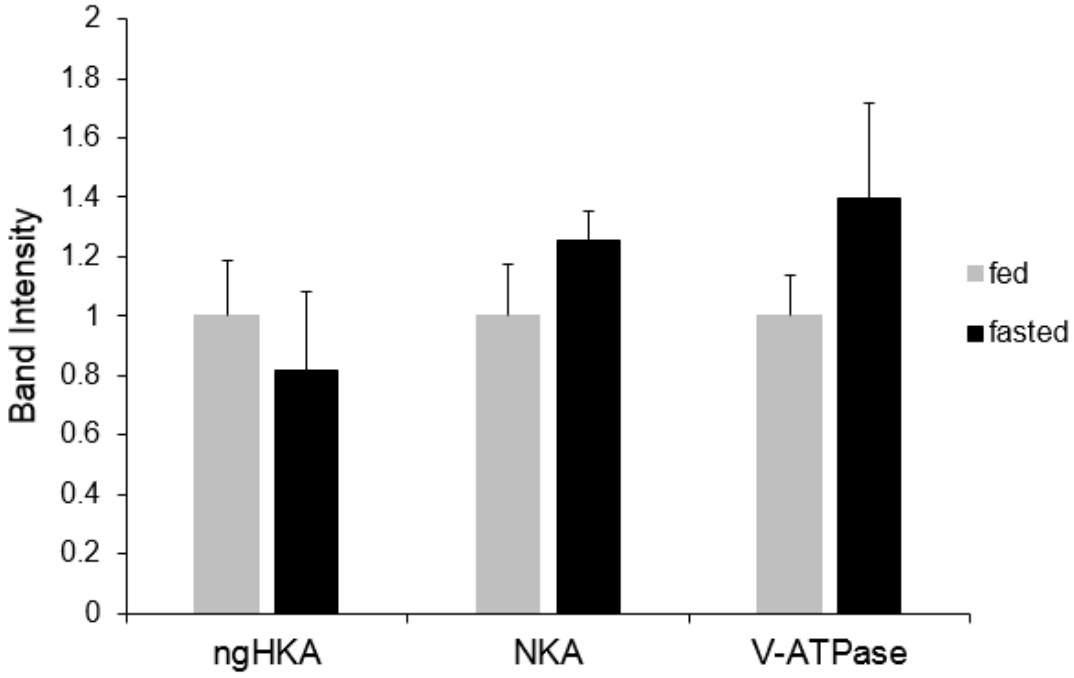

Figure 4.4: Relative band intensity of the non-gastric H^+/K^+-ATPase (ngHKA) α subunit, the Na^+/K^+-ATPase (NKA) α subunit, and the vacuolar proton pump V-ATPase B subunit, in fed (grey) and fasted (black) (n=8 for all) *Protopterus annectens* gill. No statistically significant differences were found (Man-Whitney rank sum test, p=0.44 for ngHKA; t-test, p=0.51, 0.48 for NKA and V-ATPase respectively).

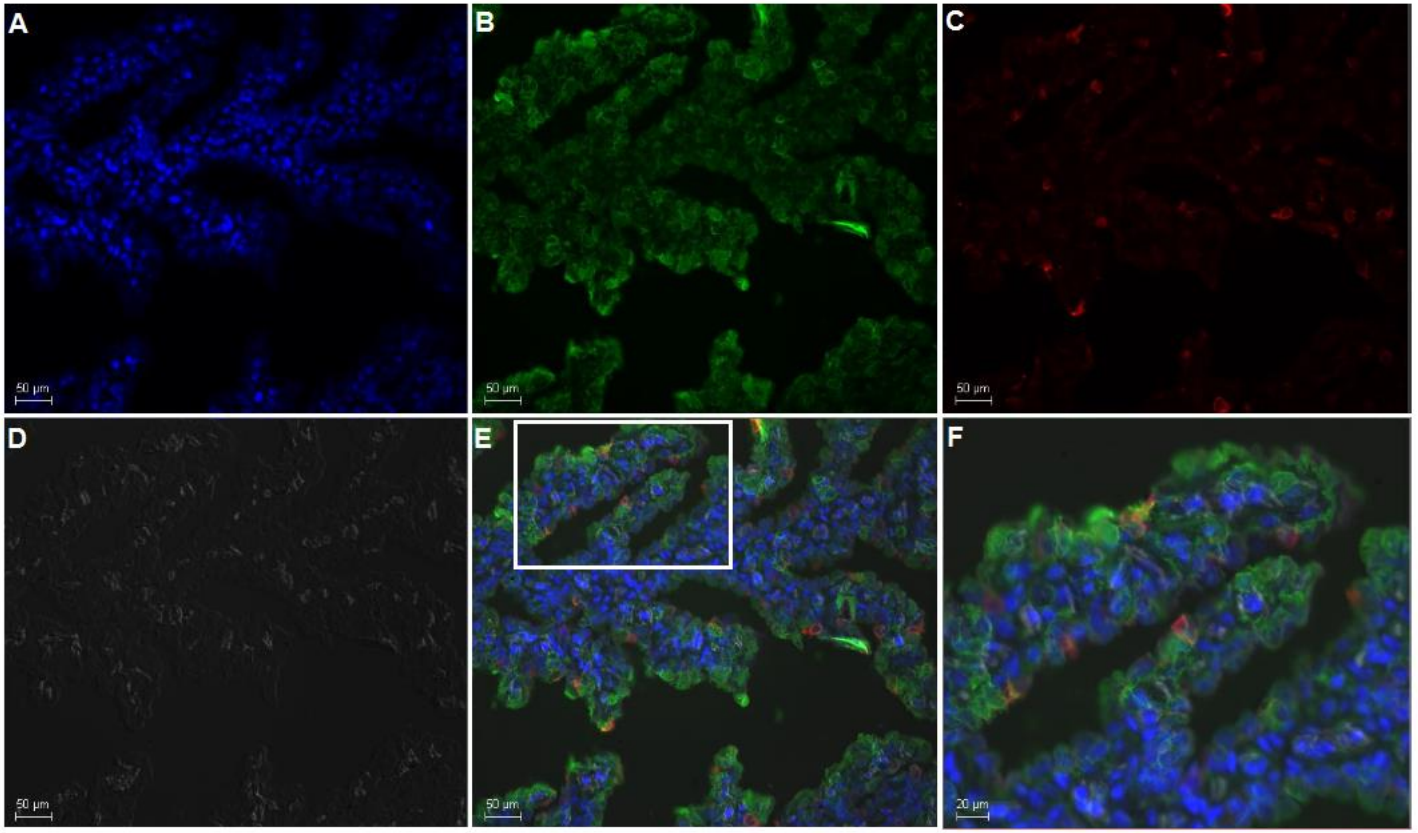

Figure 4.5: Immunohistochemistry of control lungfish *Protopterus annectens* gill A) DAPI (blue), B) non-gastric H^+/K^+-ATPase (green), D) Na^+/K^+-ATPase (red), D) DIC, E) overlay of A-D, and F) enlarged area of E. Scale bar is 50 µm A-E, 20 µm F.

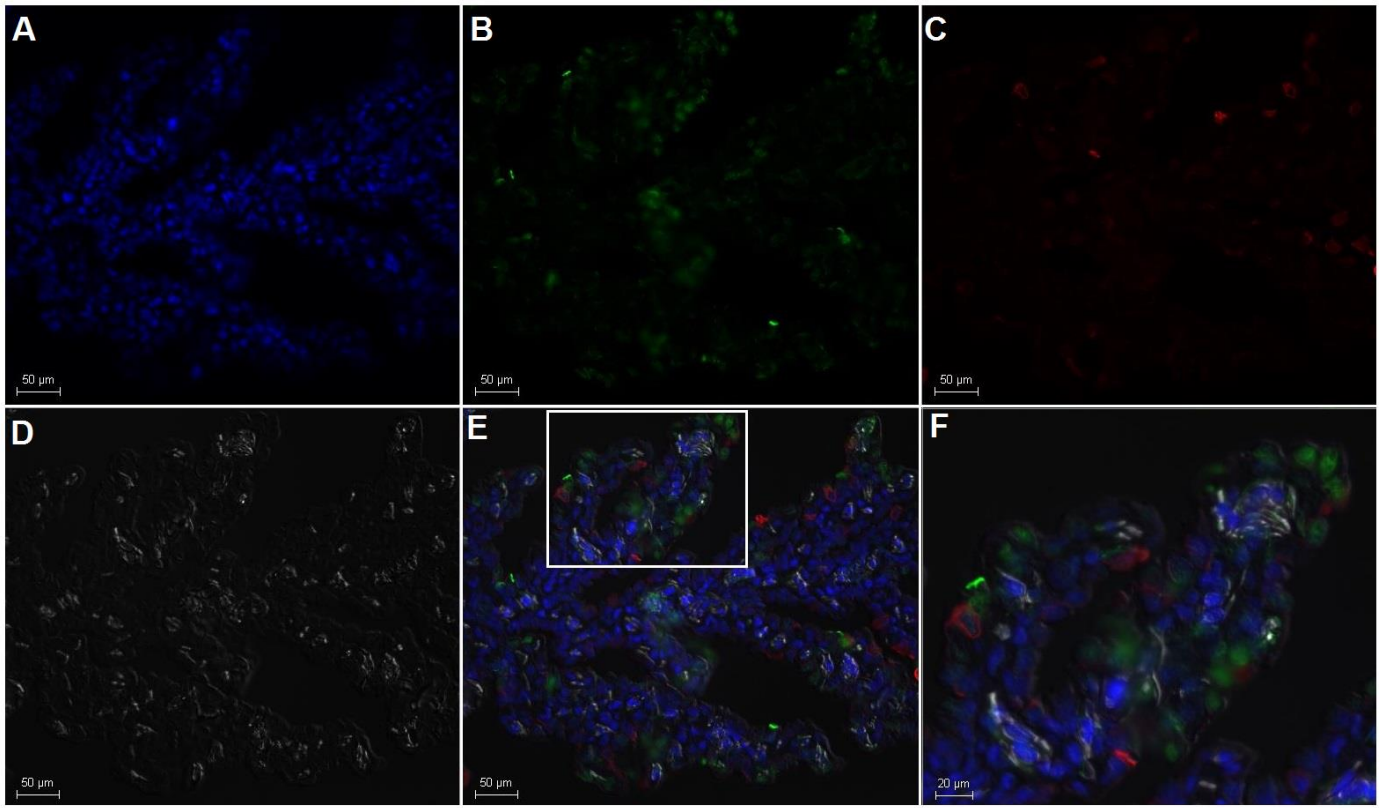

Figure 4.6: Immunohistochemistry of control lungfish *Protopterus annectens* gill A) DAPI, B) V-ATPase (green), C) Na^+/K^+-ATPase (red), D) DIC, E) overlay of A-D, and F) magnification of highlighted area in E. Scale bar is 50 µm A-E, 20 µm F.

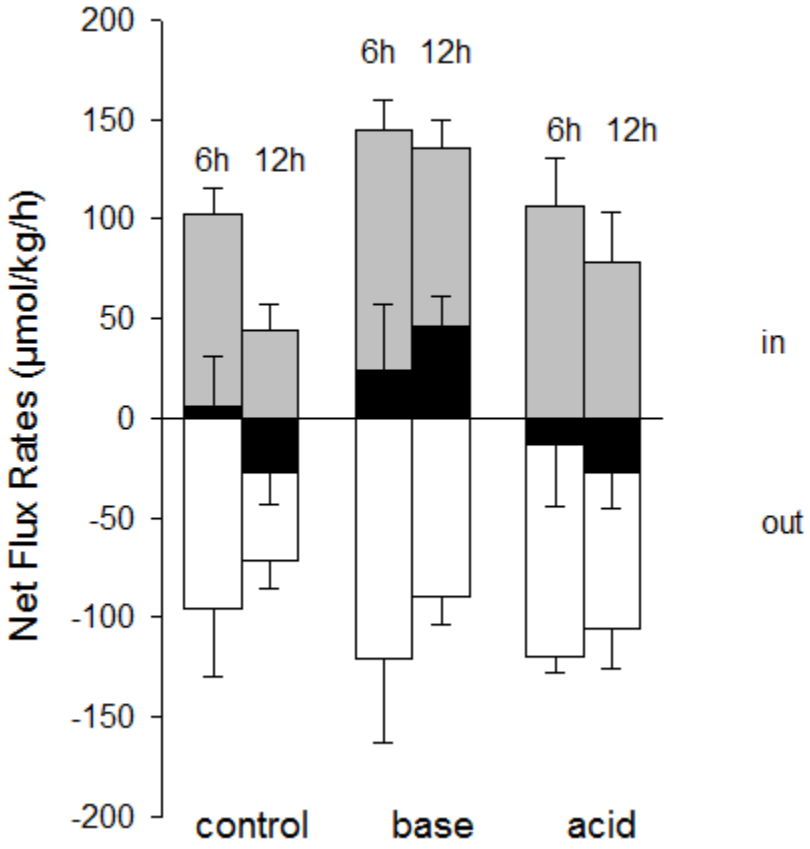

Figure 4.7: Net flux rates of ammonia (white; J_{amm}), titratable acidity (grey; J_{TA}) and acid (black; $_{H+}$) in control, base and acid loaded *Protopterus annectens* at 6 and 12 hours (n=4 for all). No statistically significant differences were found (Two-way ANOVA, p=0.07 for treatment effect, p=0.66 for time).

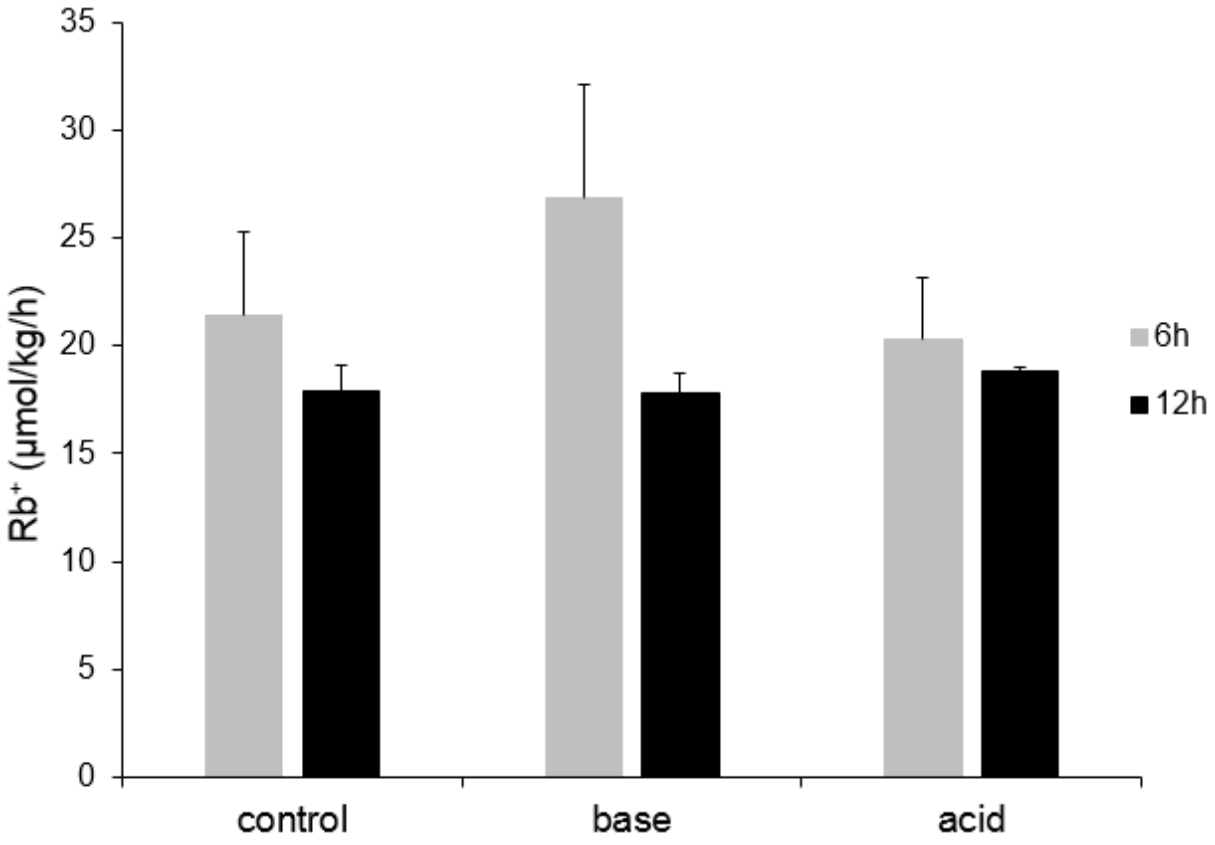

Figure 4.8: Rubidium (Rb^+) uptake rates in control, base and acid loaded *Protopterus annectens* at 6 hours (grey) and 12 hours (black) (n=4 for all). No significant differences were found (Two-way ANOVA, p=0.87 for treatment, p=0.16 for time).

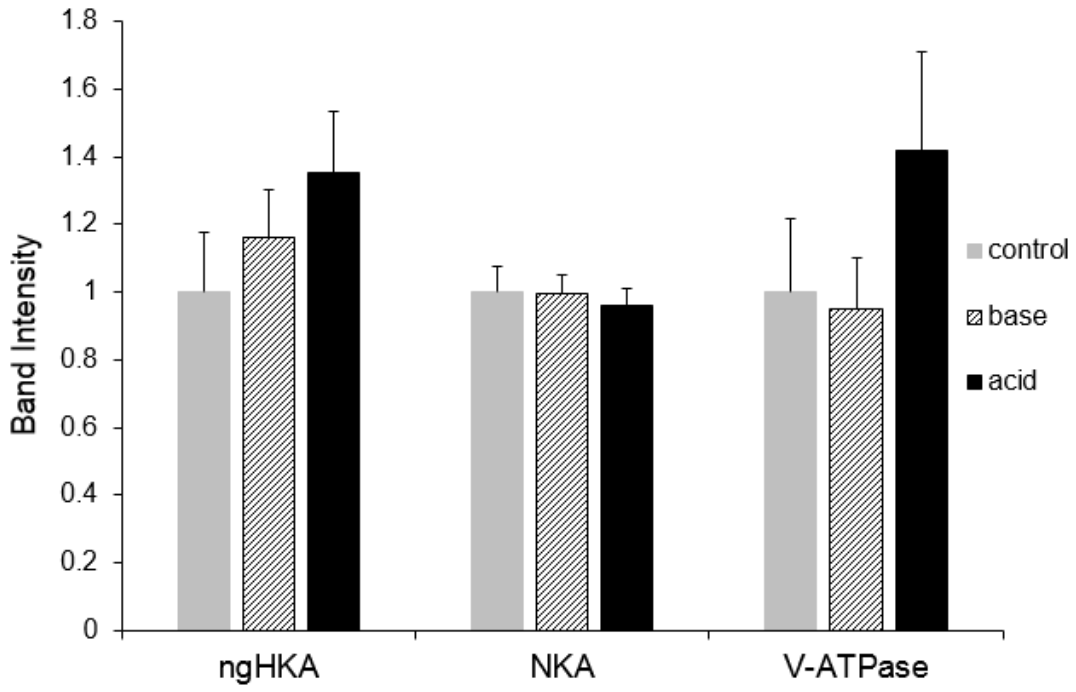

Figure 4.9: Semi-quantitative analysis of the non-gastric H^+/K^+-ATPase (ngHKA) α subunit, the Na^+/K^+-ATPase (NKA) α subunit, and the vacuolar proton pump V-ATPase, B subunit, in the gills of control (grey) base loaded (stripes) and acid loaded (black) (n=8 for all) *Protopterus annectens*. No statistically significant differences were found (Kruskal-Wallis One way ANOVA, p=0.11 for ngHKA, p=0.92 for NKA, p=0.47 for V-ATPase).

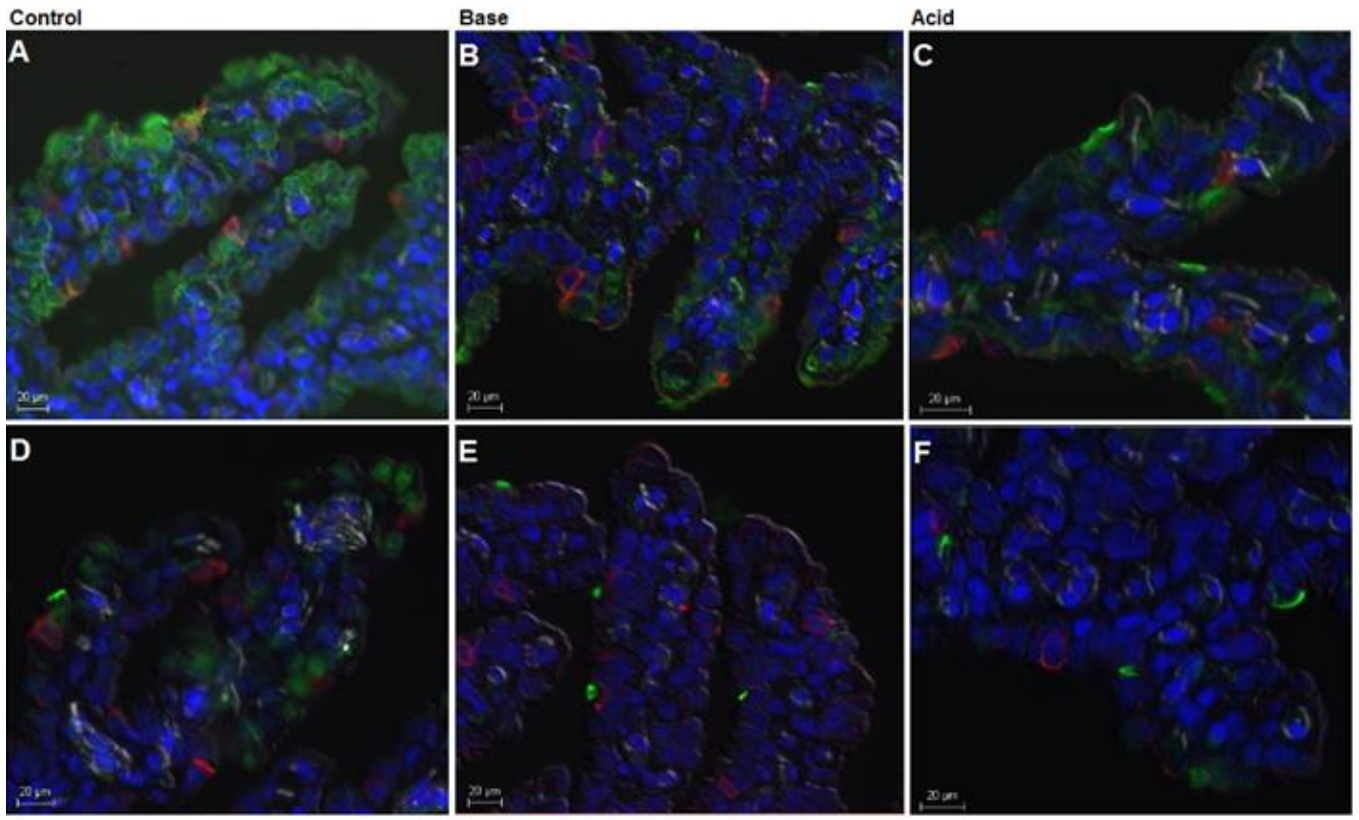

Figure 4.10: Immunohistochemistry of control (A and D), base loaded (B and E), and acid loaded (C and F) lungfish *Protopterus annectens* gill. In A, B, C sections are labelled with DAPI (blue), non-gastric H^+/K^+-ATPase (green), and Na^+/K^+-ATPase (red). In the D, E, F sections are labelled with DAPI (blue), V-ATPase (green), and Na^+/K^+-ATPase (red). Scale bar is 20 µm.

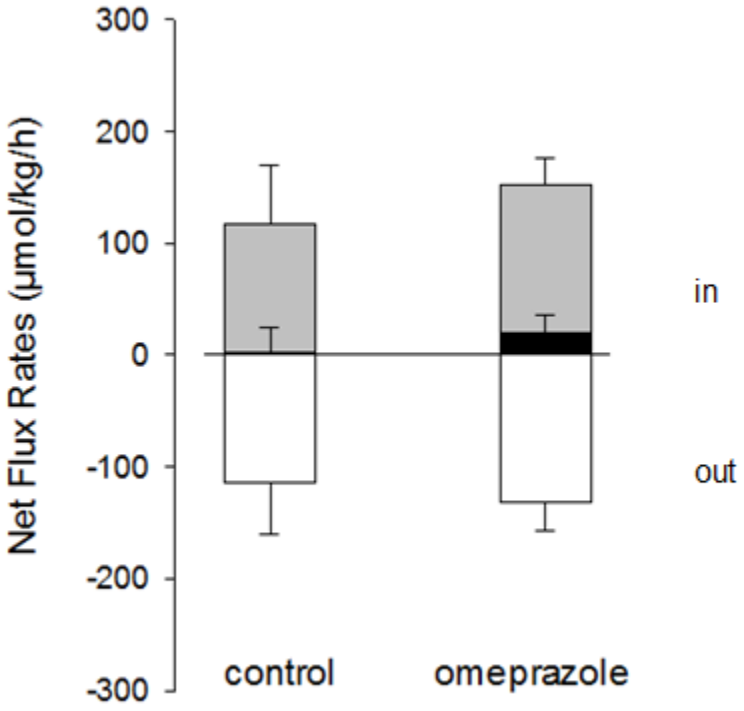

Figure 4.11: Net flux rates of ammonia (white; J_{amm}), titratable acidity (grey; J_{TA}) and acid (black; J_{H+}) in controls and omeprazole injected *Protopterus annectens* at 6 h (n=4). No statistically significant differences were found (t-test, p=0.55).

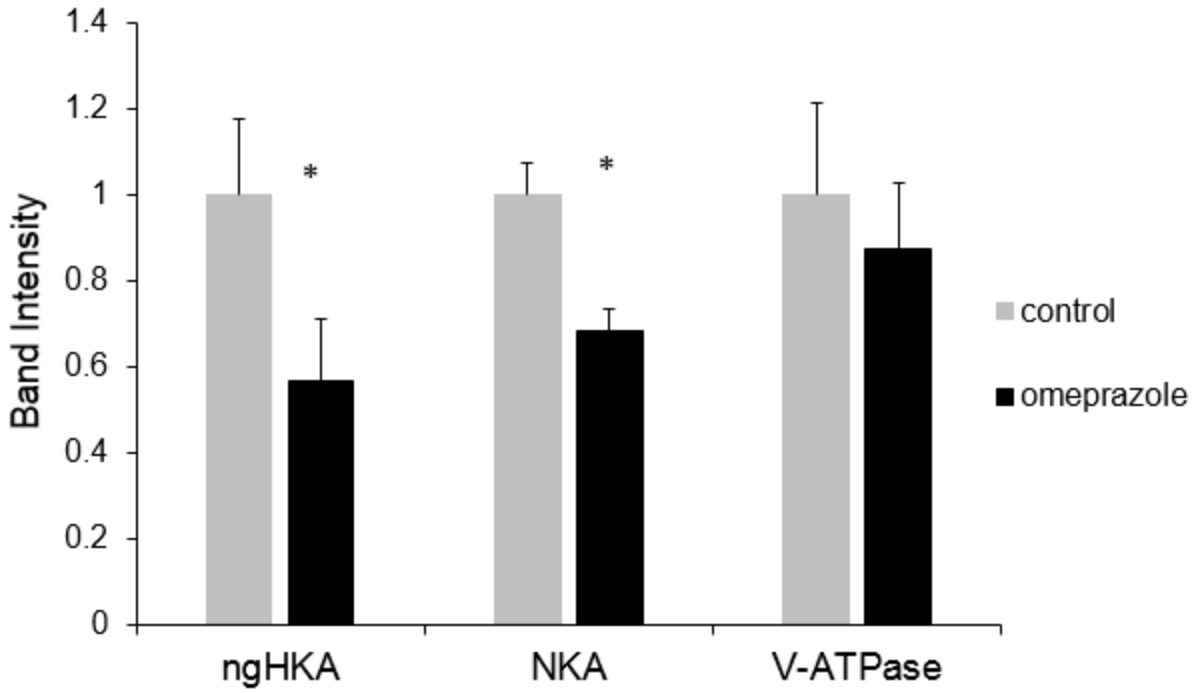

Figure 4.12: Relative band intensity of the non-gastric H^+/K^+-ATPase (ngHKA) α subunit, the Na^+/K^+-ATPase (NKA) α subunit, and the vacuolar proton pump V-ATPase B subunit in control (grey), and omeprazole injected (black) (n=8 for all) *Protopterus annectens* gill. Asterisks represent significant differences between control and omeprazole treated fish (t-test, p=0.045 for ngHKA, p=0.025 for NKA: Mann-Whitney rank sum test, p=0.65 for V-ATPase).

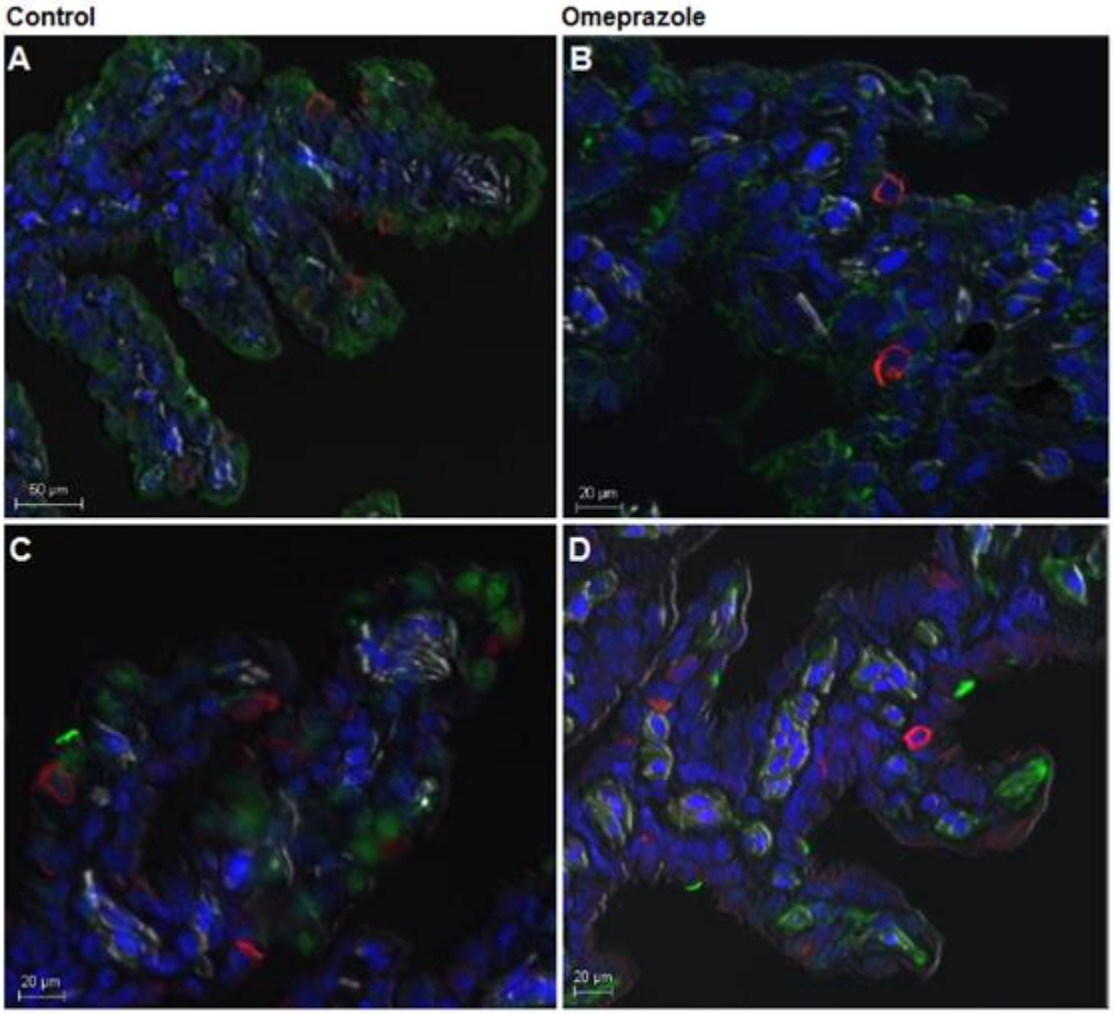

Figure 4.13: Immunohistochemistry of control (A and C), and omeprazole injected (B and D) lungfish *Protopterus annectens* gill. In A and B sections are labelled with DAPI (blue), non-gastric H^+/K^+-ATPase (green), and Na^+/K^+-ATPase (red). In C and D sections are labelled with DAPI (blue), V-ATPase (green), and Na^+/K^+-ATPase (red). Scale bar is 20 µm.

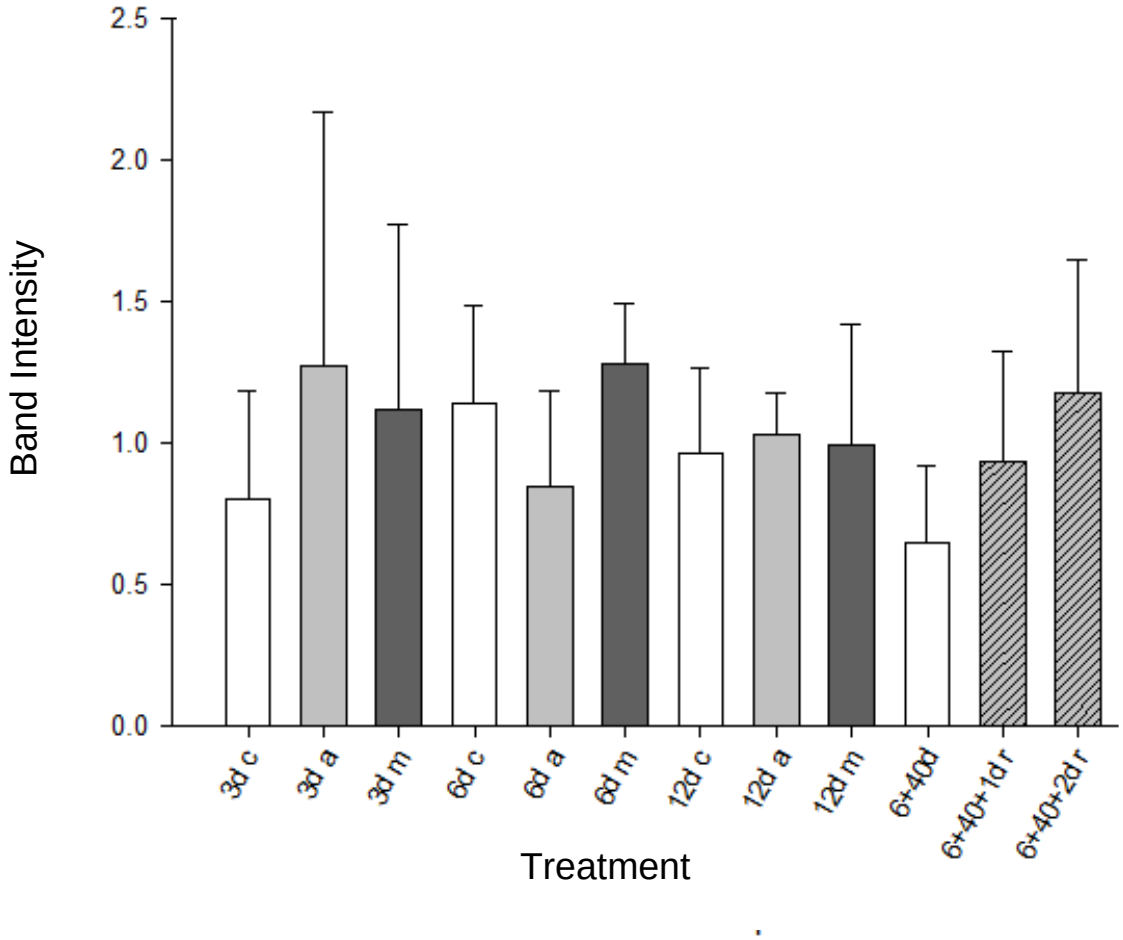

Figure 4.14: Relative band intensity of the ngHKA in *Protopterus annectens* internal gill of control (c, white), air estivating (a, light grey), and mud estivating (m, dark grey) lungfish from 3 days to 46 days, as well as some that were recovered (r, hatched bars) (n=3-5). No significant differences were found (Two-way ANOVA, p=0.6).

Chapter 5:
General Discussion

5.1 Species Integration

The overall objective of my thesis was to characterize the non-gastric H^+/K^+-ATPase (ngHKA) (*atp12a*) in two distinct fish lineages, the cyclostome (agnathan) lamprey and sarcopterygian (gnathostome lobed finned fishes) lungfish. Both of these lineages also lack the gene for the gastric H^+/K^+-ATPase (gHKA) (*atpa4a*). Even though both lamprey and lungfish have the ngHKA present, they differ significantly in terms of life history traits. Sea lamprey are a temperate anadromous species that undergo a dramatic metamorphosis from a freshwater, burrow-dwelling filter feeder, to a saltwater parasitic adult. In contrast, African lungfish are tropical stenohaline freshwater fish that have a capability and reliance of breathing air, as well as a unique ability to enter a state of estivation for years at a time during harsh environmental conditions.

Teleost fish have lost the *atp12a* gene for the ngHKA. One possible reason why could be that a different mechanism is used, which arose due to the extra round of whole genome duplication found in teleosts. One example how lamprey and lungfish differ from teleosts is by their sodium channel proteins. Lamprey and lungfish both have an epithelium sodium channel (ENaC) (Uchiyama et al., 2015; Bartels and Potter, 2004), whereas teleosts do not and instead have an acid sensing ion channel (ASIC) (Dymowska et al., 2014). Additionally, perhaps the gHKA plays the role of the ngHKA in the gill of teleost fishes as seen in the Atlantic stingray (Choe et al., 2004).

Lungfish sodium (Na^+) and chloride (Cl^-) ion flux rates are only 10% of lamprey and teleost fish (Evans, 1979; Wood, 1988; Wilkie et al., 2007). In addition Eddy (1985) estimated potassium (K^+) uptake rates to be only about 3-5% of Na^+ and Cl^- uptake rates in rainbow trout. However, in this study, lungfish rubidium (Rb^+) uptake rates were in the

same range as lamprey (50%, 20 vs. 40 µmol/kg/h). Lamprey Rb^+ flux rates were just above predicted values from known Na^+ uptake rates, while lungfish were much higher than predicted values (Wilkie et al., 1998, 2001). These differences between lungfish and lamprey may be due to differences in ion kinetics between Na^+ and Cl^- versus K^+ in these species. K^+ flux rates are already much lower compared to Na^+ and Cl^- and therefore K^+ may not follow this trend. To my knowledge, K^+ flux values have not been measured previously in any lamprey or lungfish species.

The acid flux in the acid and base loaded lamprey had significantly more acid excretion compared to the control, which is what we would expect to see. The lungfish did show a trend toward this, although not significant. This muted response in lungfish is most likely due to the fact that lungfish are capable of using air breathing as a method of adjusting acid-base homeostasis and is actually used more compared to metabolic excretion of protons into the water (Gilmour et al., 2007).

Although omeprazole is an effective inhibitor of the gHKA, its effects on the ngHKA are tissue and species dependent (Crambert 2014). Not only can omeprazole inhibit the gHKA it also appears to inhibit the Na^+/K^+-ATPase (NKA), also found by (Iwata et al., 1988). However, only in lungfish was ngHKA protein decreased with omeprazole treatment. In both lamprey and lungfish the NKA expression was significantly reduced in omeprazole treated fish. These changes were not reflected in transcript levels or Rb^+ or H^+ flux rates in either species. Additionally, the differences seen in the decrease of ngHKA in the omeprazole lungfish and not the omeprazole lamprey may have to do with species differences. In the literature there has been a wide variety of responses to inhibitors that appears to be isoform, species, and tissue dependent (Crambert, 2014). For example,

Xenopus oocytes expressing ngHKA were inhibited by ouabain (NKA inhibitor) but not to Sch28080 (gHKA inhibitor) (Cougnon et al., 1996), and human alphaHKA2 (ngHKA) expressing cells were sensitive to both ouabain and Sch28080 (Grishin et al., 1996).

Although the results for both species were not clear cut and did not provide evidence for the hypothesis, this study provides solid groundwork for future studies. Until now, no one has looked at the role of the ngHKA in these fishes. Now with the use of novel antibodies, further studies can continue to investigate the function of the ngHKA and future osmoregulation models of lamprey and lungfish should include the ngHKA (Fig. 5.1).

5.2 Future Directions and Conclusions

Very little is known about the ngHKA in fishes. This is the first study investigating the potential functions of this ion pump in fish. With the use of antibodies, future studies can begin to think about how this pump fits in to the osmoregulation strategy of lamprey and lungfish. On an evolutionary scale, the ngHKA may have an important role or it could be lost similarly like in the teleost fish. Elasmobranchs have also been confirmed to have the *atp12a* gene for the ngHKA (J.M. Wilson, personal communication).

Although, in this study none of the physiological disturbances elicited any straightforward response in terms of the predicted function, future studies are suggested to continue work using various techniques such as radiolabelled isotopes. A closer look at the kidney may also reveal important information regarding ion and acid-base regulation. Specifically in lungfish, the skin is also an important osmoregulatory organ and should be look into further (Sturla et al., 2001; Wilkie et al., 2007). Both lamprey and lungfish could be fasted for longer as both species have a sedentary lifestyle. It is also suggested that lamprey have an acclimation period, perhaps using a flow through system, before flux

measurements begin. Investigation into the different life stages of lamprey could also reveal important differences between saltwater and freshwater ionoregulatory strategies, which would help deduce function. Lastly, further inhibitors such as ouabain and SCH28080 should be tested in attempt to find an inhibitor as this would be a powerful tool to further our understanding of the ngHKA.

In the field of ion regulation there still remains many unanswered questions and inconsistent results. The difficulty lies in trying to understand how one protein operates when all of the pumps are somehow connected and a certain manipulation may effect multiple things. Although easier said than done, it would be best to study a system in its entirety rather than looking at individual pumps.

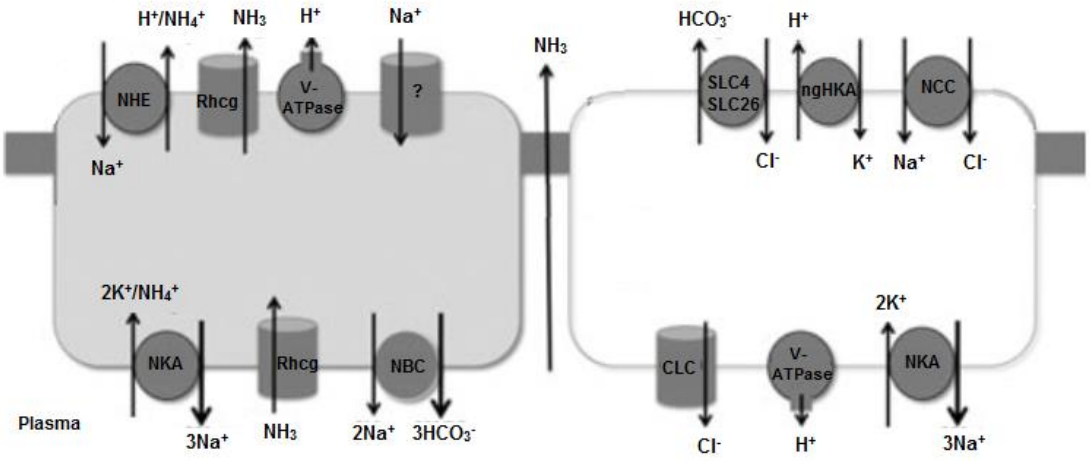

Figure 5.1: Adapted from Evans 2011 with the addition of the non-gastric H^+/K^+-ATPase. Proposed model for ion regulation in freshwater fish gill epithelium. Two cell types are shown (white and grey), distribution of pumps in specific cells are not fully understood as well as species and environmental differences most likely occur.

REFERENCES

Abbas, L., Hajihashemi, S., Stead, L. F., Cooper, G. J., Ware, T. L., Munsey, T. S., & White, S. J. (2011). Functional and developmental expression of a zebrafish Kir1.1 (ROMK) potassium channel homologue Kcnj1. *The Journal of Physiology*, 589(Pt 6), 1489–1503. http://doi.org/10.1113/jphysiol.2010.200295

Adams, J. C. (1992). Biotin amplification of biotin and horseradish peroxidase signals in histochemical stains. *The Journal of Histochemistry and Cytochemistry* 40(10), 1457-1463.

Ballantyne, J.S. & Frick, N. T. (2006). Metabolism. In J. Jorgensen Morup, J., Joss (Ed.), *The Biology of Lungfish* (pp. 305–340). Science Publisher Inc., Enfield.

Bartels, H., Moldenhauer, A., & Potter, I.C. (1996). Changes in the apical surface of chloride cells following acclimation of lampreys to sea- water. *American Journal of Physiology. Regulatory, Integrative and Comparative Physiology*, 270, R125–R133.

Bartels, H., Potter, I.C., Pirlich, K., & Mallatt, J. (1998). Categorization of the mitochondria-rich cells in the gill epithelium of the freshwater phases in the life cycle of lampreys. *Cell and Tissue Research*, 291, 337–349.

Bartels, H., & Potter, I. C. (2004). Cellular composition and ultrastructure of the gill epithelium of larval and adult lampreys: implications for osmoregulation in fresh and seawater. *The Journal of Experimental Biology*, 207(Pt 20), 3447–62. http://doi.org/10.1242/jeb.01157

Beamish, F. W. (1980). Osmoregulation in Juvenile and Adult Lampreys1. *Canadian Journal of Fisheries and Aquatic Sciences*, 37, 1739–1750.

Beamish, F.W.H. & Potter, I.C. (1975). The biology of the anadromous sea lamprey (Petromyzon marinus) in New Brunswick. *Journal of Zoology*, 177, 57–72.

Blanco, G., & Mercer, R. W. (1998). Isozymes of the Na-K-ATPase: heterogeneity in structure, diversity in function. *The American Journal of Physiology*, 275(5 Pt 2), F633–F650. http://doi.org/10.1152/ajprenal.00721.2010

Bordeaux, J., Welsh, A. W., Agarwal, S., Killiam, E., Baquero, M. T., Hanna, J. A., & Rimm, D. L. (2010). Antibody validation. *BioTechniques*, 48(3), 197–209. http://doi.org/10.2144/000113382

Brinkmann, H., Denk, A., Zitzler, J., Joss, J. J., & Meyer, A. (2004). Complete mitochondrial genome sequences of the South American and the Australian lungfish: testing of the phylogenetic performance of mitochondrial data sets for phylogenetic problems in tetrapod relationships. *Journal of Molecular Evolution*, 59(6), 834–48. http://doi.org/10.1007/s00239-004-0122-8

Brown, D., Lydon, J., McLaughlin, M., Stuart-Tilley, A., Tyszkowski, R., & Alper, S. (1996). Antigen retrieval in cryostat tissue sections and cultured cells by treatment with sodium dodecyl sulfate (SDS). *Histochemistry and Cell Biology*, 105, 261–267. http://doi.org/10.1007/BF01463929

Bublitz, M., Morth, J. P., & Nissen, P. (2011). P-type ATPases at a glance. *Journal of Cell Science*, 124(Pt 15), 2515–2519. http://doi.org/10.1242/jcs.102921

Bucking, C., & Wood, C. M. (2006). Gastrointestinal processing of Na^+, Cl^-, and K^+ during digestion: implications for homeostatic balance in freshwater rainbow trout. *American Journal of Physiology. Regulatory, Integrative and Comparative Physiology*, 291(6), R1764–R1772. http://doi.org/10.1152/ajpregu.00224.2006

Bucking, C., & Wood, C. M. (2008). The alkaline tide and ammonia excretion after voluntary feeding in freshwater rainbow trout. *The Journal of Experimental Biology*, 211(Pt 15), 2533–41. http://doi.org/10.1242/jeb.015610

Burggren, W.W. & Johansen, K. (1986). Circulation and respiration in lungfishes (Dipnoi). *Journal of Morphology*, 1(suppl.), 217– 236.

Cameron, J. N., & Kormanik, G. A. (1982). The acid-base responses of gills and kidneys to infused acid and base loads in the channel catfish, *Ictalurus punctatus*. *The Journal of Experimental Biology*, 99, 143–160.

Castro, L. F. C., Gonçalves, O., Mazan, S., Tay, B., Venkatesh, B., & Wilson, J. M. (2014). Recurrent gene loss correlates with the evolution of stomach phenotypes in gnathostome history. *Proceedings of the Royal Society London B- Biological Sciences.* 281(1775), 20132669. http://doi.org/10.1098/rspb.2013.2669

Choe, K. P., Verlander, J. W., Wingo, C. S., & Evans, D. H. (2004). A putative H^+-K^+-ATPase in the Atlantic stingray, *Dasyatis sabina*: primary sequence and expression in gills. *American Journal of Physiology. Regulatory, Integrative and Comparative Physiology*, 287(4), R981–R991. http://doi.org/10.1152/ajpregu.00513.2003

Claiborne, J. B., Edwards, S. L. & Morrison-Shetlar, A. I. (2002). Acid–base regulation in fishes: cellular and molecular mechanisms. *Journal of Experiment Zoology,* 293, 302-319.

Cougnon, M., Planelles G., Crowson, M.S., Shull, G.E., Rossier, B.C., & Jaisser, F. (1996). The rat distal colon P-ATPase alpha subunit encodes a ouabain- sensitive H^+/K^+-ATPase. *Journal of Biological Chemistry*, 271, 7277–7280.

Crambert, G. (2014). H-K-ATPase type 2: relevance for renal physiology and beyond. *American Journal of Physiology. Renal Physiology*, 306(7), F693–700. http://doi.org/10.1152/ajprenal.00605.2013

Crothers, J.M., Chow, D.R., & Forte, J.G. (1993). Omeprazole decreases H^+/K^+-ATPase protein and increases permeability of oxyntic secretory membranes in rabbit. *The American Journal of Physiology,* 265, G231- G241.

Dymowska, A. K., Schultz, A. G., Blair, S. D., Chamot, D., & Goss, G. G. (2014). Acid-sensing ion channels are involved in epithelial Na^+ uptake in the rainbow trout *Oncorhynchus mykiss*. *American Journal of Physiology. Cell Physiology*, 307(3), C255–65. http://doi.org/10.1152/ajpcell.00398.2013

Eddy, F. B. (1975). The effect of calcium on gill potentials and on sodium and chloride fluxes in the goldfish *Carassius auratus*. *Journal of Comparative Physiology*, 96, 131-142.

Eddy, F. B. (1985). Uptake and loss of potassium by rainbow trout (*Salmo gairdneri*) in fresh water and dilute sea water. *Journal of Experimental Biology*, 118(1), 277–286.

Evans, D.H. (1979). Fish. Pp. 305–391 in G.M.O. Maloiy, ed. Comparative Physiology of Osmoregulation in Animals. *Academic Press*, New York.

Evans, D. H. (2011). Freshwater fish gill ion transport: August Krogh to morpholinos and microprobes. *Acta Physiologica (Oxford, England)*, 202(3), 349–359. http://doi.org/10.1111/j.1748-1716.2010.02186.x

Evans, D. H., Piermarini, P. M., & Choe, K. P. (2005). The multifunctional fish gill: dominant site of gas exchange, osmoregulation, acid-base regulation, and excretion of nitrogenous waste. *Physiological Reviews*, 85(1), 97–177. http://doi.org/10.1152/physrev.00050.2003

Ferreira-Martins, D., Coimbra, J., Antunes, C., & Wilson, J. M. (2016). Effects of salinity on upstream-migrating, spawning sea lamprey, Petromyzon marinus. *Conservation Physiology*, 4, 1–16. http://doi.org/10.1093/conphys/cov064

Fishman, A.P., Pack, A.I., Delaney, R.G., & Galante, R.J. (1986). Estivation in Protopterus. *Journal Morphology,* Suppl. 1, 237–248.

Forte, J.G., Forte, T.M., Black, J.A., Okamoto, C., & Wolosin, J.M. (1983). Correlation of parietal cell structure and function. *Journal of Clinical Gastroenterology*, 5(Suppl 1):17–27.

Furukawa, F., Watanabe, S., Kimura, S., & Kaneko, T. (2012). Potassium excretion through ROMK potassium channel expressed in gill mitochondrion-rich cells of Mozambique tilapia. *American Journal of Physiology. Regulatory, Integrative and Comparative Physiology*, 302(5), R568–576. http://doi.org/10.1152/ajpregu.00628.2011

Galmiche, J.P., Bruley Des Varannes, S., Ducrotte, P., Sacher-Huvelin, S., Vavasseur, F., Taccoen, A., Fiorentini, P., & Homerin. M. (2004). Tenatoprazole, a novel proton pump inhibitor with a prolonged plasma half-life: effects on intragastric pH and comparison with esomeprazole in healthy volunteers. *Alimentary Pharmacology & Therapeutics*, 19, 655–662.

Galvez, F., Reid, S.D., Hawkings, G., & Goss, G.G. (2002). Isolation and characterization of mitochondria-rich cell types from the gill of freshwater rainbow trout. *American Journal of Physiology. Regulatory, Integrative and Comparative Physiology*, 282, R658–R668.

Gardaire, E., & Isaia, J. (1992). Potassium balance in freshwater-adapted trout *Onchorhynchus mykiss*. *Comparative Biochemistry and Physiology*, 103(4), 657–660.

Gardaire, E., Isaia, J., & Bornancin, M. (1991). Kinetics of potassium transport across trout gills. *Comparative Biochemistry and Physiology - Part A: Physiology*, 99(4), 615–620. http://doi.org/10.1016/0300-9629(91)90139-4

Georgalis, T., Perry, S. F. & Gilmour, K. M. (2006). The role of branchial carbonic anhydrase in acid–base regulation in rainbow trout (Oncorhynchus mykiss). *Journal of Experimental Biology*, 209, 518-530.

Gilmour, K. M. & Perry, S. F. (2007). Branchial chemoreceptor regulation of cardiorespiratory function. In Fish Physiology, Vol. 25, *Sensory Systems Neuroscience*, (ed. B. Zielinski and T. J. Hara), pp. 97-151. San Diego: Academic Press.

Gilmour, K. M., Euverman, R. M., Esbaugh, A.J., Kenney, L., Chew, S. F., Ip, Y. K., & Perry, S. F. (2007). Mechanisms of acid-base regulation in the African lungfish *Protopterus annectens*. *The Journal of Experimental Biology*, 210, 1944–1959. http://doi.org/10.1242/jeb.02776

Glass, M.L., Fernandes, M.S., Soncini, R., Glass, H. & Wasser, J.S. (1997). Effects of dry season dormancy on oxygen uptake, heart, rate, and blood pressure in the toad Bufo parracnemis. *Journal of Experimental Zoology*, 279. 330-336.

Glass, M.L. (2010). Respiratory Function in Lungfish (Dipnoi) and a Comparison to Land Vertebrates. In J. Jorgensen Morup, J., Joss (Ed.), *The Biology of Lungfish* (pp. 266-276). Science Publisher Inc., Enfield.

Goss, G. G., Perry, S. F., Wood, C. M. & Laurent, P. (1992). Mechanisms of ion and acid–base regulation at the gills of freshwater fish. *Journal of Experimental Zoology*, 263, 143-159.

Goss, G. G., Perry, S. F., Fryer, J. N. & Laurent, P. (1998). Gill morphology and acid–base regulation in freshwater fishes. *Comparative Biochemistry and Physiology*, 119A, 107-115.

Grant, G. A. (2002). Synthetic peptides for production of antibodies that recognize intact proteins. *Current Protocols in Protein Science*, 18-30.

Grishin, A.V., Bevensee, M.O., Modyanov, N.N., Rajendran, V., Boron, W.F., & Caplan, M.J. (1996). Functional expression of the cDNA encoded by the human ATP1AL1 gene. *American Journal of Physiology – Renal Physiology*, 271, F539–F551.

Gumz, M. L., Lynch, I. J., Greenlee, M. M., Cain, B. D., & Wingo, C. S. (2010). The renal H^+-K^+-ATPases: physiology, regulation, and structure. *American Journal of Physiology. Renal Physiology*, 298(1), F12–F21. http://doi.org/10.1152/ajprenal.90723.2008

Hamm, L.L., Hering-Smith, K. S., & Nakhoul, N. L. (2013). Acid-base and potassium homeostasis. *Seminars in Nephrology*, 33(3), 257–64. http://doi.org/10.1016/j.semnephrol.2013.04.006

Hardisty, M.W., Potter, I.C., & Hilliard, R. (1989). Physiological adaptations of the living agnathans. In *Environments and physiology of fossil organisms*, (Vol. 80, pp. 241–254). Edinburgh: Royal Soc Edinburgh.

Harlow, E. & Lane, D. (1999). Using Antibodies: A Laboratory Manual, *Cold Spring Harbor Laboratory Press*, Cold Spring Harbor, New York.

Heisler, N. (1986). Comparative aspects of acid–base regulation. In Acid–base Regulation in Animals (ed. N. Heisler), pp. 397-449. Amsterdam: Elsevier.

Heisler, N. (1989). Parameters and methods in acid–base physiology. In C. R. B. and P. J. Butler (Ed.), *Techniques in Comparative Respiratory Physiology: an Environmental Approach* (pp. 305–332). Cambridge: Cambridge University Press.

Hiong, K. C., Ip, Y. K., Wong, W. P., & Chew, S. F. (2014). Brain Na^+/K^+-ATPase α-subunit isoforms and aestivation in the African lungfish, *Protopterus annectens*. *Journal of Comparative Physiology.B, Biochemical, Systemic, and Environmental Physiology*, 184(5), 571-587.

Hirata, T., Kaneko, T., Ono, T., Nakazato, T., Furukawa, N., Hasegawa, S., Wakabayashi, S., Shigekawa, M., Chang, M.-H., & Romero, M. F. (2003). Mechanism of acid adaptation of a fish living in a pH 3.5 lake. *American Journal of Physiology*, 284, R1199-R1212.

Hirose, S., Kaneko, T., Naito, N. & Takei, Y. (2003). Molecular biology of major components of chloride cells. *Comparative Biochemistry and Physiology B,* 136, 593- 620.

Holeton, G. F., Neuman, P. & Heisler, N. (1983). Branchial ion exchange and acid–base regulation after strenuous exercise in rainbow trout (*Salmo gairdneri*). *Respiratory Physiology,* 51, 303–318.

Hunyady, B., Krempels, K., Harta, G., & Mezey, E. (1996). Immunohistochemical signal amplification by catalyzed reporter deposition and its application in double immunostaining. *Journal of Histochemistry and Cytochemistry,* 44*, 1353-1362.*

Hwang, P.P., Lee, T.H., & Lin, L.Y. (2011). Ion regulation in fish gills: recent progress in the cellular and molecular mechanisms. *American Journal of Physiology. Regulatory, Integrative and Comparative Physiology,* 301(1), R28–47. http://doi.org/10.1152/ajpregu.00047.2011

Iftikar, F., Patel, M., Ip, Y. K. & Wood, C. M. (2008). The influence of feeding on aerial and aquatic oxygen consumption, nitrogenous waste excretion, and metabolic fuel usage in the African lungfish *Protopterus annectens*. *Canadian Journal of Zoology*, 86, 790–800.

Im, W. B., Sih, J. C., Blakeman, D. P., & McGrath, J. P. (1985). Omeprazole, a specific inhibitor of gastric (H^+-K^+)-ATPase, is a H^+-activated oxidizing agent of sulfhydryl groups. *The Journal of Biological Chemistry*, 260(8), 4591-4597.

Iwata, H., Iwata, C., & Matsuda, T. (1988). Difference between Two Isozymes of (Na^+ K^+) -ATPase in the Interaction with Omeprazole. Japan. *Journal of Pharmacology*, 46, 35–42.

Kieffer, J. D., Currie, S. & Tufts, B. L. (1994). Effects of environmental temperature on the metabolic and acid–base responses of rainbow trout to exhaustive exercise. *The Journal of Experimental Biology,* 194, 299–317.

Koelz, H. R. (1992). Gastric acid in vertebrates. *Scandinavian Journal of Gastroenterology*. Supplement, 193(769144705), 2–6. http://doi.org/10.3109/00365529209095998

Krishna, G.G., Chusid, P., & Hoeldtke, R.D. (1987). Mild potassium depletion provokes renal sodium retention. *Journal of Laboratory and Clinical Medicine,* 109, 724–730.

Kühlbrandt, W. (2004). Biology, structure and mechanism of P-type ATPases. *Nature Reviews Molecular Cell Biology*, *5*(4), 282-295.

Lahiri, S., Szidon, J.P., & Fishman, A.P. (1970). Potential respiratory and circulatory adjustments to hypoxia in the African lungfish. *Federation Proceedings*, 29, 1141–1148.

Laurent P., Delaney, R.G., & Fishman, A.P. (1978). The vasculature of the gills in the aquatic and aestivating lungfish (*Protopterus aethiopicus*). *Journal of Morphology*, 56, 173–208.

Laurent, P. & Dunel, S. (1980). Morphology of gill epithelia in fish. *American Journal of Physiology. Regulatory, Integrative and Comparative Physiology*, 238, R147–R159.

Lenfant, C. & Johansen, K. (1968). Respiration in the African lungfish, Protopterus aehiopicus. 1. Respiratory properties of blood and normal patterns of breathing and gas exchange. *Journal of Experimental Biology*, 49, 437-452.

Lewis, S.V. (1980). Respiration of lamprey. *Canadian Journal of Fisheries and Aquatic Sciences*, 37, 1711-1722.

Li, J., Codina, J., Petroske, E., Werle, M.J., Willingham, M.C., & DuBose, T.D. Jr. (2004). The effect of beta-subunit assembly on function and localization of the colonic H^+/K^+-ATPase alpha-subunit. *Kidney International*, 66, 1068–1075.

Lin, H., & Randall, D. (1995). Proton pumps in fish gills. In C. M. W. and T. J. Shuttleworth (Ed.), Cellular and Molecular Approaches to Fish Ionic Regulation (pp. 229–255). New York: Academic Press.

Livak, K. J., & Schmittgen, T. D. (2001). Analysis of relative gene expression data using real-time quantitative PCR and the 2(-delta delta C(T)) method. *Methods* (San Diego, Calif.), 25(4), 402-408.

Mähler, J., & Persson, I. (2012). A study of the hydration of the alkali metal ions in aqueous solution. *Inorganic Chemistry*, 51(1), 425-438.

Major, S.M., Nishizuka, S., Morita, D., Rowland, R., Sunshine, M., Shankavaram, U., Washburn, & F., Asin, D. (2006). AbMiner: a bioinformatic resource on available monoclonal antibodies and corresponding gene identifiers for genomic, proteomic, and immunologic studies. *BMC Bioinformatics*, 7, 192.

Marshall, W.S. & Grosell, M. (2006). The Physiology of Fishes. (J. Evans & J. B. Claiborne, Eds.) (third). Taylor and Francis Group.

McDonald, D.G., Tang, Y. & Boutilier, R.G. (1989). Acid and ion transfer across the gills of fish: mechanisms and regulation. *Canadian Journal of Zoology*, 67, 3046–3054.

McNamara, J. & Worthley, L. L. G. (2001). Acid–base balance: Part I. *Physiology. Critical Care and Resuscitation*, 3, 181-187.

Milligan, C. L. & Wood, C. M. (1986). Intracellular and extracellular acid–base status and H^+ exchange with the environment after exhaustive exercise in the rainbow trout. *The Journal of Experimental Biology*, 123, 93–121.

Morris, R. (1972). The biology of lampreys. In Osmoregulation (vol 2, pp. 193–239). London: Academic Press.

Namimatsu, S., Ghazizadeh, M., & Sugisaki, Y. (2005). Reversing the effects of formalin fixation with citraconic anhydride and heat: a universal antigen retrieval method. *Journal of Histochemistry and Cytochemistry*, 53(1), 3–11. http://doi.org/10.1369/jhc.4C6466.2005

Novak, I., Wang, J., Henriksen, K.L., Haanes, K.A., Krabbe, S., Nitschke R., & Hede, S.E. (2011). Pancreatic bicarbonate secretion involves two proton pumps. *The Journal of Biological Chemistry*, 286, 280–289.

Oduleye, S. O. (1977). Unidirectional water and sodium fluxes and respiratory metabolism in the African lungfish, *Protopterus annectens*. *Journal of Comparative Physiology*, 119, 127–139.

Patel, M., Iftikar, F. I., Leonard, E. M., Ip, Y. K., & Wood, C. M. (2009). Ionoregulatory physiology of two species of African lungfishes *Protopterus dolloi* and *Protopterus annectens*. *Journal of Fish Biology*, 75(4), 862–884. http://doi.org/10.1111/j.1095-8649.2009.02335.x

Perry, S. F., Furimsky, M., Bayaa, M., Georgalis, T., Shahsavarani, A., Nickerson, J. G. & Moon, T. W. (2003a). Integrated responses of Na^+/HCO_3^- cotransporters and V-type H^+-ATPases in the fish gill and kidney during respiratory acidosis. *Biochimica et Biophysica Acta,* 1618, 175-184.

Perry, S. F., Shahsavarani, A., Georgalis, T., Bayaa, M., Furimsky, M. & Thomas, S. (2003b). Channels, pumps, and exchangers in the gill and kidney of freshwater fishes: their role in ionic and acid–base regulation. *Journal of Experimental Zoology*, Part A Ecol. Genet. Physiol. 300, 53-62.

Perry, S. F., Gilmour, K. M., Swenson, E. R., Vulesevic, B., Chew, S. F. & Ip, Y. K. (2005). An investigation of the role of carbonic anhydrase in aquatic and aerial gas transfer in the African lungfish *Protopterus dolloi*. *The Journal of Experimental Biology,* 208, 3805-3815.

Perry, S. F., & Gilmour, K. M. (2006). Acid-base balance and CO2 excretion in fish: Unanswered questions and emerging models. *Respiratory Physiology and Neurobiology,* 154(1-2), 199–215. http://doi.org/10.1016/j.resp.2006.04.010

Rabon, E.C. & Reuben, M.A. (1990). The mechanism and structure of the gastric H, K-ATPase. *Annual Review of Physiology*, 52, 321–344.

Rahim, S.M., Delaunoy, J.P. & Laurent, P. (1988). Identification and immunocytochemical localization of two different carbonic anhydrase isoenzymes in teleostean fish erythrocytes and gill epithelia. *Histochemistry*, 89(5), pp.451-459.

Reid, S.D., Hawkings, G.S., Galvez, F. & Goss, G.G. (2003). Localization and characterization of phenamil-sensitive Na^+ influx in isolated rainbow trout gill epithelial cells. *Journal of Experimental Biology*, 206, 551-559. doi: 10.1242/jeb.00109

Reis-Santos, P., McCormick, S. D., & Wilson, J. M. (2008). Ionoregulatory changes during metamorphosis and salinity exposure of juvenile sea lamprey (*Petromyzon marinus* L.). *The Journal of Experimental Biology,* 211(Pt 6), 978–88. http://doi.org/10.1242/jeb.014423

Sachs, G., Chang, H., Rabon, E., Schackman, R., Lewin, M., & Saccomani, G. A. (1976). A nonelectrogenic H^+ pump in plasma membranes of hog stomach. *The Journal of Biological Chemistry*, 251, 7690–7698.

Sachs, G., Prinz, C., Loo, D., Bamberg, K., Besancon, M., & Shin, J. M. (1994). Gastric acid secretion: activation and inhibition. *The Yale Journal of Biology and Medicine*, 67(3-4), 81–95.

Sanders, B. Y. M. J., & Kirschner, L. B. (1983). Potassium metabolism in seawater. *Journal of Comparative Physiology. B*, Biochemical, Systemic, and Environmental Physiology, 28, 15–28.

Shi, S.R., Chaiwun, B., Young, L., Cote, R.J., & Taylor, C.R. (1993). Antigen retrieval technique utilizing citrate buffer or urea solution for immunohistochemical demonstration of androgen receptor in formalin-fixed paraffin sections. *Journal of Histochemistry and Cytochemistry*, 41(11), 1599-604.

Shin, J. M., Munson, K., Vagin, O., & Sachs, G. (2009). The gastric HK-ATPase: Structure, function, and inhibition. *Pflugers Archiv European Journal of Physiology*, 457(3), 609–622. http://doi.org/10.1007/s00424-008-0495-4

Skou, J. (1957). The influence of some cations on an adenosine triphosphatase from peripheral nerves. *Biochimica et Biophysica Acta*, 23, 394–401.

Smith, H. W. (1931). Observations on the African Lungfish, Protopterus Aethiopicus, and on Evolution from Water to Land Environments. *Ecology*, 12(1), 164. http://doi.org/10.2307/1932938

Smolka, A.J., Lacy, E.R., Luciano, L., & Reale, E. (1994). Identification of gastric H,K-ATPase in an early vertebrate, the Atlantic stingray *Dasyatis sabina*. *Journal of Histochemistry and Cytochemistry*, 42, 1323–1332.

Stanton, B. A., & Giebisch, G. (1982). Effects of pH on potassium transport by renal distal tubule. *American Journal of Physiology*, (242), F544–51.

Stewart, P.A. (1983). Modern quantitative acid–base chemistry. *The Canadian Journal of Physiology and Pharmacology*, 61, 1444–1461.

Sturla, M., Masini, M.A., Prato, P., Grattarola, C., & Uva, B. (2001). Mitochondria-rich cells in gills and skin of an African lungfish, *Protopterus annectens*. *Cell and Tissue Research*, 303(3), 351–358. http://doi.org/10.1007/s004410000341

Swenson, E. R. (2000). Respiratory and renal roles of carbonic anhydrase in gas exchange and acid–base regulation. EXS 90, 281-341.

Takeyasu, K., Tamkun, M.M., Renaud, K.J., & Fambrough, D.M. (1988). Ouabain-sensitive (Na^+ , K^+)-ATPase activity expressed in mouse L cells by transfection with DNA encoding the a-subunit of an avian sodium pump. *Journal of Biology and Chemistry*, 263, 4347-4354.

Tipsmark, C. K., & Madsen, S. S. (2001). Rapid modulation of Na^+/K^+-ATPase activity in osmoregulatory tissues of a salmonid fish. *The Journal of Experimental Biology,* 204, 701-709.

Tresguerres, M., Katoh, F., Fenton, H., Jasinska, E. & Goss, G. G. (2005). Regulation of branchial V-H^+-ATPase, Na^+/K^+-ATPase and NHE2 in response to acid and base infusions in the Pacific spiny dogfish (*Squalus acanthias*). *The Journal of Experimental Biology*, 208, 345-354.

Tresguerres, M., Parks, S. K., Katoh, F. & Goss, G. G. (2006). Microtubule-dependent relocation of branchial V-H^+-ATPase to the basolateral membrane in the Pacific spiny dogfish (*Squalus acanthias*): a role in base secretion. *The Journal of Experimental Biology*, 209, 599-609.

Tresguerres, M., Parks, S. K., Wood, C. M., & Goss, G. G. (2007). V-H^+ -ATPase translocation during blood alkalosis in dogfish gills: interaction with carbonic anhydrase and involvement in the post feeding alkaline tide. *American Journal of Physiology. Regulatory, Integrative and Comparative Physiology*, 292(5), R2012–R2019. http://doi.org/10.1152/ajpregu.00814.2006

Uchiyama, M., Konno, N., Shibuya, S., & Nogami, S. (2015). Cloning and expression of the epithelial sodium channel and its role in osmoregulation of aquatic and estivating African lungfish *Protopterus annectens*. *Comparative Biochemistry and Physiology.Part A, Molecular & Integrative Physiology,* 183, 1-8.

Ura, K., Soyano, K., Omoto, N., Adachi, S., & Yamauchi, K. (1996). Localization of Na-KATPase in tissues of rabbit and teleosts using an antiserum directed against a partial sequence of the α - subunit. *Zoological Science,* 13, 219-227.

Van Heusden, J., de Jong, P., Ramaekers, F., Bruwiere, H., Borgers, M., & Smets, G. (1997). Fluorescein-lled tyramide strongly enhances the detection of low

bromodeoxyuridine incorporation levels. *The Journal of Histochemistry and Cytochemistry*: Official Journal of the Histochemistry Society, 45(2), 315-319.

Verdouw, H., Van Echteld, C. J. A., & Dekkers, E. M. J. (1978). Ammonia determination based on indophenol formation with sodium salicylate. *Water Research*, 12(6), 399–402. http://doi.org/10.1016/0043-1354(78)90107-0

Wand, Y., Heigenhauser, G. J. F. & Wood, C. M. (1994). Integrated responses to exhaustive exercise and recovery in rainbow trout white muscle: acid–base, phosphagen, carbohydrate, lipid, ammonia, fluid volume and electrolyte metabolism. *The Journal of Experimental Biology*, 195, 227–258.

Wang, G., Achim, C. L., Hamilton, R. L., Wiley, C. A., & Soontornniyomkij, V. (1999). Tyramide signal amplification method in multiple-label immunofluorescence confocal microscopy. *Methods* (San Diego, Calif.), 18(4), 459-464.

Weiner, I. D., & Wingo, C. S. (1997). Hypokalemia--consequences, causes, and correction. *Journal of the American Society of Nephrology: JASN*, 8(7), 1179-1188.

Weiner, I. D., & Wingo, C. S. (1998). Hyperkalemia: A potential silent killer. *Journal of the American Society of Nephrology: JASN*, 9(8), 1535-1543.

Wilkie, M., Couturier, J., & Tufts, B. (1998). Mechanisms of acid-base regulation in migrant sea lampreys (*Petromyzon marinus*) following exhaustive exercise. *The Journal of Experimental Biology*, 201 (Pt 9), 1473–82.

Wilkie, M. P., Bradshaw, P. G., Joanis, V., Claude, J. F., & Swindell, S. L. (2001). Rapid metabolic recovery following vigorous exercise in burrow-dwelling larval sea lampreys (*Petromyzon marinus*). *Physiological and Biochemical Zoology: PBZ*, 74(2), 261-272.

Wilkie, M. P., Morgan, T. P., Galvez, F., Smith, R. W., Kajimura, M., Ip, Y. K., & Wood, C. M. (2007). The African lungfish (*Protopterus dolloi*): ionoregulation and osmoregulation in a fish out of water. *Physiological and Biochemical Zoology*, 80(1), 99–112. http://doi.org/10.1086/508837

Willingham, M. C. (1999). Conditional epitopes. Is your antibody always specific? *Journal of Histochemistry and Cytochemistry*, 47(10), 1233–1236. http://doi.org/10.1177/002215549904701002

Wilson, J. M., & Laurent, P. (2002). Fish gill morphology: Inside out. *The Journal of Experimental Zoology*, 293(3), 192-213.

Wilson, J. M. (2007). The use of immunochemistry in the study of branchial ion transport mechanisms. In B. Baldisserotto, J. M. Mancera, & B. G. Kapoor (Eds.), Fish Osmoregulation (pp. 358–394). Enfield: Science Publisher Inc.

Wilson, J.M., Leitão, A., Gonçalves, A.F., Ferreira, C., Reis-Santos, P., Fonseca, A-V., da Silva, J.M., José Antunes, J.C., Pereira-Wilson, C., & Coimbra, J. (2007). Modulation of branchial ion 194 transport protein expression by salinity in glass eels (*Anguilla anguilla* L). *Marine Biology*, 151, 1633-1645.

Wilson, J. M. (2011). From Genome to Environment. In : Farrell A.P. (Ed.), Encyclopedia of Fish Physiology (volume 2, pp. 1381–1388). SanDiego: Academic Press.

Wilson, J. M., & Castro, L. F. C. (2010). Morphological diversity of the gastrointestinal tract in fishes. The Multifunctional Gut of Fish. In C. Grosell, M, Farrell, AP, Brauner (Ed.), (volume 30, pp. 1–55). Elsevier Inc.

Wingo, C.S. & Smolka, A.J. (1995). Function and structure of H-K-ATPase in the kidney. *American Journal of Physiology – Renal Physiology*, 269, F1–F16.

Witters, H., Berckmans, P. & Vangenechten, C. (1996). Immunolocalization of Na^+,K^+-ATPase in the gill epithelium of rainbow trout, *Oncorhynchus mykiss*. *Cell and Tissue Research*, 283, 461–468.

Wood, C. M., & Caldwell, F. H. (1978). Renal regulation of acid-base balance in a freshwater fish (1). *The Journal of Experimental Zoology*, 205(2), 301-307.

Wood, C. M. (1988). Acid-base and ionic exchanges at gills and kidney after exhaustive exercise in the rainbow trout. *The Journal of Experimental Biology*, 136(1), 461–481.

Wood, C. M., Bucking, C., & Grosell, M. (2010). Acid-base responses to feeding and intestinal cl- uptake in freshwater- and seawater-acclimated killifish, *Fundulus heteroclitus*, an agastric euryhaline teleost. *The Journal of Experimental Biology*, 213, 2681-2692.

Wright, P. A., Randall, D. J., & Perry, S. F. (1989). Fish gill water boundary layer: a site of linkage between carbon dioxide and ammonia excretion. *Journal of Comparative Physiology B*, 158(6), 627–635. http://doi.org/10.1007/BF00693000

Wright, P. A., Wood, C. M., & Wilson, J. M. (2014). Rh versus pH: the role of Rhesus glycoproteins in renal ammonia excretion during metabolic acidosis in a freshwater teleost fish. *The Journal of Experimental Biology*, 217(Pt 16), 2855–65. http://doi.org/10.1242/jeb.098640

Youson, J., & Potter, I. (1979). A description of the stages in the metamorphosis of the anadromous sea lamprey, *Petromyzon marinus* L. *Canadian Journal of Zoology*, 57(1976), 1808–1817. http://doi.org/10.1139/z79-235

APPENDICES

All typed protocols courtesy of Jonathan Wilson

A: Paraffin Tissue Embedding Procedure

Alcohol: Histology grade alcohol.
Xylene: Fisher Scientific.
Paraffin: Richard Allen type 6 paraffin

1. Set to program D on Citadel 1000 machine.
2. Plug in heating mantles for paraffin (Steps #11 and 12).
3. Start in position 1 – where remote holder is → to change press step on remote
4. Remove 2 lids
5. Take out polypropylene reagent containers – need to rotate on remote
6. Skip #2 (use white buckets #1,3-7). Fill with histo alcohol in the following order:
    1. 70% histo alcohol 1 hr
    3. 70% 1 hr
    4. 95% 1 hr
    5. 100% 1 hr
    6. 100% 1 hr
    7. 100% 2 hr

7. Metal reagent containers – 3 xylene – 1, 1, 2 hr (pour xylene in fume hood).
8. There are 2 paraffin heating mantels– do not remove. Plug in.
   – 2 and 3 hours
9. Place cassettes in metal rack(slide in from top) [max 60 cassettes]
10. Place weighted lid on top
11. Hang in and press **auto start** to lower into first reagent container.
12. Total time: 16 hours

Next day:

13. At ~15 hrs plug in HistoStat embedding station. Check that there is sufficient paraffin in reservoir– press heat button.
14. Once ready to start press cool
15. Empty wax overflow tray
16. Take out heating mantle from last stage and drop cassettes in (press life on remote). Unplug heating mantle from step #11.
17. Press rotate on remote to clear position to lift out heating mantle.
18. Plug heating mantle in next to HistoStat.
19. Place metal moulds on heating plate.
20. Fill metal molds with wax until they just overflow the centre well of the mold.
21. Empty contents of cassette into mold and place empty cassette onto hot plate.
22. Position tissue in centre of mold with fine tip probe.
23. Slide mould to cold block and quickly orientate and then gently press down on tissue with probe.
24. Put cassette on top and press down. Make sure liquid paraffin passes through slits in cassette.

25. After ~20 mins gently separate the metal mold from the cassette.
26. Clean the edges of the cassette – get rid of excess wax on all side
27. Empty all reagent containers back in to their respective glass storage jars.
28. Place stopper where wax comes out in HistoStat and turn off machine.
29. Put paper towel on cold plate to absorb any condensation.

B: Immunohistochemistry Protocol

SLIDE PREPARATION
Acid wash slides. 1%HCl in 70% EtOH for 15min at 60°C in sonicating bath
Rinse slides under running tap water and let sit (15 mins). Rinse further in dH_2O (15 mins).
Dry in drying oven 37C and allow to cool to room temperature.
Submerge slides in 2% APS in acetone for 2 min.
Briefly rinse in dH_2O.
Dry in oven. When completely dry store in slide box.
Notes:
Use plastic slide holders and containers.
Reuse 1%HCl in 70% EtOH.
7ml HCl conc. (37%) + 250 ml 70%EtOH (175ml EtOH + 75ml dH_2O)
Diluted APS solution only stable for 8h. Therefore prepare slides in batches of >100.
5ml APS + 250ml dry acetone. (Sigma A3648).
Store in a dry place at room temperature. Treated slides can be kept indefinitely.

SECTIONING
For new blocks
Orientate block in microtome chuck and mark upper side with a pencil.
Advance into block until tissue starts to appear in sections and a full block face is reached. Use course advance with care. Fine advance can be set at 10-20 um.
Final sectioning
Cool and hydrate blocks by placing face down in an ice-water bath for 5-10min.
Dry block face and surrounding area completely with tissue paper. Place block back into chuck in same orientation (marked side up).
Take care in advancing knife toward block. Set fine advance to 5-10um and begin collecting section.
Transfer a ribbon of sections to a dark piece of cardboard and with care transfer sections to APS coated slides dry. The shiny side of the sections should be face down (2-4 per slide depending on size of block face).
Add dH_2O to the **uncoated slides** using a plastic pipette to float the sections. Using fine tip probes try and flatten out section and chase out air pockets.
Place on heating mantle (setting 5-5.5 depending on room temperature) a glass Petri dish filled to brim with dH2O. Once warm (30min) slip sections in by gently lowering slide in at a slight angle using slide forceps. Wait until sections have expanded, retrieve sections with **coated slide**, drain off water by titling slide and drawing off the water with an absorbent material (cloth or paper).
Label frosted end of slides using a pencil. Place in plexiglas slide drying rack.
Dry slides overnight at 37°C or at room temperature until completely dry. This is important in order to ensure that the sections remain attached to the slide.

DEWAXING
Place slides to immunolabel in rack at 60C for 30 min allow to cool for 5-10 mins
Take slides through Xylene (3x5min) Xylene solublizes wax. Rinse 3x 100% EtOH*
3 mins in 70% EtOH
5 mins in DiH2O
* continue to rehydration to water for citraconic anhydride pretreatment. 70%EtOH, water, water. Do not dry slides.

PRETREATMENT (OPTIONAL)
CITRACONIC ANHYRIDE

Prepare 0.05% citraconic anhydride (Sigma **125318**) adjust pH to 7.4. Preheat in boiling water bath in sealed container.
Note: Dewax slides and rehydrate to water. Do NOT use hydrophobic barrier pen yet.
30 min at boil in water bath.
transfer directly to water and allow to cool. Remove rack and air dry slides at 37C.
Circle tissue section with a hydrophobic marker pen (DAKO PEN) and allow to dry (2-3 min).
SDS
Cover the sections with 50-100ul of 1%SDS in phosphate buffered saline (PBS) for 5min at room temperature OR submerge batch in Coplin jar.
Rinse sections with running tap water until free of foaming. Transfer to metal rack and 3x5min dH2O. Transfer to Coplin jar (8 or 16 slides per jar) with TPBS.

* If using TSA technique go to step 1 under Tyramide signal amplification
Note:
The SDS pre-treatment is particularly effective for antibodies generated against denatured proteins (AE1t, T4 α5). Background labelling however does tend to increase with pre-treatment. Citraconic anhydride and SDS pre-treatments can be used in series.

BLOCKING
Incubate section with 25-100 ul of 5% normal goat serum (NGS) / 1% bovine serum albumin (BSA) in TPBS (pH 7.4) or BLØK for 20 minutes at room temperature. Make sure hydrophobic circle is dry before adding solution.
Note:
At this time prepare primary antibody solutions. Dilute aliquots of antisera 1:20 to 1:500 times in 1%BSA/TPBS. Use 0.05% sodium azide as a preservative.
NGS is used in the blocking because the secondary antibodies are of goat origin. The pre-blocking reduces non specific background labelling of the sections. Modify the blocking buffer serum accordingly.

PRIMARY INCUBATION
Tap off blocking buffer (tap edge of slide onto tissue paper).
Add 25-100ul of diluted primary antibody to sections. Control incubations should also be done (i.e. normal mouse (NMS) and/or normal rabbit serum (NRS) equivalently diluted as primaries, and only buffer).
Incubate sections in a humidity chamber at 37°C for 1-2h or overnight 4°C.
WASH
Tap off primary antibody solutions as above and place slides in Coplin jar with TPBS.
Immediately change TPBS and then after 5,10 and 15 min. Agitate periodically.

SECONDARY INCUBATION
Incubate sections with appropriate secondary antibodies for 1h at 37°C in the humidity chamber.
Notes:
Select secondary antibodies according to the host species used to generate your primaries. The secondary antibodies are species specific. (i.e. *rabbit* anti-chicken CAII primary polyclonal antibody; use a *goat anti-rabbit* FITC labelled secondary. *Mouse* anti-human NKCC monoclonal antibody; use a *goat anti-mouse* Cy3 labelled secondary.
Select the type of secondary conjugate you wish to use. Fluorochromes (i.e. FITC, Cy3, Alexa dyes etc) are sensitive and allow double labelling but require a fluorescence microscope. ***Alexa dyes can be used at high dilutions 1:500.*** Enzyme conjugates such as horse radish peroxidase

(HRP) and alkaline phosphatase (AP) require the incubation of an enzyme substrate and are not as sensitive. They can however be permanently mounted.

HRP is sensitive to azide so do not use it in buffers used to dilute or rinse slides.
AP is sensitive to phosphates so use a non phosphate based buffer to rinse slides (i.e. TRIS).

WASH

1. Rinse slides as above.
2. However for fluorescence add DAPI to second wash buffer. 5ul (5mg/ml) in 60ml TPBS.

ENZYME SUBSTRATE REACTIONS

1. HRP use SIGMA Fast DAB Tabs. Monitor reaction under the microscope. Typically 30 seconds to 10 min.
2. AP use SIGMA Fast Red Tabs
3. Stop reaction by placing slides in Coplin jar with TPBS.

MOUNTING

1. Use glycerol based mounting media to mount sections labelled with either fluorochromes or AP. (1:1 glycerol:PBS with 0.1% azide, DAKO fluorescent mounting media S3023; Prolong Gold, or see homemade fluorescence mounting media file)
2. HRP labelled sections can be dehydrated, clearing and mounted with a permanent mounting media (Entellan, Merck)

*** <u>Tyramide Signal Amplification</u>**

Peroxidase Labeling
1. If necessary, quench endogenous peroxidase activity by incubating in peroxidase quenching buffer for 15 minutes at room temperature.
2. Incubate the specimen with 1% blocking reagent for 20 minutes at room temperature or 37°C.
3. Label the cells or tissue with primary antibody diluted in 1% blocking reagent for 60 minutes at room temperature or overnight at 4°C.
4. Rinse the cells or tissue three times with TPBS.
5. Prepare a working solution of the HRP conjugate by diluting the stock solution at the appropriate dilution in 1% blocking solution.
6. Apply 25-100 µL of the HRP conjugate working solution to the cells or tissue and incubate For 60 minutes at 37°C
7. Rinse the cells or tissue 5 min in TPBS, 10 min in DAPI, and 15 min in TPBS.
Tyramide Labeling
8. Prepare a tyramide working solution by diluting the tyramide stock solution 1:100 in amplification buffer/0.0015% H_2O_2 just prior to labeling. Prepare 100 µL of working solution per specimen. This quantity is sufficient to cover a standard 18 × 18 mm coverslip.
9. Apply 100 µL of the tyramide working solution to the cells or tissue and incubate for 10 minutes at room temperature.
10. Rinse the cells or tissue three times with PBS. Fluorescence detection of deposited biotin-XX tyramide requires the application of a fluorophore-labeled streptavidin conjugate.
11. Mount the specimen and examine by fluorescence microscopy or other appropriate imaging method.

C: Western Blotting Protocol

SDS-PAGE

1. Check that all stock solutions are available (Page 8). Make up gel formulation according to needs.
Prepare fresh 10% Ammonium persulfate solution (APS).

2. Prepare resolving and stacking gel solutions. Mix gently by inversion after adding all components. DO NOT SHAKE OR VORTEX! (See solutions section at end)
Note1: APS and TEMED (polymerisation catalysts) should be added to each solution immediately prior casting.
Note2: Unpolymerized acrylamide is NEUROTOXIC. Handle with care! Once polymerized it is non toxic and can be disposed off in regular garbage.

3. Degas gel solutions for 15 min prior to adding APS and TEMED.

4. Set up the glass plates in their holders according to BioRad instruction.
Mark plates at 5.2 cm from bottom (1cm below end of comb).

5. Add APS and TEMED to degassed resolving gel, almost at the same time mixing gently by inversion without shaking, and pour it in the glass plates with a 3ml disposable plastic pipette to a point slightly above the mark as the top of the gel will not polymerise.

6. Gently layer EtOH 95% using a disposable plastic pipette, to keep oxygen out as it will inhibit polymerisation.
Wait about 20minutes (Should gel within 30 minutes or something wrong)
Note1: Check polymerization by aspirating the left gel remaining in the tube, pipette should become blocked attempting to.
Note2: At this point the resolving gel can be stored at room temperature overnight. Add 5ml of 1:4 dilution of 1.5M Tris-HCl, pH 8.8 buffer (for Laemmli System) to the resolving gel to keep it hydrated. If using another buffer system, add 5ml 1x resolving gel buffer for storage.

7. Decant EtOH and rinse with dH_2O and insert dry filter paper to draw off water. Do not touch top of gel.

8. Prepare 1X Running buffer. For 4 gels (2 setups). 60 ml 10x to 600 ml is sufficient.

9. Add TEMED and APS to degassed Stacking gel sol^n and pour the solution between the glass plates using a disposable plastic pipette. Continue to pour until the top of the short plate reached. Insert the desired comb (10 or 15) at an angle between the spacers starting at the top of the Spacer Plate making sure that the tabs on each end of the comb are guided between the spacers. Avoid trapping bubbles!
Wait 5 minutes for polymerisation. (Should gel within 10 minutes or something wrong)
Note: Check polymerization by aspirating the left gel remaining in the tube, pipette should become blocked attempting to.

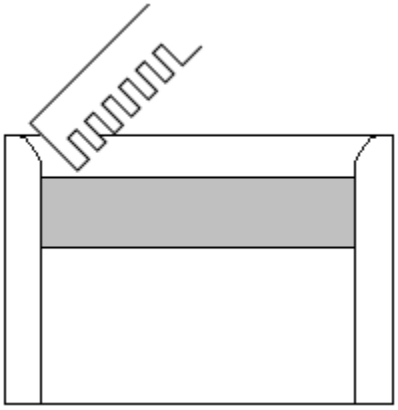

10. Mount gel assembly into module. Fill inner (upper) reservoir with running buffer and check for leaks. Then place module into tank and add running buffer to lower reservoir until bottom edge of glass plates are submerged. Wait at least 30 min for stacking gel to completely polymerize. Gels can be stored overnight in fridge or on bench top.
Note: Pour the running buffer down sides of tank and avoid trapping bubbles between bottom edge of plates.

11. BioRad MW std (Molecular Weight standard) are ready to load (5 ul). Vortex and spin. Do the same for all samples.

12. Remove the comb and with a 200µl pipette use a jet of running buffer to gently dislodge unpolymerized material from wells.

13. Insert sample loading guides (10 or 15 spacer) and load standards and samples using a gel loading tip cut to the depth of the well. Use one tip for all samples, rinsing inbetween.
Note: First well MW std and last wells Positive Control and/or 1xLB.

14. Place lid on and connect to BioRad power supply. Set to constant voltage at 75V and run for 15 minutes. Then increase voltage to 150V and run for approximately 1h.

15. While gel is running prepare Blotting Paper. Cut to size both thick filter paper (9.24 x 8.14 cm; 3 per gel) and PVDF or nitrocellulose membranes (7.5 x 9 cm). Mark the bottom (and/or top) right-hand corners (slash or box) of the membranes for identification and orientation. Equilibrate filter paper and membranes in transfer buffer for 30 minutes with gentle agitation (orbital shaker).
Note: PVDF membranes must be first dipped in MeOH for 10sec and then rinsed in dH2O before equilibration in transfer buffer. PVDF membrane transfer does not require MeOH in the buffer (but we use the buffer with 10% MeOH). Nitrocellulose membranes are directly equilibrated in transfer buffer that must contain MeOH (20%).

TRANSFER

1. After the run is complete remove gel assembly one at a time. Remove top plate using the plastic spatula. Mark the bottom and/or top right-hand corners (slash or box) of the gels (opposite to MW std), using the plastic spatula, for identification and orientation. Cut away all stacking gel and dispose. Score the edges of the gel with the plastic spatula and at an angle gently place the

plate gel side down directly into a container with transfer buffer (for equilibration), it should fall out easily. Equilibrate for 20min with gentle agitation.

By convention

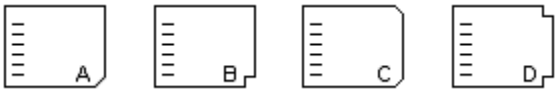

2. Construct transfer stacks in the Trans-blot SD:

Blotting paper, roll out bubbles using a cylinder (glass pipette).
Second blotting paper, roll out bubbles using the cylinder.
Transfer membrane.
Gel.
Third blotting paper, roll out bubbles using a cylinder.

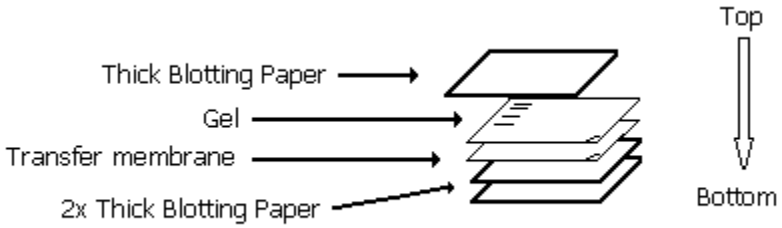

Note: DO NOT allow membranes to dry!

3. Place lid on and connect to power supply (Hoffer 2A200).
Set to constant voltage 100 V and time 1 hr, and start.

4. Once transfer is complete, carefully remove lid and check transfer of MW markers. Mark the location of MW std marker bands, dye front and gel limits on membrane, using a clean needle, by poking holes through gel and membrane.

5. Remove any acrylamide that may stick to the membrane and place membranes in TTBS for 10 min on orbital shaker.

6. Air dry membranes and then cut the excess, near the limits marked with the needle. You can write on the edge of blot with Signo Uni-ball UM-151.12 pens. Remark position of MW standards in ink. Store at 4ºC in sealed plastic bag.

PROBING AND DETECTION

1. Rehydrate PVDF membranes by passing them 10sec by methanol and then wash 5-10min in TTBS, on rocker or orbital shaker. Nitrocellulose can go straight to TTBS.

2. Ponceau S staining (0.5% in 1% acetic acid) incubate for 5min.
Destain in 5% acetic acid. A few changes 5min.
Lay out face up on acetate sheet. Overlay with second acetate sheet and photograph with regular camera. Water → picture → TTBS

3. Transfer the membranes to 10% blotto/TTBS (Blocking Buffer – skim milk powder), for 1h or overnight, on rocker or orbital shaker.
Note: Unoccupied sites on the membrane are saturated to prevent non-specific binding of antibodies, which are proteins themselves, to the membrane.

4. Decant the blotto and rinse the membranes with TTBS (3x 5min), on rocker or orbital shaker.

5. Incubate membranes with the primary antibodies diluted (1: 250 to 1:20 000 depending on antibody) in 1%BSA/TTBS/0.05% azide, for 1h at rt or overnight at 4°C, on rocker or orbital shaker. For small volumes (2.5 ml), membranes can be inserted face side up in 50 ml falcon tubes and placed on the rotissery (LabQuake).

6. Recover the primary antibodies and rinse the membranes with TTBS (quick rinse and changes after 5,10 and 15 min; 30 min total).

7. Incubate membranes with HRP secondary conjugated antibodies in TTBS (avoid azide!) for 1 h at rt.
Note1: 2µl Anti-mouse antibody + 50ml TTBS (25ml for each primary antibodies).
Note2: AP-BCIP/NBT *note phosphate inhibits AP enzymatic reaction. Do not use PBS. Dilute 1:10.000; HRP-ECL * Azide inhibits HRP catalyzed reaction. Avoid use in wash buffers.

8. Rinse membranes with TTBS (Step 25).

9. Prepare Millipore Immobilon ECL Western Blotting Detection 1A:1B (lab fridge).
Note: For each membrane 1ml solution. Prepare the solution in 5ml tubes, mix gently by inversion. Warm to rt.
DO NOT PIPETTE DIRECTLY FROM STOCK BOTTLES, with cross contamination this solutions will be rendered useless.

10. Switch on c600 Azure Biosystems and tablet. Settings: Type: Chemi, Exposure Time: 30 sec, Sensitivity/Resolution: normal, set tray position.

11. Cut a sheet of A4 acetate into two. Trim 2cm off one half piece (TOP), the other will be the BOTTOM piece.
Place the membranes face up on the BOTTOM piece of acetate. Blot dry.

12. Add 1 ml ECL solution and spread equally using the edge of pipette tip. Place TOP piece on. Incubate membranes for 5min at rt.

13. Tap off excess ECL solution and place sandwich inside imager on tray.

14. Adjust focus and START acquisition.
Adjust intensity histogram to optimize image.
Stop acquisition when desired or if image saturates (red).
Save selected images as tiff 16 bit. Do not save all images.

15. Take an additional set of images in precision mode with digitize. Set appropriate exposure time for ECL acquisition based on results from 14.

SOLUTIONS

AMMONIUM PERSULFATE SOLUTION (APS)
0.030 g Ammonium persulfate + 300µl dH_2O
(Desicator in the centre shelf)
NOTE: Use a 500 µl eppendorf tubes and weight in the precision balance.

RESOLVING GEL

1.5 mm	12%T 4gels	10% 4gels	8% 4gels
1.5M Tris HCl pH 8.8 (WB Shelf)	7.5 ml	7.5 ml	7.5 ml
dH_2O	13.0ml	14.5 ml	16.0 ml
10%SDS (WB Shelf)	0.3 ml	0.3 ml	0.3 ml
40% Bis/Acrylamide sol^n (fridge)	9.0 ml	7.5 ml	6.0 ml
10% APS (WB Shelf)	150µl	150µl	150µl
TEMED*	30(60)µl	30(60)µl	30(60)µl
Final volume	30ml	30ml	30ml

* TEMED is old so higher than normal concentration required. Use 20µl/10ml

Note: Resolving gel sieves and separates the proteins by size. Percentage gel depends upon the size of target proteins.

Acrylamide %	Range of separation (kDa)
15	12-43
10	16-68
7.5	36-94
5	57-212

STACKING GEL 0.75mm thick gels	4%T 4gels	4% 2gels	1.5mm 4% 4 gels
0.5M Tris HCl pH 6.8 (WB Shelf)	2.5 ml	1.25 ml	3.75 ml
dH_2O	6.1 ml	3.05 ml	9.7 ml
10%SDS	0.1 ml	0.05 ml	0.15 ml
40% Bis/Acrylamide sol^n	1.3 ml	0.65 ml	1.50 ml
0.5% Bromphenol Blue	100µl	50µl	150µl
10% APS	50µl	25µl	75µl
TEMED*	20µl(40µl)	10(20)µl	30 (60) µl
Final volume	10ml	5ml	15ml

* TEMED is old so higher than normal concentration required. Use 40µl/10ml
Don't add APS and TEMED until right before use

Note1: APS and TEMED are polymerisation catalysts required for gel formation. TEMED catalyses the formation of persulphate free radicals from APS, Which in turn initiates polymerisation. TEMED is always the last reagent added to the gel.
Note2: SDS is a denaturating reagent used at a final concentration of 0.1%. Binds proteins so they all become negatively charged, therefore separation is on the basis of size alone and not the intrinsic protein charge.

Acrylamide/BIS 30%T, 2.67%C	50ml	100ml	300ml
Acrylamide	14.6g	29.2 g	87.6 g
N'N'-bis-methylene-acrylamide	0.4g	0.8 g	2.4 g

Make with dH_2O, filter (pore size 0.2µm) and store at 4°C in the dark. (30 days maximum).

1.5M Tris HCl, pH 8.8
27.23 g Tris base
Use 6N HCl to adjust pH 8.8, qs to 150ml. Autoclave and store at rt.

0.5M Tris HCl, pH 6.8
6 g Tris base
Use 6N HCl to adjust pH to 6.8, qs to 100ml. Autoclave and store at rt.

RUNNING BUFFER (fridge)

	10X
Tris	30g
Glycine	144g
SDS	10g

qs to 1 l with dH_2O and store at 4°C

Note: Running Buffer 5x is kept in the lab fridge. (pH ±9.2)

1x RUNNING BUFFER
600ml
60 ml RB 10X
540 ml dH_2O

10x TRANSFER BUFFER (BioRad Buffer B) (fridge)

48mM Tris	58.2 g
39mM Glycine	29.3 g
0.0375% SDS	3.75 g) Optional

Bring volume to 1L with dH_2O. Do not adjust pH. Should be ~9.2

Note: *MeOH is not necessary for PVDF membranes but 20% is required for nitrocellµlose membranes (but we use the buffer with 10% MeOH for PVDF).

1x TRANSFER BUFFER		PVDF	Nitrocellulose
1L	10x Transfer Buffer	100ml	100ml
	MeOH	100ml	200ml
	dH_2O	800ml	700ml

Note: Transfer Buffer 10x is kept in the lab fridge.

TBS
10X (WB table)

20mM Tris	Tris HCl	27.4 g
	Tris base	3.2 g
500mM	NaCl	292.2 g

qs to 1L
Note: Filter (pore size 0.2µm) and store at room temperature.

TTBS

1L	TBS 10x	100ml
	dH_2O	900ml
	Tween 20	500µl

Note: 0.05% Tween 20. TTBS is stored at room temperature.

Ponceau S
0.5% in 1% acetic acid

BLOCKING BUFFER

Skim milk powder (WB table)	5g
TTBS	50ml

Note: 10% skim milk. If we want to keep the blocking buffer azide (0.05%) should be added.
Alternative: Roche blocking buffer (5ml aliquots in the –20ºC freezer) 10x concentrated.
Antibody dilution Buffer (1%BSA/TTBS/0.05% azide)

50ml	TTBS		50ml
BSA (lab Desicator)		0.5g (1%)	
Sodium azide 10% (WB table)		250µl (0.05%)	

2x Lämmli sample buffer

Stock	Volume		
0.125M Tris-HCl pH 6.8	0.5M	12.5	3.75
20% Glycerol		12.6g(10ml)	3.78g(3ml)
4% SDS	10%	20ml	6 ml
0.01% Bromphenol blue	0.5%	1.0ml	300µl
ddH_2O		1.5ml	450µl
100mM Dithiothreitol (DTT)*	1M	(5.0ml)	1.5ml
		45ml	15ml

Make up without DTT, filter with a 0.22µm syringe filter and divide into 0.9ml aliquots. Store at -20°C.
* add 100µl of 1M DTT to each thawed aliquot when needed.

Note: For ATPase assay gills are homogenise, afterwards what was left it was used for WB, by adding 2x Lämmli sample buffer in an equal volume (1:1) to the homogenate.

Immunoprecipitation – Biorad SureBeads™ Protocol

Preparation and Binding

1. Thoroughly resuspend the SureBeads in their solution and transfer 100 µl (1 mg at 10 mg/ml) of SureBeads to 1.5 ml tubes. Magnetize beads and discard supernatant.
2. Wash with 1,000 µl PBS-T (PBS + 0.1% Tween 20): a. Resuspend the beads thoroughly b. Magnetize beads and discard supernatant, repeat three times (3x).
Tip: Resuspension can be achieved by vortexing or pipetting while the magnet slider is outside of the tube holder. If vortexing, spin down the tubes before magnetization to bring down drops from the tube cap.
3. Add 1–10 µg antibody in final volume of 200 µl and resuspend the beads.
4. Rotate 10 min at room temperature (RT).
5. Magnetize beads and discard supernatant.
6. Wash with 1,000 µl PBS-T: a. Resuspend the beads thoroughly b. Magnetize beads and discard supernatant, repeat three times (3x).
7. Add the antigen-containing lysate, 100–500 µl.
8. Rotate for 1 hr at room temperature (RT).
9. Magnetize beads and discard supernatant. SureBeads Magnetic Beads Standard Immunoprecipitation Protocol 2
10. Wash with 1,000 µl PBS-T: a. Resuspend the beads thoroughly b. Magnetize beads and discard supernatant, repeat three times (3x). Before the last magnetization, transfer the resuspended beads to a new tube.
11. Spin down all tubes for several seconds.
12. Magnetize beads and aspirate residual buffer from the tubes.

Elution

Elution Strategy 1:
a. Add 20 µl glycine 20 mM pH 2.0 and incubate 5 min at RT
b. Magnetize beads and move eluent to a new vial
c. Neutralize eluent with 2 µl (10% eluent volume) 1 M phosphate buffer pH 7.4.

Elution Strategy 2:
a. Add 40 µl 1x Laemmli buffer and incubate for 10 min at 70°C
b. Magnetize beads and move eluent to a new vial.

D: RNA extractions and PCR/qPCR

RNA Agarose Formaldehyde Gel

- Clean everything with ZAP, rinse with milliQ
- 0.3 g of agarose
- 21.75 mL of milliQ
- 5.25 mL of formaldehyde
- 3 mL of 10x MOPS
- 5 µl of Gel Red
- (all values x 2 for larger sized gel)
- 2 µl of ladder, 10µl of sample
- Run gel in 250 mL of 1x MOPS buffer for 30 min at 80V

cDNA Reverse Transcriptase

For 1 sample

- 10x RT buffer: 2 µl
- 25x dNTP mix: 0.8 µl
- 10x RT primers: 2 µl
- Multiscribe RT: 1 µl
- + 14.2 µl of RNA

Running conditions

Volume 20 µl
Hot start? No

1. RT (25°C): 10 min
2. 37°C: 2 x 60 min
3. 85°C: 5 min
4. 4°C: ∞

Actin PCR Reaction Mix:

Per 1 sample

- 2x MasterMix: 10 µl
- Act SBR F1: 0.5 µl
- Act SBR R1: 0.5 µl
- Water: 8 µl
- cDNA: 1 µl

Running conditions for actin PCR using C1000 Touch Thermal Cycler

Lid temperature: 105°C
Sample volume: 10 µl

1. 94°C, 3:00 min
2. 94°C, 0:30 sec
3. 58°C, 0:30 sec
4. 72°C, 0:30 sec
5. Go to 2 29x
6. 72°C, 0: 30 sec

7. 4°C, ∞

1% agarose TBE gel

- 0.6 g agarose
- 54 mL milliQ
- 6 mL of 10x TBE
- 5 µl of Gel Red
- 2 µl ladder, 5 µl sample
- Run in 1L of 1x TBE for 30 min at 80V

qPCR Reaction Mix:

Per 1 sample

- CyberGreen (2x): 10 µl
- Forward primer: 0.5 µl
- Reverse primer: 0.5 µl
- Water: 4 µl
- Sample: 5 µl

qPCR Running Conditions using CFX96 Real-Time

Lid temperature: 105°C
Sample volume: 20 µl

7. 95°C, 3:00 min
8. 95°C, 0:10 sec
9. 60°C, 0:30 sec
10. Plate read
11. Go to 2. 39x
12. 55°C, 0:31 sec
7. 55°C, 0:05 sec

E: Immunohistochemistry pre-immune controls

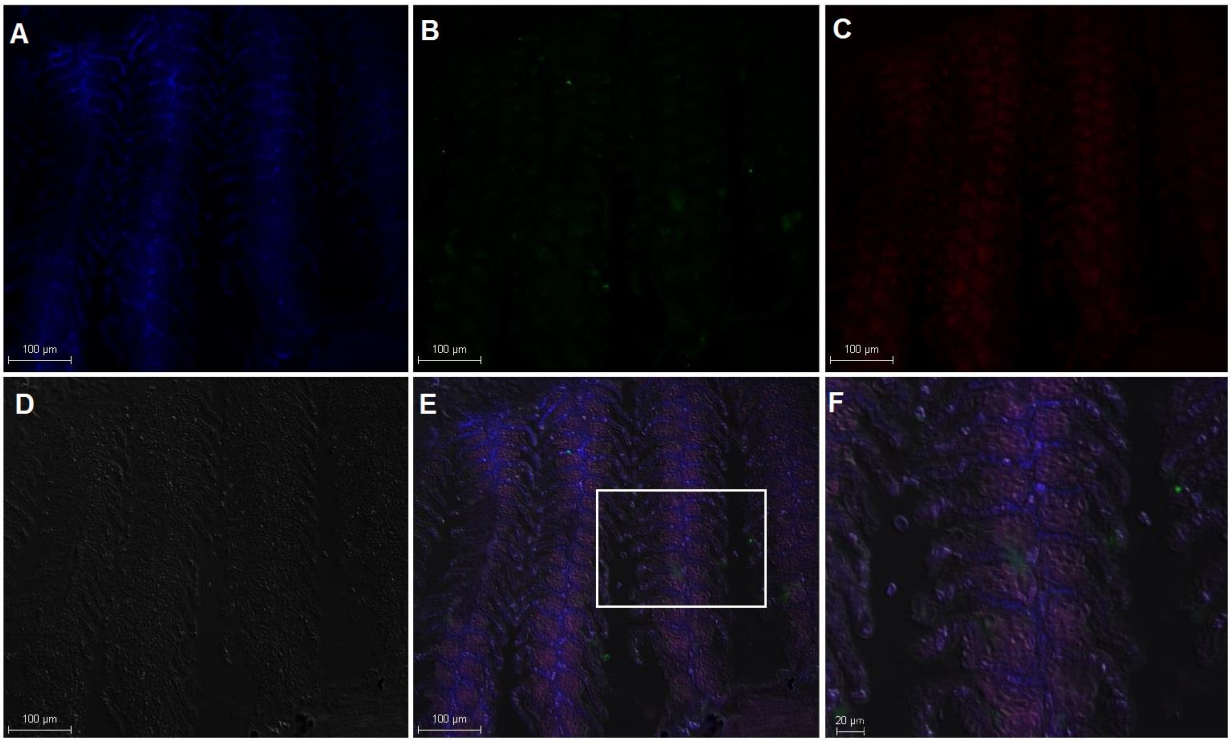

Figure E1: Immunohistochemistry of lamprey *Petromyzon marinus* gill A) DAPI B) pre-immune serum D) J3 D) DIC E) overlay of A-D and F) magnification of E. No specific staining seen. Scale bar is 100 µm A-E, 20 µm F

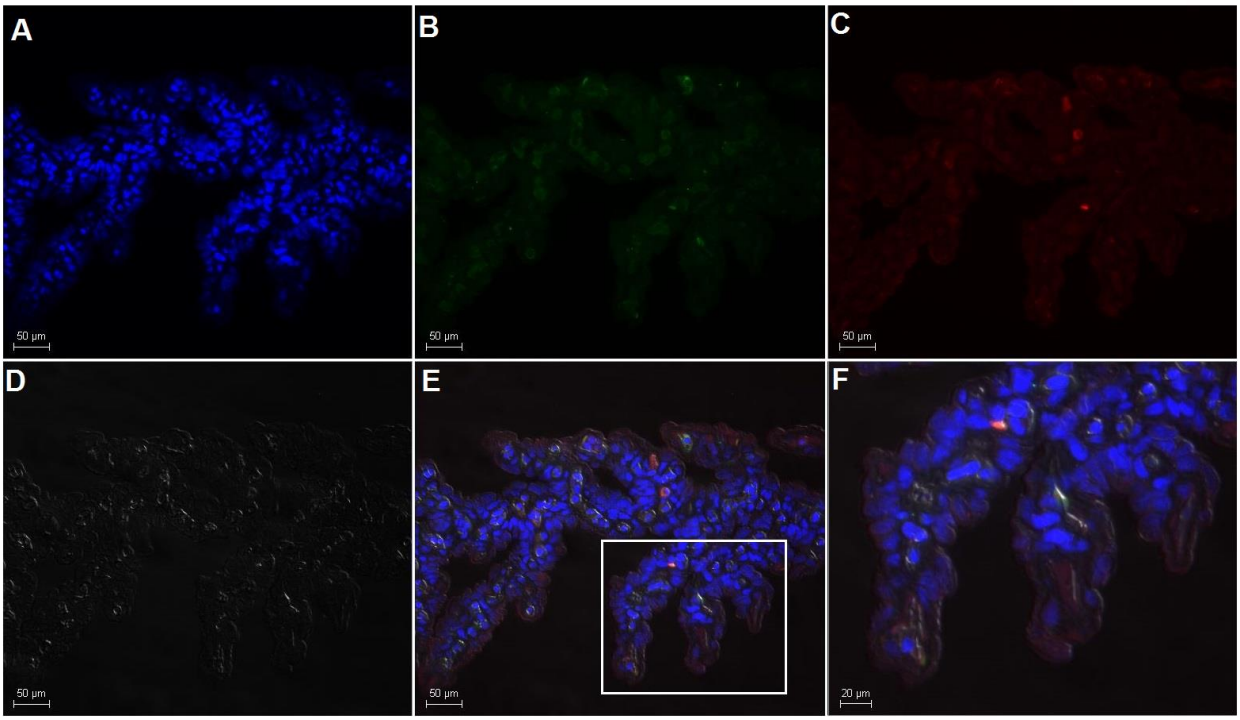

Figure E2: Immunohistochemistry of lungfish *Protopterus annectens* gill A) DAPI B) pre-immune serum D) J3 D) DIC E) overlay of A-D and F) magnification of E. No green staining seen. Scale bar is 50 µm A-E, 20 µm F